Portland State University
PDXScholar

Dissertations and Theses

Dissertations and Theses

1982

A geophysical study of the North Scappoose Creek, Alder Creek, Clatskanie River lineament, along the trend of the Portland Hills fault, Columbia County, Oregon

Nina Haas
Portland State University

Follow this and additional works at: https://pdxscholar.library.pdx.edu/open_access_etds

Part of the Geology Commons, and the Tectonics and Structure Commons
Let us know how access to this document benefits you.

Recommended Citation
Haas, Nina, "A geophysical study of the North Scappoose Creek, Alder Creek, Clatskanie River lineament, along the trend of the Portland Hills fault, Columbia County, Oregon" (1982). *Dissertations and Theses.* Paper 3254.
https://doi.org/10.15760/etd.3244

This Thesis is brought to you for free and open access. It has been accepted for inclusion in Dissertations and Theses by an authorized administrator of PDXScholar. Please contact us if we can make this document more accessible: pdxscholar@pdx.edu.

AN ABSTRACT OF THE THESIS OF Nina Haas for the Master of Science in Geology presented December 15, 1982.

Title: A Geophysical Study of the North Scappoose Creek - Alder Creek - Clatskanie River Lineament, Along the Trend of the Portland Hills Fault, Columbia County, Oregon.

APPROVED BY MEMBERS OF THE THESIS COMMITTEE:

[redacted]

Ansel G. Johnson, Chairman

[redacted]

Gilbert T. Benson

[redacted]

Marvin H. Beeson

The Portland Hills fault forms a strong northwest trending lineament along the east side of the Tualatin Mountains. An en echelon lineament follows North Scappoose Creek, Alder Creek, and the Clatskanie River along the same trend, through Columbia County, Oregon. The possibility that this lineament follows a fault or fault zone was investigated in this study. Geophysical methods were used, with seismic

refraction, magnetic and gravity lines run perpendicular to the lineament. The seismic refraction models indicate the near surface basalt is broken in many places, with 15 - 30 meters (50 - 100 feet) vertical displacement, down to the west, at Bunker Hill along the Alder Creek fault. Gravity models required a faulted zone approximately two kilometers wide across the lineament. The proposed fault zone is more clearly defined in the south, becoming more diffuse and branching in the northern part of the study area. The Bouguer gravity values from this study distort the -40 milligal contour farther to the northwest than is shown on the Complete Bouguer Gravity Anomaly Map of Oregon (Berg and Thiruvathukal, 1967b). The existence of sharp topographic features and the geophysical evidence indicate fault activity along the zone.

A GEOPHYSICAL STUDY OF THE NORTH SCAPPOOSE CREEK - ALDER CREEK - CLATSKANIE RIVER LINEAMENT, ALONG THE TREND OF THE PORTLAND HILLS FAULT, COLUMBIA COUNTY, OREGON

by

NINA HAAS

A thesis submitted in partial fulfillment of the requirements for the degree of

MASTER OF SCIENCE
in
GEOLOGY

Portland State University

1983

TO THE OFFICE OF GRADUATE STUDIES AND RESEARCH:

The members of the Committee approve the thesis of Nina Haas presented December 15, 1982.

[redacted]

Ansel G. Johnson, Chairman

[redacted]

Gilbert T. Benson

[redacted]

Marvin H. Beeson

APPROVED:

[redacted]

Gilbert T. Benson, Head, Department of Geology

[redacted]

Stanley E. Rauch, Dean of Graduate Studies and Research

ACKNOWLEDGEMENTS

I would like to thank Dr. R. W. Couch at Oregon State University for loaning the gravimeter and thumper, and for his advice; Steve Pitts and Northwest Geophysical Associates, Corvallis, for computer assistance with corrections to the gravity data; and Longview Fibre Company for allowing access to their timberlands.

Funding for this study was from Reichhold Energy Corporation, Tacoma, Washington, and St. Helens, Oregon, and the Paul Howell Fund, administered by the Geology Department of Portland State University.

Special thanks are due Dr. Ansel Johnson, my thesis advisor, Dr. Tom Benson and Dr. Marvin Beeson, my thesis committee, all who gave advice and assistance, and especially to my friends who helped with the field work.

TABLE OF CONTENTS

	PAGE
ACKNOWLEDGEMENTS	iii
LIST OF TABLES	vi
LIST OF FIGURES	vii
INTRODUCTION	1
PURPOSE	1
LOCATION	1
PREVIOUS WORK	5
GEOLOGIC SETTING	7
NORTHWESTERN OREGON, COLUMBIA COUNTY	7
Stratigraphy Structure	
TECTONIC HISTORY	12
METHODS OF INVESTIGATION	15
LINEAMENT ANALYSIS	15
WELL LOGS	17
GRAVITY	22
Purpose Field Procedure Regional Trend Data Reduction Equipment Used	
REFRACTION	28
Purpose Field Procedure	

PAGE

Data Reduction
Equipment Used

MAGNETICS 34

Purpose
Field Procedure
Data Reduction
Equipment Used

MODELLING AND RESULTS 36

GRAVITY 36

General
Regional Models
Local Models
Comparison

REFRACTION 50

General
Bunker Hill Line
Shaffer Road Line
Little Clatskanie River Road Line
Comparison

MAGNETICS 65

General
Bunker Hill Line
Shaffer Road Line
Little Clatskanie River Road Line
Comparison

DISCUSSION AND CONCLUSIONS 74

REFERENCES 82

APPENDIX A. GRAVITY DATA AND FORMULAS 92

APPENDIX B. REFRACTION DATA AND FORMULAS 101

APPENDIX C. MAGNETIC DATA 106

APPENDIX D. WATER WELL LOGS 109

LIST OF TABLES

TABLE		PAGE
I	Complete Bouguer Gravity Anomaly Values for Apiary, Pittsburg-Yankton and Spitzenberg Gravity Lines	49

LIST OF FIGURES

FIGURE		PAGE
1.	Regional Map	2
2.	Study Area	4
3.	Formations in Study Area	8
4.	Lineaments in Columbia County, Oregon	16
5.	North Scappoose Creek - Alder Creek - Clatskanie River Lineament (SLAR)	18
6.	Lineament, North Scappoose Creek - Alder Creek (photo)	19
7.	Lineament, Clatskanie River (photo)	20
8.	Lineament, North of Apiary-Oak Ranch Road	21
9.	Regional Bouguer Gravity Map	26
10.	Bunker Hill Refraction Line	30
11.	Typical Refraction Line Layout	31
12.	Shaffer Road and Little Clatskanie River Road Refraction Lines	32
13.	Location of Regional Gravity Models	39
14.	Apiary Regional Gravity Model	41
15.	Spitzenberg Regional Gravity Model	42
16.	Apiary Local Gravity Model	45
17.	Spitzenberg Local Gravity Model	46
18.	Bouguer Gravity Anomaly Contour Map	48

FIGURE PAGE

19. Bunker Hill Refraction, Time-distance Plot . . 54
20. Bunker Hill Refraction, Projected Cross Section 54
21. Shaffer Road Refraction, Time-distance Plot 58
22. Shaffer Road Refraction, Projected Cross Section 58
23. Lineament Offset at North End of Shaffer Road 61
24. Little Clatskanie Refraction, Time-distance Plot 62
25. Little Clatskanie Refraction, Projected Cross Section 62
26. Bunker Hill Magnetic Data, Graph 68
27. Bunker Hill Magnetic Data, Projected Cross Section 68
28. Shaffer Road Magnetic Data, Graph 70
29. Shaffer Road Magnetic Data, Projected Cross Section 70
30. Little Clatskanie Magnetic Data, Graph 72
31. Little Clatskanie Magnetic Data, Projected Cross Section 72
32. Complete Bouguer Gravity Map of Northwestern Oregon with Study Data 81

INTRODUCTION

PURPOSE

The Portland Hills fault lineament extends southeast into the upper Clackamas River drainage. This study was undertaken to investigate 1) the possible extension of the Portland Hills fault lineament to the northwest, into Columbia County, Oregon, and 2) the form this extension would take, whether as a continuation of the Portland Hills fault itself, as another fault along the same trend, or as a zone of parallel or en echelon faults. The thick vegetative cover in northwestern Oregon makes geophysical and remote sensing techniques the most logical way to investigate this problem. Photo and map analysis, and a combination of gravity, magnetic, and seismic refraction surveys were used to study the lineament trends.

LOCATION

This study was conducted in Columbia County, Oregon. Three gravity lines, and three refraction and magnetics lines were run (Figure 1).

The Spitzenberg gravity line begins at the intersection of Kappler Road and the St. Helens-Pittsburg (Old Vernonia) Road in T4N, R1W, Sec. 6, and follows Kappler Road to Cater Road (T4N, R2W), through Spitzenberg, then follows

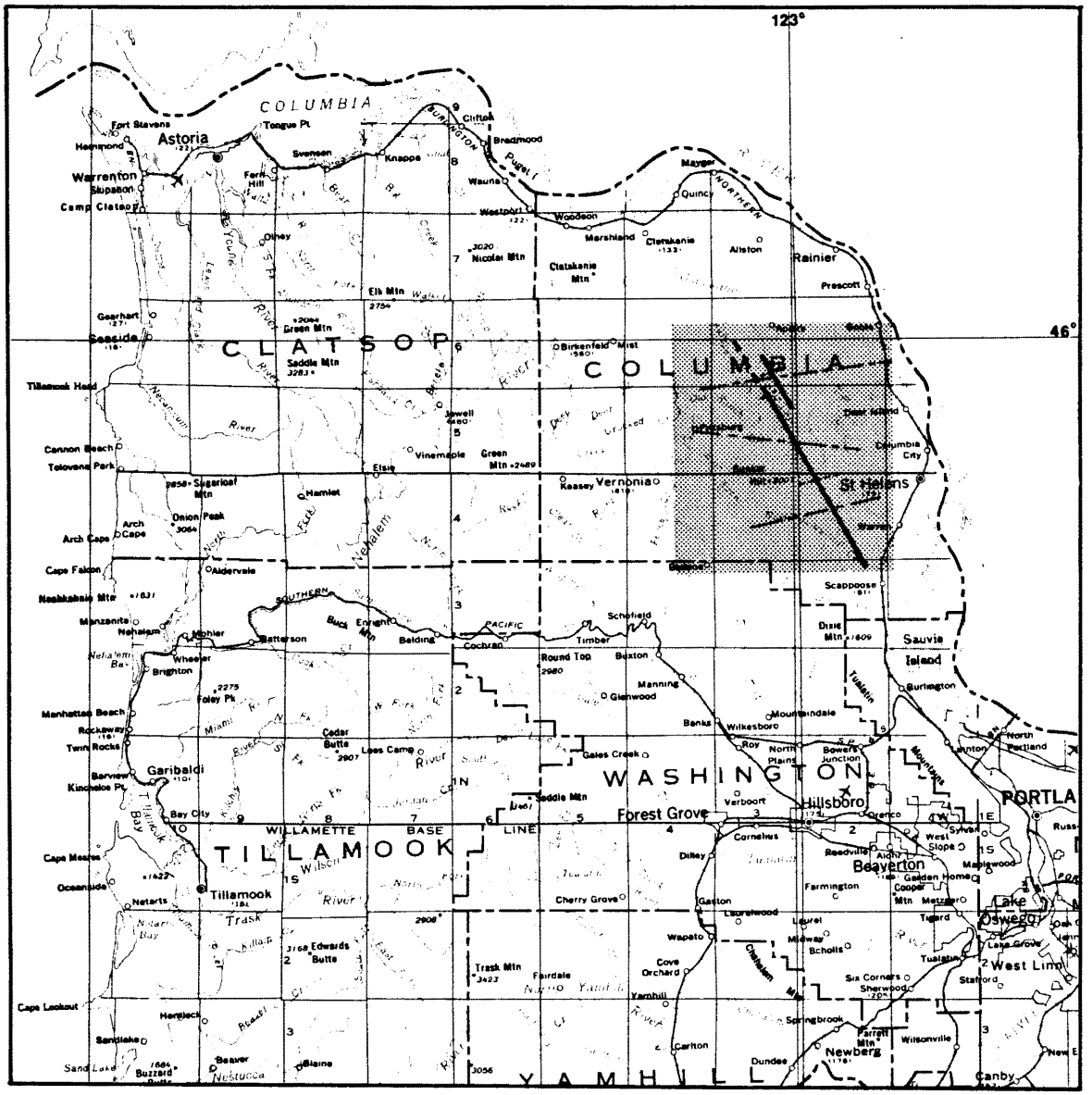

Figure 1. Regional map (from USGS map of Oregon, 1979 rev., 1:500,000).

the Scappoose-Vernonia Highway west past Chapman and Tunnel Road to the line's western end in T4N, R3W, Sec. 16 (Figure 2).

The Pittsburg-Yankton gravity line follows the St. Helens-Pittsburg (Old Vernonia) Road west from Yankton school (T5N, R2W, SW corner of Sec. 36) to its intersection with the Scappoose-Vernonia Highway and Oregon Highway 47 (T5N, R4W, Sec. 23) near Pittsburg (Figure 2).

The Apiary gravity line begins at the intersection of Tide Creek Road and U.S. Highway 30 (T6N, R2W, Sec. 36) and proceeds west via Tide Creek Road, Anliker Road, Meissner Road, Janshaw Road, Little Clatskanie River Road and the Apiary-Oak Ranch Road to the intersection with Oregon Highway 47 (T5N, R4W, Sec. 3) about 13 kilometers (8 miles) north of Vernonia (Figure 2).

The Bunker Hill refraction and magnetics line follows Bunker Hill Road east and west of its intersection with the Wilark 247 Road, in T4N, R2W, Sec. 6 (Figure 2). The Shaffer Road refraction and magnetics line follows the northernmost 1.5 kilometers (0.9 miles) of Shaffer Road to its intersection with the Apiary-Oak Ranch Road, then east along the Apiary-Oak Ranch Road for 0.3 kilometer (0.2 mile) in T5N, R3W, Sec. 3. The Little Clatskanie refraction and magnetics line follows the Little Clatskanie River Road east from the Apiary-Oak Ranch Road to the Little Clatskanie River, T6N, R3W, Sec. 34 and 35 (Figure 2).

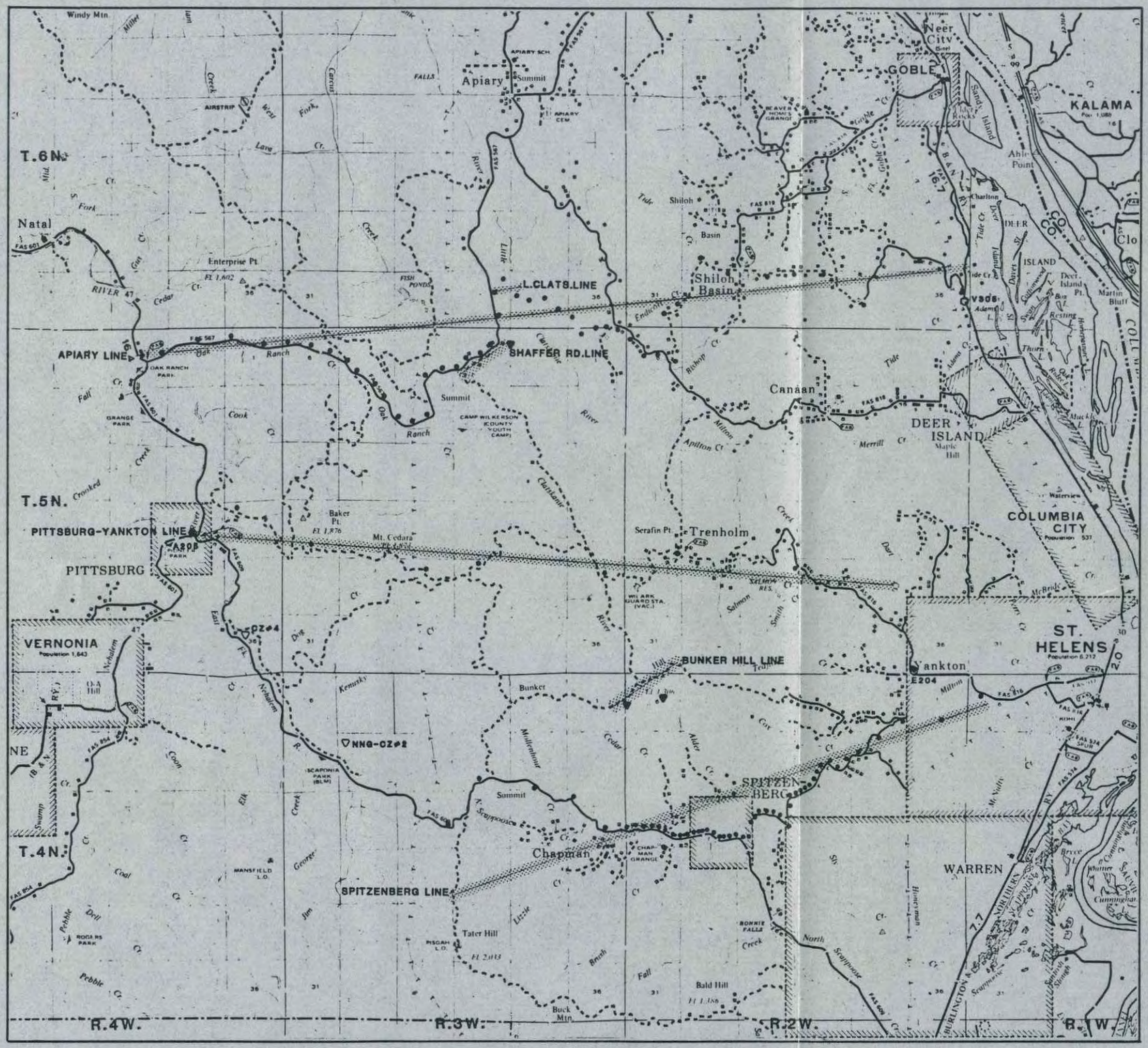

Geophysical line

Gravity station

Deep well

Water well

Building

Benchmark to anchor surveying

Figure 2. Study area (from map of Columbia County, Oregon, prepared by Oregon State Hwy. Division, 1971, scale 1:62,500).

The Shaffer Road and Little Clatskanie refraction and magnetics lines are located along sections of the Apiary gravity line. The Pittsburg-Yankton gravity line is 8.4 kilometers (5.2 miles) southeast of the Apiary line, and the Bunker Hill refraction and magnetics line is 3.5 kilometers (2.2 miles) south of the Pittsburg-Yankton gravity line. The Spitzenberg gravity line is 4.5 kilometers (2.8 miles) south of the Bunker Hill line.

PREVIOUS WORK

The Portland Hills fault, along the eastern edge of the Tualatin Mountains (Portland Hills), has been studied by Johnson and others (1977) and Beeson and others (1976), who noted gravity anomalies and offset Columbia River basalt flows. Schlicker and others (1964) and Couch and Lowell (1971) noted earthquake epicenters and their probable agreement with postulated faults in the Portland area. The gravity work of Jones (1977) and Perttu (1980) could be interpreted as evidence of the fault. Topographic evidence for the Portland Hills fault is cited by Beeson and others (1976) and Balsillie and Benson (1971). Extension of the Portland Hills fault trend into the Clackamas River drainage has been studied by Schmela (1971) and Anderson (1978).

The structure and stratigraphy of northwestern Oregon and Columbia County has been described by Diller (1896), Newton and Van Atta (1976), Benson and Donovan (1974), Warren, Norbisrath and Gravetti (1945), Snavely and Wagner

(1964), Trimble (1963), Kelty (1981) and Kadri (1982) among others. The St. Helens Quadrangle has been described by Wilkinson and others (1946).

Gravity of northwestern Oregon has been surveyed and analyzed by Bromery and Snavely (1964), Berg and Thiruvathukal (1967), and Thiruvathukal and others (1970). Gravity surveys in the Portland area have been conducted by Schmela (1971), Cash (1973), Johnson and others (1977), Jones (1977) and Perttu (1980).

Regional tectonic models have been offered by Atwater (1970) and Dickinson (1976, 1979). The Basin and Range province in Oregon was discussed by Lawrence (1976) and possible rotation of northwestern Oregon was discussed by Beck and Burr (1979), Magill and Cox (1981), and Simpson and Cox (1977). These models are described in the section on tectonic history.

GEOLOGIC SETTING

NORTHWESTERN OREGON - COLUMBIA COUNTY

Stratigraphy

A chart of formations in the study area is given in Figure 3. The following description is based primarily on the work of Newton and Van Atta (1976), Wilkinson and others (1946) and Snavely and Wagner (1964).

The upper Eocene Goble Volcanic series is the oldest unit in the study area and is considered slightly younger than the Tillamook-Siletz River Volcanics. The Goble Volcanics consist of dark grey submarine and subaerial basalt flows, breccias, and pyroclastics, often with calcite or zeolite filling fractures, intercalated with Cowlitz Formation sediments (Newton and Van Atta, 1976). The Cowlitz sedimentary rocks consist of siltstone, sandstone, shale, and in the lower part of the section, conglomerates. These sediments were deposited in near shore marine (littoral to sublittoral) environments. The siltstone is arkosic, finely laminated, argillaceous, and micaceous, with low angle cross lamination and cut and fill structures. The sandstone is grey, arkosic, silty, micaceous, and fine to medium grained. The shale is dark grey, thinly laminated, and micaceous, with some sandstone and tuffs (Newton and Van Atta, 1976; Snavely and Wagner, 1964).

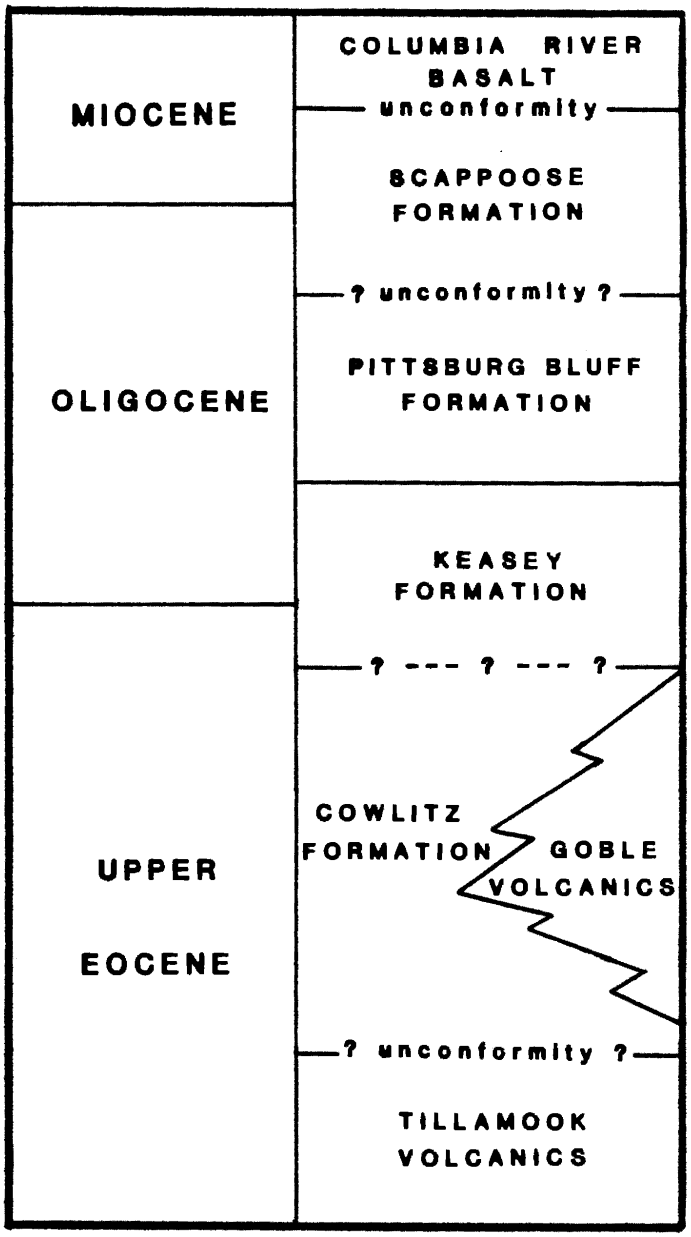

Figure 3. Formations in study area (from Kelty 1981, Newton and Van Atta 1976).

The upper Eocene to lower Oligocene Keasey Formation rests conformably on the Cowlitz Formation (Newton and Van Atta, 1976). The Keasey sediments were deposited in a bathyal to sub-bathyal environment and consist of tuffaceous mudstone, siltstone and shale, with some glauconitic sand. The Keasey beds are typically greenish grey and weather to a buff color. Fossils are abundant and structures include cross laminations, ripple laminations and load casts. Limestone concretions are found locally. An unconformity separates the Keasey from the younger Pittsburg Bluff Formation (Wilkinson and others, 1946; Newton and Van Atta, 1976).

The middle Oligocene to lower Miocene Pittsburg Bluff and Scappoose Formations are similar, and have been mapped as undifferentiated (Newton and Van Atta, 1976). The lower Pittsburg Bluff sediments are similar to the Keasey but contain more siltstone (Newton and Van Atta, 1976). Concretionary limestone beds are also found in the Pittsburg Bluff Formation. The upper Pittsburg Bluff beds are arkosic sandstone and siltstone. The sandstones are medium to fine grained, locally cross bedded, with iron stained laminae, and with wood fragments and locally developed coal. The Pittsburg Bluff sediments were deposited in shallow marine and delta environments, and are very fossiliferous. White ash layers, now altered to clay, are present. The Scappoose Formation, also fossiliferous, is composed of tuffaceous, arkosic sandstone, siltstone and mudstone, more quartzose,

but with less ash than the Pittsburg Bluff, and is a shallow marine, brackish water deposit. There is a disconformity between the Pittsburg Bluff and Scappoose Formations (Kelty, 1981; Warren and Norbisrath, 1946; Newton and Van Atta, 1976).

The Miocene Columbia River Basalt Group unconformably overlies the Scappoose Formation (Wilkinson and others, 1946). It is grey-black, aphanitic, and vesicular near flow tops (Snavely and Wagner, 1964). Most of the Columbia River basalt has been weathered at the surface to ferruginous bauxite, often containing pisolites. Below the surface the ferruginous bauxite contains angular, broken basalt fragments which appear to grade down gradually to solid rock. In the upper portions of the weathered layer the basalt fragments are commonly completely altered so only relict texture remains. Limonite staining is common (Wilkinson and others, 1946). The groundmass is altered to an orange clay and the feldspar phenocrysts are altered to white clay.

For geophysical modelling the Keasey, Pittsburg Bluff and Scappoose Formations have been grouped together as "sediments", and the Columbia River basalt and Goble Volcanics as "basalt". The Cowlitz Formation can fit into either category depending on its local expression since it contains both sediments and interbedded basalt. The density of the upper Eocene basalts is about 2.8 g/cm^3 (range 2.45 - 2.97); that of the Columbia River basalt is 2.8 g/cm^3

(range 2.31 - 2.98); and the late Eocene to late Oligocene sediments are about 2.4 g/cm^3 (Snavely and Wagner, 1964; Bromery and Snavely, 1964; Pfaff, 1981). Magnetic susceptibility of upper Eocene rocks has been measured as .00046 to .002 cgs units and the Miocene volcanics as .00015 to .002 cgs units. These susceptibilities agree with averages from other sources for basalt, such as .007 (Dobrin, 1976), .006 (Telford and others, 1976) and .0005 to .0017 (Heiland, 1968). Seismic velocities (P wave) are estimated, for local near surface materials, to be about 1830 m/s (6000 f/s) for sediments and about 3050 - 4570 m/s (10,000 - 15,000 f/s) for volcanics (Mike Alger, personal communication, 1982). These values agree with other sources which list 400 - 610 m/s (1300 - 2000 f/s) for clayey soil, 915 - 1800 m/s (3000 - 5900 f/s) for clay and claystone, 1830 - 2440 m/s (6000 - 8000 f/s) for sandstone, and 2750 - 4270 m/s (9000 - 14,000 f/s) for fractured basalt (Redpath, 1973).

Structure

Heavy vegetation and poor exposure limit the quality of the structural interpretation from surface data. The Tillamook Volcanics and northern Coast Range form a northward plunging anticline (or high) with the Eocene sediments deposited around it (Newton and Van Atta, 1976). The Oligocene sediments have been deposited on the eastern side only. The Goble Volcanics also formed a topographic high. Uplift and erosion in the early Miocene produced an

erosional surface with a relief of approximately 100 meters (300 feet) and some gentle folding (Wilkinson and others, 1946; Newton and Van Atta, 1976), which was overlain by the Columbia River basalt flows. Northwest - southeast folds which cross the area are believed to have formed during the time the Columbia River basalt was being laid down (Newton and Van Atta, 1976). Mapped faults are oriented northwest - southeast, east - west, and northeast - southwest (Newton and Van Atta, 1976; Kelty, 1981). Evidence of vertical movement can be found in the field but unequivocal evidence of strike-slip movement has not been found. The principal compressional stress is north - south (Crosson, 1972; Dehlinger and Couch, 1969), and this would favor strike-slip movement on the northeast and/or northwest trending faults.

TECTONIC HISTORY

There are several models of the Mesozoic and Cenozoic history of northwestern Oregon, however much work remains to be done before any one is generally agreed upon. Most researchers agree that the Siletz River - Tillamook Volcanics are oceanic islands which were rafted in by eastward or northeastward moving plates, and collided with the Mesozoic rocks of the North American continent during the Cenozoic era (Dickinson, 1976). A subduction zone was located west of the continental mass, but its location and that of the coastline during the Mesozoic and early Cenozoic are not known. Most hypotheses, however, place the

subduction zone and continental coastline well east of the present southern Washington - northern Oregon coastline (Dickinson, 1976, 1979; Simpson and Cox, 1977; Magill and Cox, 1980; Hamilton, 1978). During the early Eocene the subduction zone moved from east of the present Cascades to the present inner continental shelf of Oregon (Snavely and others, 1980). Paleomagnetic evidence has been interpreted to indicate Eocene and later rotation of the Coast Range - Klamath Mountain block. The oldest rocks of the Coast Range show about $75^{\circ} \pm 17^{\circ}$ clockwise rotation and younger rocks show progressively less rotation. The Goble Volcanic series rotated about $25^{\circ} \pm 13^{\circ}$, but possibly as a separate block (Beck and Burr, 1979). The Coast Range rotation is suggested as a two phase rotation, about $50^{\circ} \pm 15^{\circ}$ during the Eocene (40 - 50 mybp) and about $25^{\circ} \pm 20^{\circ}$ during the Miocene Basin and Range extension (20 mybp). The earlier rotation may have been associated with accretion and/or shear associated with plate movement (Beck and Plumley, 1980; Magill and others, 1981, 1982; Magill and Cox, 1980, 1981; Simpson and Cox, 1977; Hamilton, 1978). The Coast Range does not appear to be an exotic terrane which was rafted in from a great distance as has been proposed for other West Coast terranes (Hamilton, 1978; Jones and others, 1982), but could have been formed nearby. The inclination of the remnant magnetism indicates no detectable northward movement of the block (Beck and Burr, 1979). The current tectonic status appears to be north - south compression with

right lateral movement on northwest trending strike-slip faults due to possible subduction of the Farallon plate. The present location of the subduction zone is not known (Crosson, 1972; Dehlinger and Couch, 1969; Dehlinger, 1969).

METHODS OF INVESTIGATION

LINEAMENT ANALYSIS

Side looking airborne radar (SLAR) (1:250,000), Landsat bands 6 and 7 (1:1,000,000), and high altitude U-2 (1:130,000) photographs were studied for lineaments. A map of the study area with significant lineaments noted is shown in Figure 4. The SLAR provided the best contrast and lineament enhancement. This is due primarily to the low spatial resolution, about 10 meters (30 feet), which acts as a filter to remove vegetation "noise" and enhances the topography (Sabins, 1978, p. 207). The radar look direction is south. Since features perpendicular to the look direction are enhanced and those parallel are subdued, north - south trending lineaments are not obvious. Some east - west artifacts are evident due to image quality and the mosaic process, especially in enlargements, and make special care necessary for recognition of true east - west lineaments.

The Landsat photos lacked contrast and sharpness. Band 6, visible light, and band 7, infrared, were examined. Band 7 was better for lineament analysis and was generally a better image than band 6. Both SLAR and Landsat images were in black and white.

High altitude (U-2) aerial photographs were also

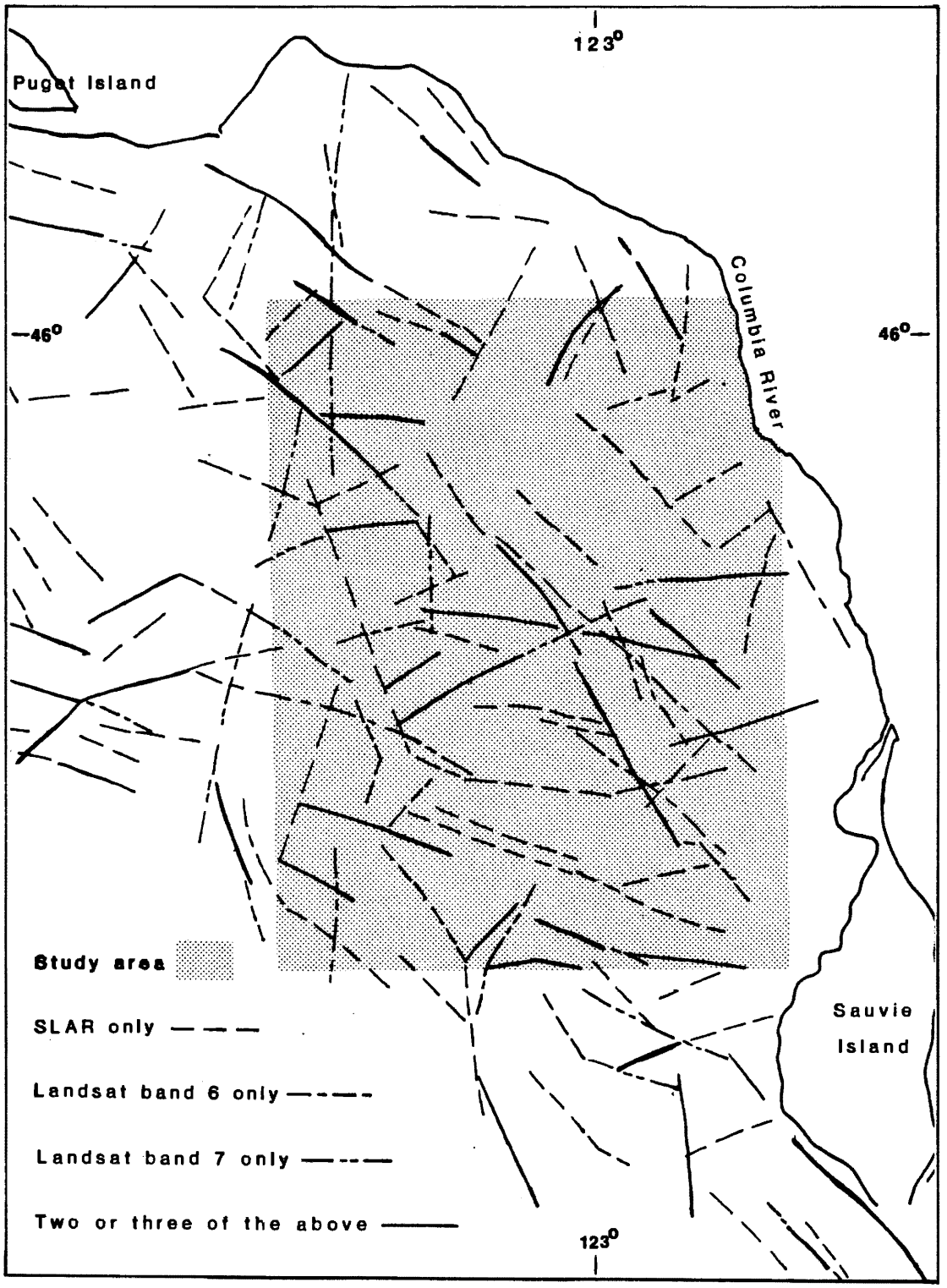

Figure 4. Lineaments in Columbia County, Oregon.

examined for evidence of lineaments along the trend of the Portland Hills fault. The black and white photos were slightly dark but do show the lineaments. Color infrared photos were excellent and show topographic features quite well.

The smaller scale did not allow analysis of lineaments over as large an area as desired and these photographs were used primarily for detail and verification of linear features seen on the SLAR and Landsat photos.

The linear feature selected for study, North Scappoose Creek - Alder Creek - Clatskanie River, is prominent on SLAR, Landsat band 7 and U-2 photos (Figure 5). A small plane flight was also made over the area and the lineament showed up very prominently from 1067 meters (3500 feet), as seen in Figures 6, 7 and 8.

WELL LOGS

Lithologic and electric logs from deep oil and gas wells, and driller's logs for water wells in the area were examined. The deep wells are all located west of the study area and show thick sedimentary sequences, intercalated in some cases with the Goble Volcanic Series. Water wells are scattered throughout the area with depths varying from 15 meters (50 feet) to 183 meters (600 feet). Many water wells penetrated basalt and almost all were drilled through 3 to 46 meters (10 to 150 feet) of clay before hitting "broken rock" (weathered basalt?), sandstone or "shale" (mudstone?).

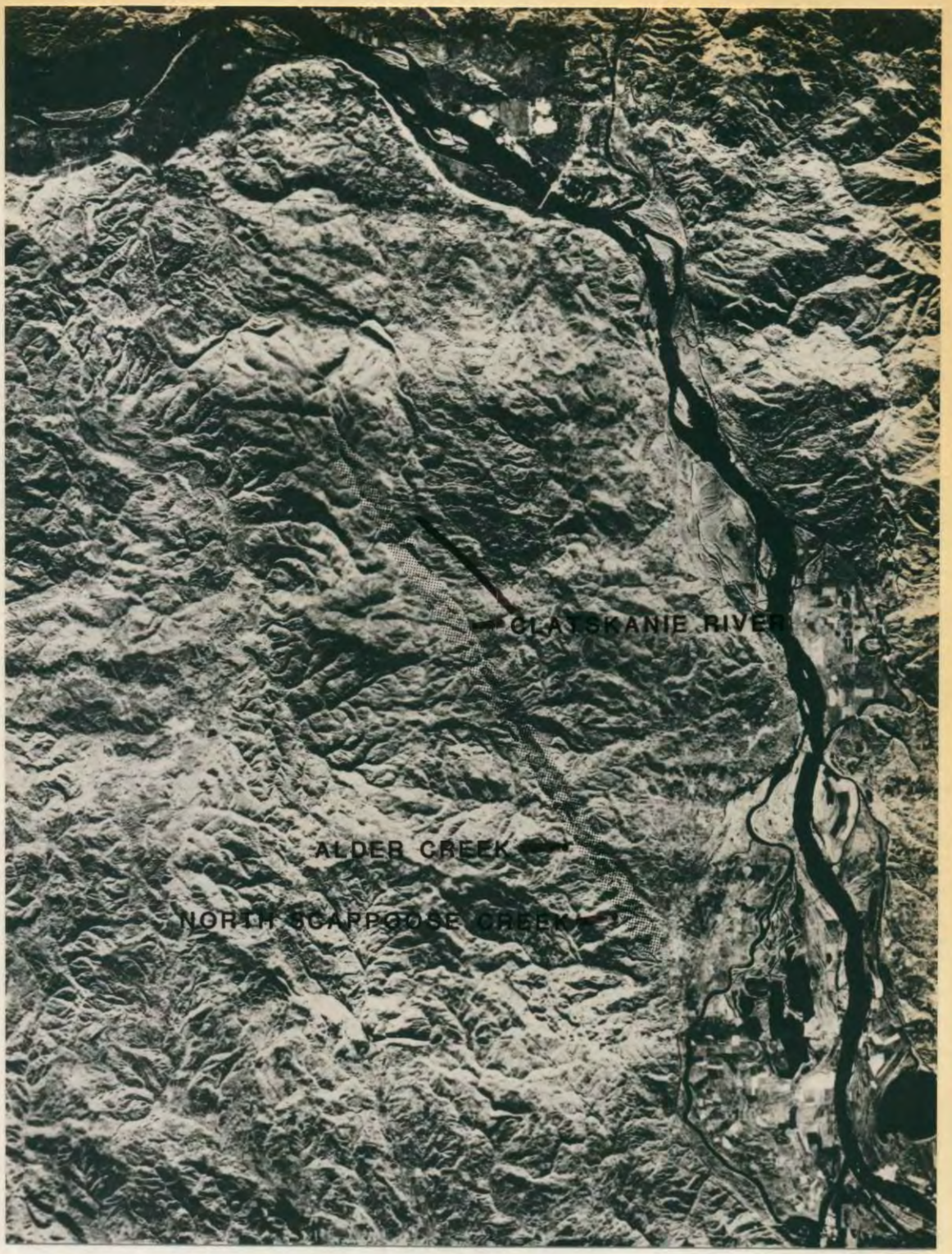

Figure 5. North Scappoose Creek - Alder Creek - Clatskanie River lineament (SLAR).

Figure 6. Lineament, North Scappoose Creek - Alder Creek (photo).

Figure 7. Lineament, Clatskanie River (photo).

Figure 8. Lineament north of Apiary - Oak Ranch Road (photo).

The basalt ranges from very thin (2 or 3 meters) in the southeastern part of the area to sixty or more meters in the northeast. Very few of the water wells were drilled through the basalt so there is only scattered data on the depth of the bottom of the Columbia River Basalt. The lack of good lithologic descriptions and imprecise locations are major drawbacks to depending on this data. Well data used in modelling is listed in Appendices A and D.

GRAVITY

Purpose

A gravity survey was conducted to gather information for structural modelling of the area. The northwest trending lineaments along North Scappoose Creek, Alder Creek, the Clatskanie River (Shaffer Road), and the Little Clatskanie River were chosen for geophysical study (Figure 5). These lineaments follow the trend of the Portland Hills fault and have roads crossing them perpendicular to their trend. Three lines were run to give coverage over an area 16 kilometers (10 miles) along the lineament trend and 16 to 24 kilometers (10 to 15 miles) perpendicular to it, or approximately 325 square kilometers (125 square miles). The lines extend several kilometers beyond the lineaments both east and west to avoid the influence of edge effects on the modelling. The density contrasts found through the gravity modelling process should show the faulting, if it exists, as basalt (~ 2.8 g/cm^3) is juxtaposed against sediments

($\sim$2.4 g/cm^3). A total straight line distance of 60 kilometers (37.5 miles) of gravity line was run.

Field Procedure

The three gravity lines chosen are described in the Location section. A straight line was drawn on the map approximately perpendicular to the lineament trend from one end of the line to the other, and distances between gravity stations were scaled off on the straight line and projected onto the roads. The road distance between stations is therefore variable. Gravity stations on the Spitzenberg line are spaced 0.16 kilometer (0.1 mile) apart for about 4 kilometers (2.5 miles) on either side of the North Scappoose Creek - Alder Creek lineament. For 1.5 kilometers (1 mile) beyond this the spacing was spread to 0.32 kilometer (0.2 mile), and finally 0.8 kilometer (0.5 mile) for a total straight line of 16 kilometers (10 miles). Gravity was tied to the Portland State University base station. In the field, the stations were tied to a station at the Spitzenberg junction approximately every two hours. This allowed a drift curve for the gravimeter to be established. Three readings were taken at each station and averaged. The station locations and elevations were surveyed using a theodolite and stadia rods and tied at the eastern end to benchmark E204 (USC&GS) at the Yankton school yard. No other benchmarks were available along the line or at the western end to tie into (Figure 2). Gravity data is in

Appendix A.

The Apiary line crossed two strong lineaments, the Clatskanie River - Shaffer Road and the Little Clatskanie River (Figure 2). Due to the wider area to be covered the gravity stations were spaced at 0.32 kilometer (0.2 mile) for about 10 kilometers (6.3 miles) across the lineament zone, widening to 0.8 kilometer (0.5 mile) for 5 kilometers (3 miles) on either side of the zone, and 1.6 kilometers (1 mile) apart at the east end for a straight line of 24 kilometers (15 miles). This line was read in several segments; each segment tied to the Portland State University base station, and the field stations were tied to an anchor station on the line every two hours to establish gravimeter drift. The station locations were surveyed with a theodolite and stadia rods, and one section with an Electronic Distance Meter (EDM), to establish elevations. The surveying was tied on the eastern end to benchmark V305 (OSHD) at the bridge over Tide Creek on U.S. Highway 30. No benchmarks were available along the line or near the west end, however the west end intersection map elevation was used as a crude guide and agreed with the surveyed elevation (Figure 2).

On the Pittsburg-Yankton line, gravity was read at established benchmarks only. The purpose of this line was to fill in between the Spitzenberg and Apiary lines and more frequent readings were not deemed necessary. The line was tied to the Portland State University base station but

intermediate repeated readings at a station on the line were not made. The line was tied to benchmark E204 (USC&GS) at Yankton school on the east end, and benchmark A205 (USC&GS) at the bridge over the east fork of the Nehalem River on Highway 47 on the west end. The straight line length is 21 kilometers (13 miles) (Figure 2).

Regional Trend

Complete Bouguer gravity anomaly values in northwestern Oregon generally decrease from zero at the Oregon Coast to -80 to -100 at the Cascade Range (Bromery and Snavely, 1964; Berg and Thiruvathukal, 1976b). There is a high over the Tillamook Highlands (+60 mgal), a low in the Tualatin Valley (-60 mgal), and a fairly steep north - south trending gradient from Longview, Washington, through central and western Columbia County, western Washington County and continuing south. A high from the Willapa Hills of southwestern Washington projects into northern Columbia County near Clatskanie (Figure 9).

The Apiary and Pittsburg-Yankton lines cross the eastern part of the north - south gradient, and the Spitzenberg line is in an area of constant anomaly. Regional anomaly values across the gravity lines range from -15 mgal to -38 mgal. The complete Bouguer gravity anomaly contours from this study's data are discussed in the chapter on Modelling.

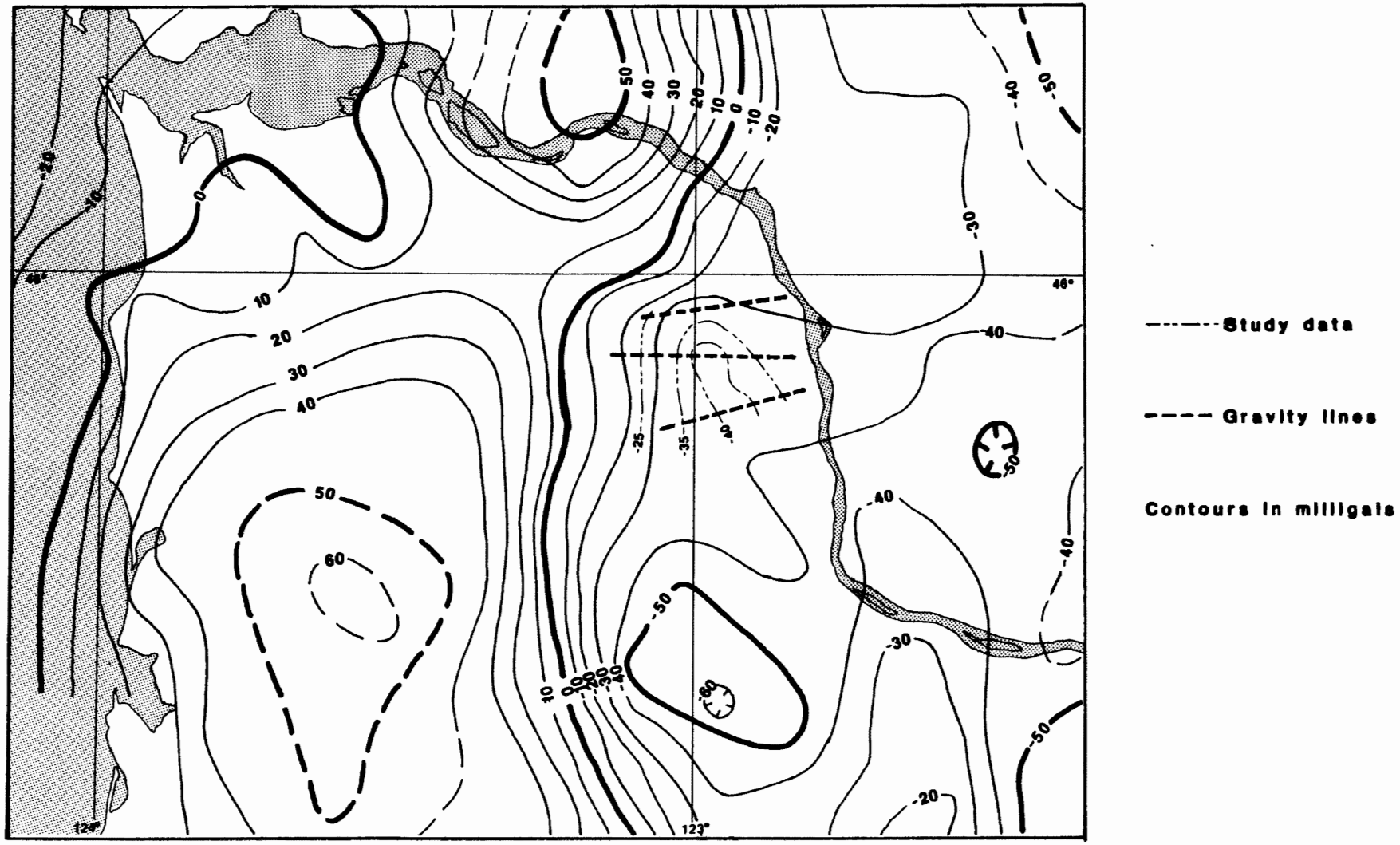

Figure 9. Regional Bouguer gravity map (from Berg and Thiruvathukal 1967, and Bonini and others 1974).

Data Reduction

Gravity readings must be corrected for 1) instrument drift, 2) earth tides (due to the gravitational attraction of the sun and moon), 3) latitude, 4) elevation, and 5) the surrounding terrain. The distance from the equator (latitude) must be corrected for since the earth is a rotating ellipsoid, bulging at the equator, which results in the attraction of gravity increasing toward the poles. The elevation correction is composed of two parts, free-air and Bouguer. The free-air correction accounts for the differences in gravity due to changes in elevation. The surveyed elevations and a sea level datum were used. Differences in mass between the gravity station and sea level are accounted for by the Bouguer correction. A density of 2.67 g/cm^3 was used for the Bouguer correction to correct for the mass between the station and sea level. Terrain corrections compensate for the decreased gravitational attraction due to hills above the station pulling upward and the decreased gravitational attraction due to valleys (lack of mass) surrounding the gravity stations. This correction was done with Hammer charts, by hand for rings C through G, using 7½' topographic maps and tables in Dobrin (1960), corrected for 2.67 g/cm^3 density. Terrain corrections from ring H out to 167 kilometers were done by computer by Northwest Geophysical Associates. Elevations for gravity stations were taken from the topographic maps. Standard correction formulas from Telford and others (1976) and Dobrin (1960),

and the computer program used to determine station elevation from survey data, are in Appendix A. Gravity meter readings are convertible to relative gravity but must be referenced to a known base station to obtain observed gravity values. The base station established at Portland State University's Geology Department office is the reference with an absolute gravity of 980641.35 mgal. Most corrections to gravity data were done by computer by Northwest Geophysical Associates.

Equipment Used

Worden Gravity Meter, Model III (Master), No. 575; sensitivity - .10374 mgal/scale division (loaned by Oregon State University).

Wild T2 theodolite.

Topcon DMS-1 Electronic Distance Meter (rented).

Stadia rods (Philadelphia rods).

REFRACTION

Purpose

Seismic refraction lines were run across the lineaments to look for near surface (0 to 60 meters) evidence of faulting. Displacements may not be visible on the surface but if there had been recent activity on the faults displacements of sediments and basalt should be evident at shallow depths. Cross-sections drawn from the time-distance curves would show any near-surface faulting.

Field Procedure

Refraction lines were run on isolated dirt or gravel roads as close to the gravity lines as possible. This eliminated vehicle noise and vibration, and in most instances avoided road fill. The locations of the three lines are shown in Figures 2, 10 and 12, and described in the Location section. The refraction lines were reversed. The energy source was a 300 or 500 pound weight dropped from the Oregon State University thumper tripod a distance of about three meters (nine feet) onto a steel plate on the ground.

The Bunker Hill Road line is about 4.5 kilometers (2.8 miles) northwest of the Spitzenberg junction and 3.5 kilometers (2.2 miles) southeast of the Wilark junction on the Pittsburg-Yankton line (Figures 2 and 10).

Bunker Hill Road is a dirt road without a rock base. The refraction line runs 2200 feet (670.6 meters) east and west of the Bunker Hill Road - Wilark 247 Road junction, along Bunker Hill Road, for a total length of 4400 feet (1341 meters). One line of 12 geophones was run with 20 foot (6.1 meter) phone spacing to determine the velocity of the weathered or surface layer. The rest of the reversed lines had 50 foot (15.2 meter) geophone spacing and were shot with double coverage at the 1100 foot (335.3 meter) distances. Figure 11 shows a typical layout. A 300 pound weight was used for 550 foot (167.6 meter) lines and a 500 pound weight for the 1100 foot (335.3 meter) lines.

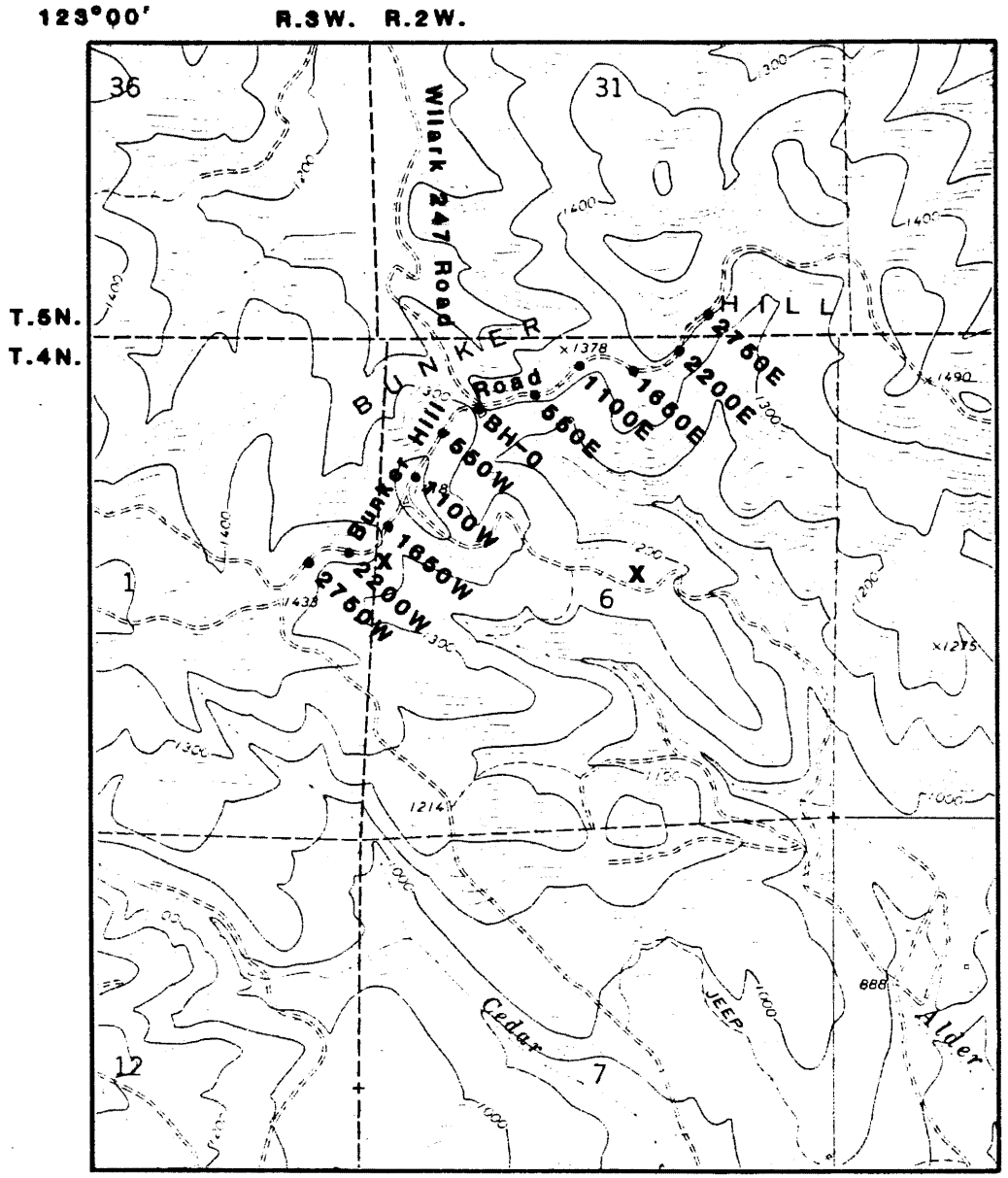

• Refraction station

X Water well (approx.)

Figure 10. Bunker Hill refraction line (from USGS 7½' Chapman quadrangle map, 1971).

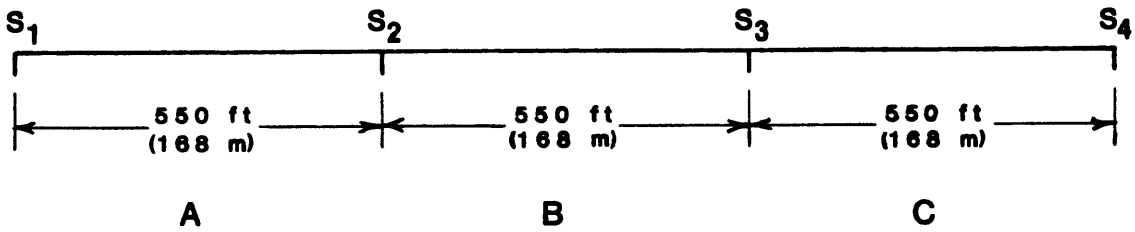

Figure 11. Typical refraction line layout.

For example, line A was thumped with 300 pounds at S_1 and S_2, line B with 300 pounds at S_2 and S_3. and line C with 300 pounds at S_3 and S_4. The 1100 foot (335.3 meter) line AB was thumped with 500 pounds at S_1 with geophones at B and with 500 pounds at S_3 with geophones at A. The line BC was similarily thumped at S_2 and S_4, so the B section is covered twice. This continued down the total length of the line. The refraction data for this line is in Appendix B.

The Shaffer Road line parallels (within 0.1 mile) the Apiary-Oak Ranch Road for approximately 3800 feet (1158 meters), then follows the Apiary Road east for another 600 feet (183 meters) from the Shaffer Road - Apiary Road junction (Figures 2 and 12). One line with 20 foot (6.1 meter) geophone spacing was run to determine the surface layer velocity. The entire 4400 foot (1341 meter) line was run with 50 foot (15.2 meter) spacing in the same manner as the Bunker Hill line, however two sections of 1100 foot (335.3 meter) line were not reversed due to operator error.

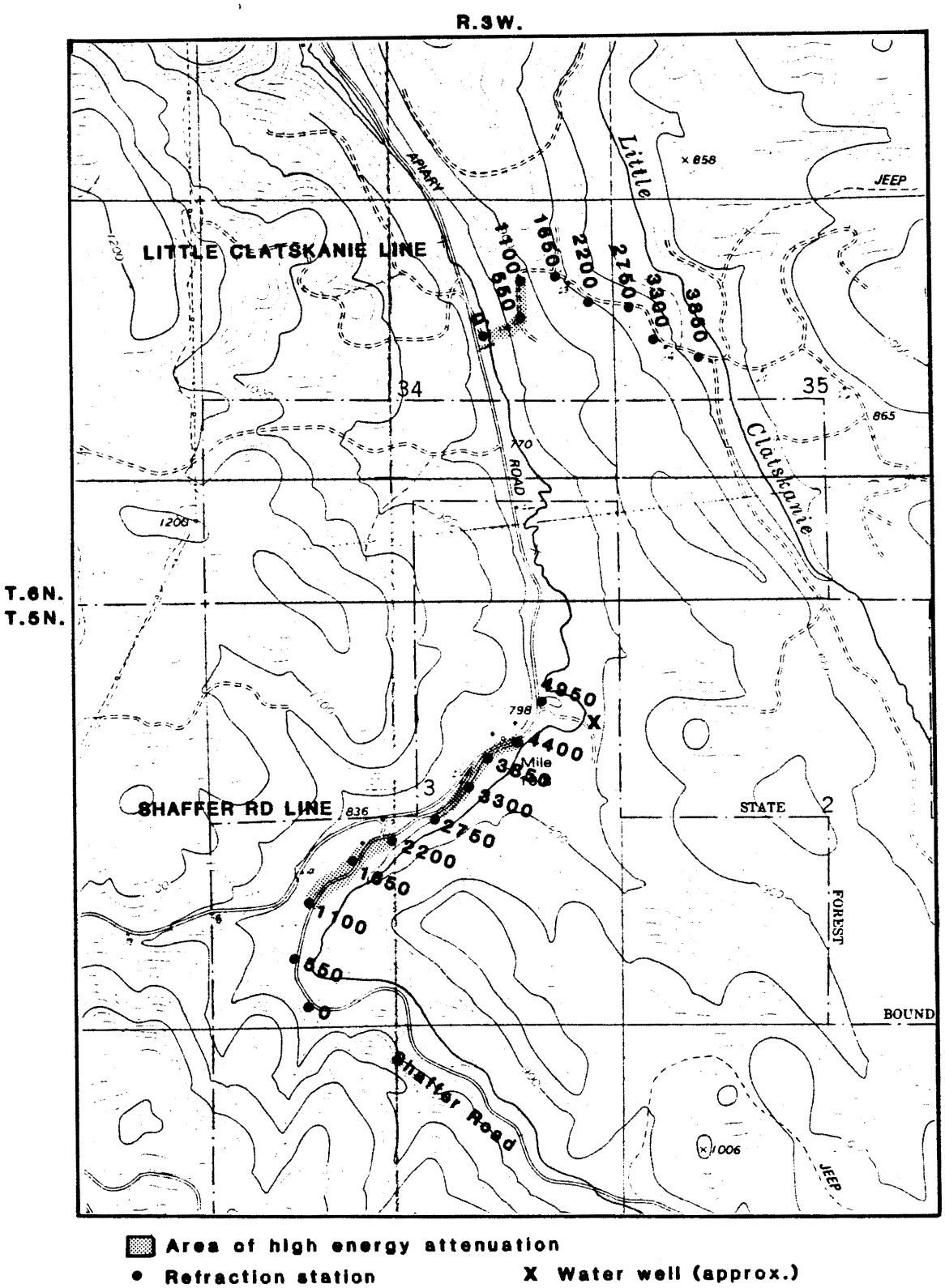

Figure 12. Shaffer Road and Little Clatskanie River Road refraction lines (from USGS 7½' Baker Point quadrangle map, 1979).

They were not shot at a later time because the 1100 foot (335.3 meter) records were so poor on this line that it was felt no additional information would be gained from them. Shaffer Road is gravelled and the Apiary Road is paved. The refraction data for this line is in Appendix B.

The Shaffer Road line could not extend across the entire Clatskanie River - Little Clatskanie River lineament zone because of restricted access, so a section was offset north 1.5 miles (2.4 kilometers) and continued east for 3300 feet (915 meters) along the Little Clatskanie River Road, which is a gravelled logging road. The technique was the same as the other lines except that no line with 20 foot (6.1 meter) spacing was run (Figures 2 and 12). The refraction data for this line is in Appendix B.

Data Reduction

The first break of each geophone trace on a record was picked and the time vs. distance graphed. (The seismic record has time lines spaced 100 ms apart). Straight line segments were fitted to the data points, and the velocities, depths, and dips for the different layers determined by standard formulas in Dobrin (1960), Nettleton (1940), Ewing and others (1939), Mota (1954) and Heiland (1968). Corrections for elevation changes along the lines were made according to Nettleton (1940, p.266). Formulas used are shown in Appendix B, with the data.

Equipment Used

SIE recording amplifier, Model RA-44, 12 channels.

SIE recording oscillograph, Model R-4.

Mark Products 7½ Hz geophones.

Thumper trailer with 300 pound and 500 pound weights, loaned by Oregon State University.

MAGNETICS

Purpose

Magnetics lines were run to complement the near-surface refraction data. The different magnetic susceptibilities of basalt and sediments should be evident if faulting has displaced blocks of either type of rock. These anomalies should show up in a cross section drawn from magnetic anomaly data.

Field Procedure

A magnetic survey was run along the same lines as refraction. Readings were taken every 30.5 meters (100 feet) with a total field nuclear precession magnetometer. The distances were paced. Readings were repeated at each station three times, or until three readings were obtained with no more than one gamma variation. A station at the center of the line was read at the beginning and end to establish drift.

Data Reduction

The readings at each station were averaged and plotted against distance, at the same distance scale as the refraction plots (See figures 26, 28 and 30). No drift corrections were made since total variations over an entire day were no more than 20 gammas. No other corrections were made. Data is in Appendix C.

Equipment Used

Geometrics G816 Magnetometer.

MODELLING AND RESULTS

The three types of geophysical data have been modelled and interpreted separately. They are compared and integrated in the section on Discussion and Conclusions.

GRAVITY

General

The gravity method measures differences in the earth's gravitational acceleration. Differences in the measured values, after corrections, indicate lateral changes in the densities of the subsurface rocks. The acceleration of gravity at the earth's surface is about 980 cm/s^2 or 980,000 milligals. Variations as small as one part in 10^8 are measured in gravity prospecting. Interpretation of gravity data requires some familiarily with the regional geology which can be used to establish "reasonable" limits on possible depths and density contrasts. Since the anomalies (variations in density) of interest in the study area are near-surface and partly above sea level, all modelling and most interpretation has been done with the free-air anomaly values.

Determination of the density of subsurface rocks is difficult and may vary within a formation or type of rock. Thus a density of 2.8 - 2.9 g/cm^3 for basalt is the average

of a range from 2.7 to 3.3 g/cm^3, although the values within one formation would not necessarily vary this amount. Variables affecting the density ranges for igneous and sedimentary rocks include grain type, size, shape and sorting, depth of burial, age, and porosity. Weathering usually lowers the density of rocks. The density of igneous rocks increases with a decrease in silica content, for example, rhyolite averages 2.5 g/cm^3 and basalt averages 2.9 g/cm^3. For gravity modelling in this study, the following density averages have been assumed: basalt 2.8 - 3.0 g/cm^3, post Eocene sediments 2.4 g/cm^3, Eocene sediments and interbedded volcanics 2.5 g/cm^3, silicic volcanics 2.3 - 2.6 g/cm^3 (Snavely and Wagner, 1964; Hammond, 1980; Telford and others, 1976), alluvium, unconsolidated sand and gravel 2.0 g/cm^3 (Heiland, 1968; Telford and others, 1976). These values are similar to those used by Pfaff (1981), Jones (1977) and Perttu (1980).

Assumptions made in modelling include 1) the "average" density is representative of the rock type or formation, 2) gravity can be modelled in two dimensions, i.e., modelled as two dimensional blocks with the third dimension infinite, 3) the "regional" values from very deep structures do not mask local anomalies, and have not been removed. Modelling was not extended deeper than six kilometers since there is no geologic information readily available that would allow reasonable assumptions of rock type below that depth.

Modelling was done on the Portland State University Honeywell computer using the program FREEAIR. This program was adapted from Oregon State University programs by Terry Jones (1977). A program listing is included in Appendix A.

Regional Models

The trends of the Apiary and Spitzenberg gravity lines were extended approximately 75 kilometers (47 miles) west (to the Oregon coast) and 100 kilometers (63 miles) east (to the vicinity of Swift Reservoir) (Figure 13) to allow regional modelling and eliminate any influence of the edge of the model on the actual gravity lines being studied. The "edge effect" is the effect of the density contrast between the model and air at the ends. This has an overwhelming influence on the anomaly amplitude since it is a contrast of 2.4 - 2.8 g/cm^3 (to zero for air), compared with density contrasts of 0.2 - 0.5 g/cm^3 within the model. Oregon free-air gravity values were taken from the Free-Air Gravity Anomaly Map of Oregon (Berg and Thiruvathukal, 1967a). Free-air values for Washington were not available so complete Bouguer values (Bonini and others, 1974) were used with the Bouguer correction added back into the anomaly values. Elevations were determined from a 1:500,000 topographic map. These free-air values are only approximate but adequate for the general regional model. Modelling was begun using known densities, depths and locations of formations and available cross sections and well data.

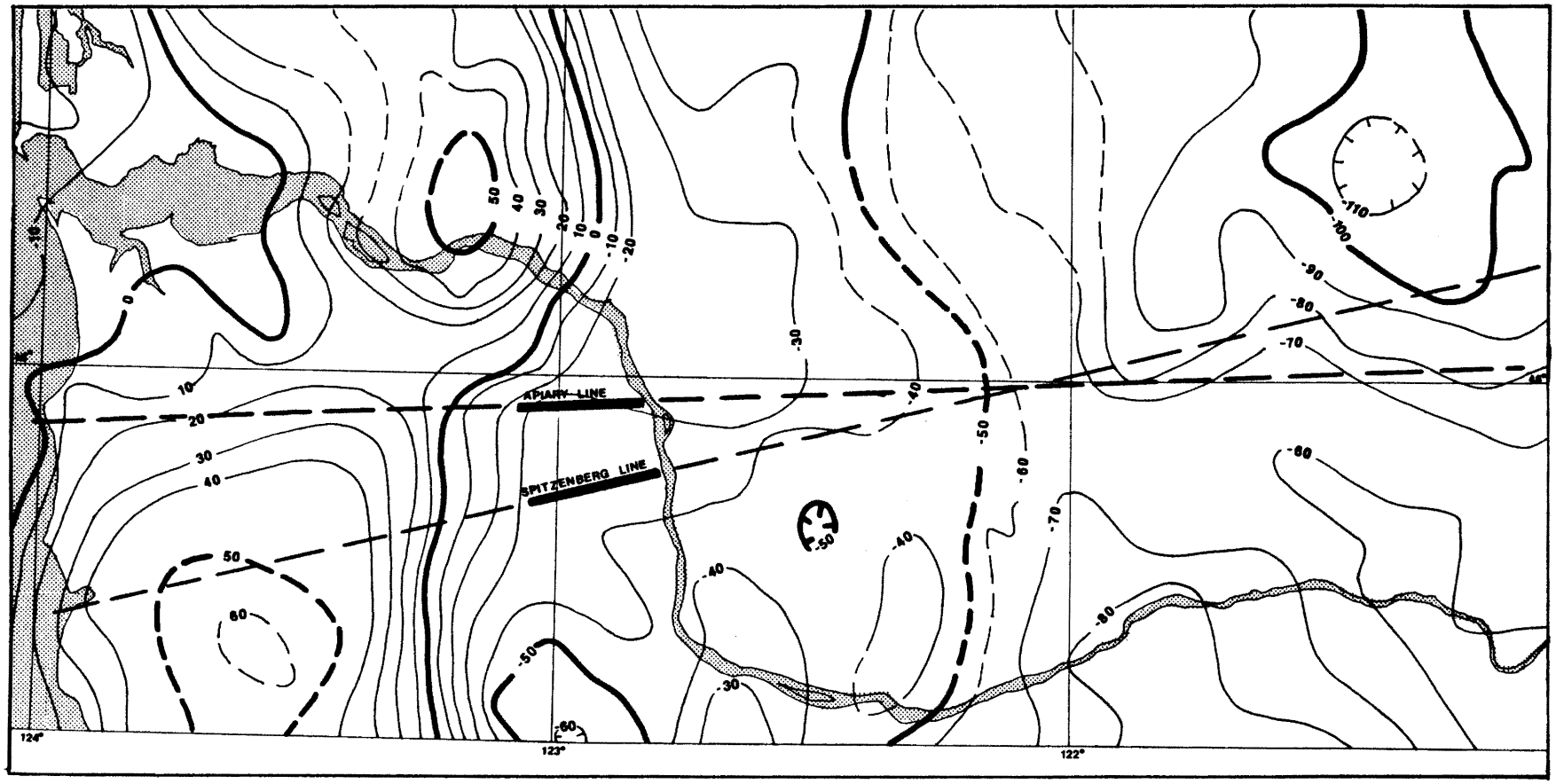

Figure 13. Location of regional gravity models (from Bonini and others 1974).

The Apiary regional free-air gravity model (Figure 14) has approximately one kilometer (3000 feet) of 2.4 g/cm^3 sediments on top of 2.8 g/cm^3 igneous rocks, probably basalt, in the west. The Nehalem Valley to Lake Merwin section of the model consists of 600 meters (1800 feet) of 2.4 g/cm^3 sediments above 2.5 g/cm^3 sediments, with a block of 2.7 g/cm^3 rock, probably igneous, about four kilometers (12,200 feet) deep at the east side. The Washington Cascade volcanics model as a block of 2.3 g/cm^3 material 1.5 kilometers (4575 feet) deep, with 2.5 g/cm^3 material below it.

The 2.4 g/cm^3 sediments in the western and central sections are the post Eocene Keasey, Pittsburg Bluff and Scappoose Formations, above Tillamook Highlands volcanic rocks on the west, and above Cowlitz Formation in the central section. The block of 2.7 g/cm^3 material may be Goble Volcanics or a local eruptive center of similar age. This block was necessary to bring the model into agreement with the regional anomaly values (Figure 14). The Washington Cascades area is less well known stratigraphically but the 2.3 g/cm^3 and 2.5 g/cm^3 values fit the brecciated, tuffaceous and volcaniclastic nature of the Ohanapecosh Formation. Rock types below this formation are not known but model with a similar density of 2.5 g/cm^3.

The Spitzenberg regional free-air gravity model is generally similar to the Apiary regional model (Figure 15). The Tillamook Highlands in the west have no sediments on top, and the igneous rocks model with a density of 2.9 g/cm^3.

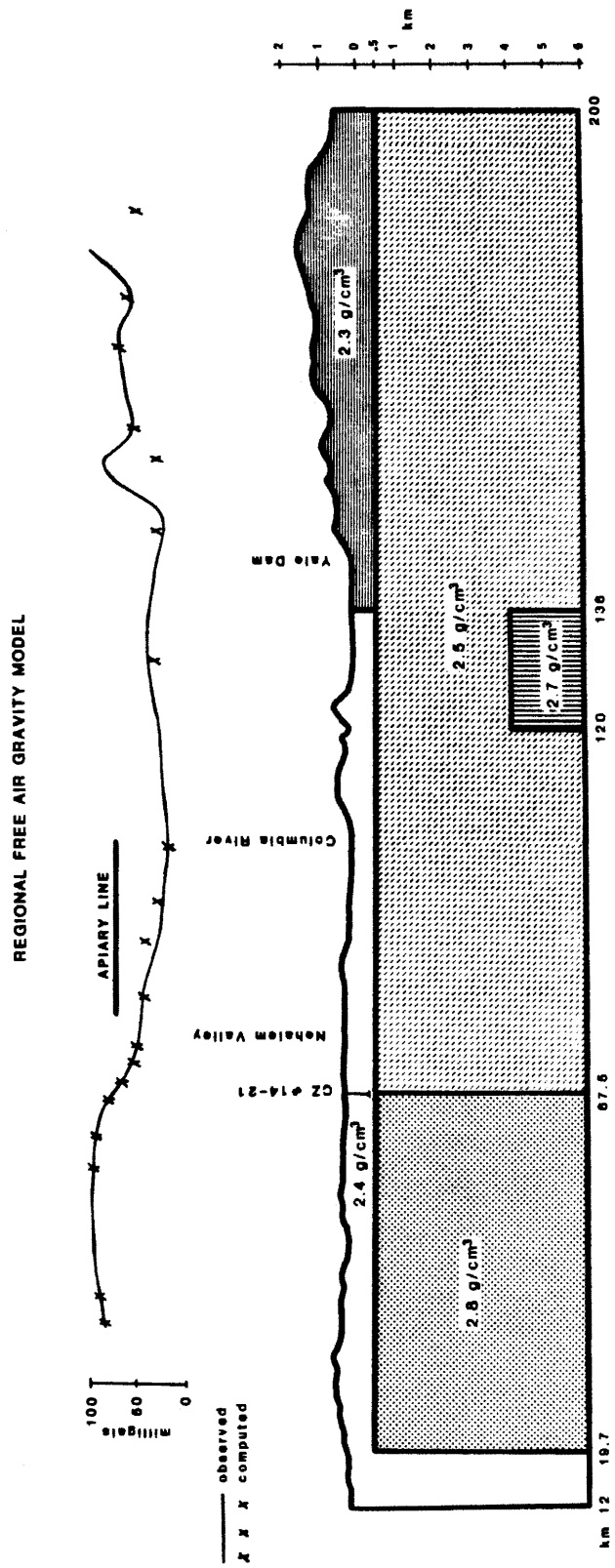

Figure 14. Apiary regional gravity model.

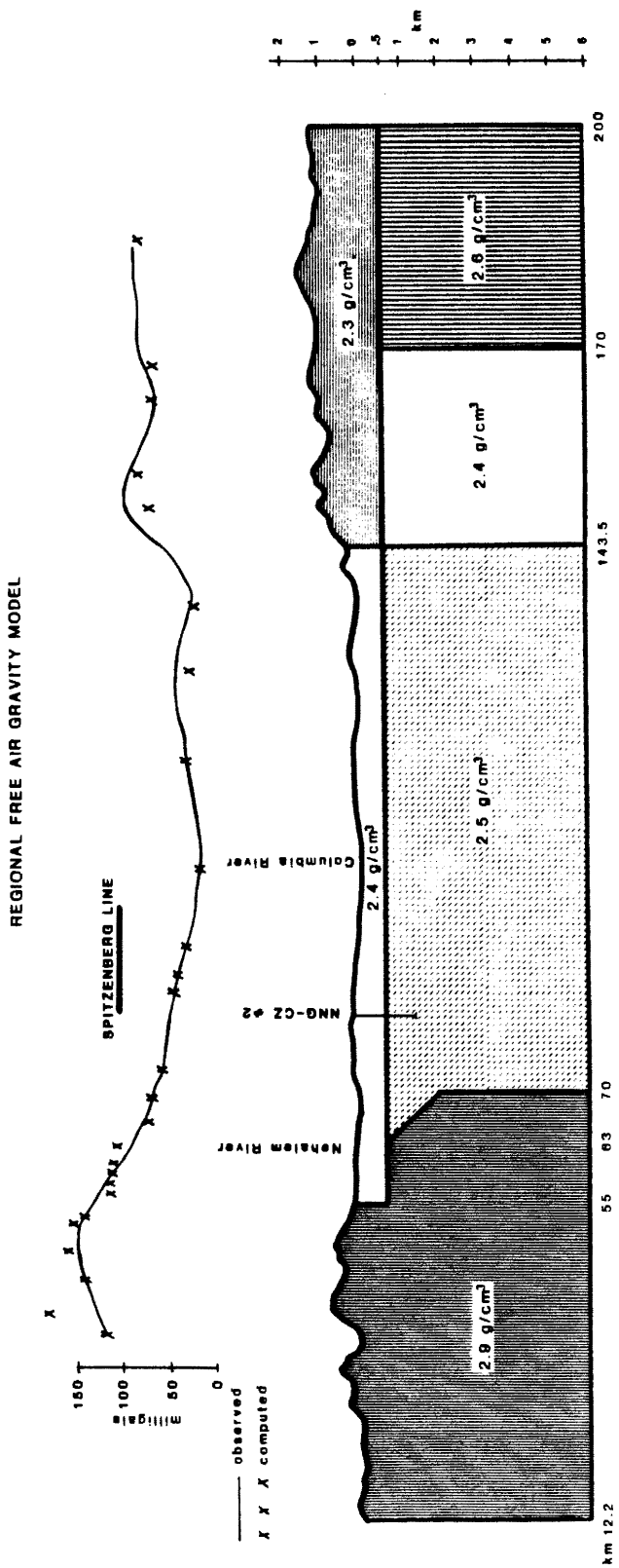

Figure 15. Spitzenberg regional gravity model.

Sediments lap onto the igneous rocks on the east side of the Tillamook Highlands and continue across the center section. Onlap of both Eocene (Cowlitz) and post Eocene sediments was necessary for the model to fit. The eastern section of the model, in the Washington Cascades, is again lower density volcanics with those below increasing in density to the east. The deeper 2.7 g/cm^3 block in the central section of the Apiary model is not necessary to model this line.

The regional view for both models is quite similar, especially in the sections where the local gravity lines were run, indicating that differences between the local lines are due to near-surface contrasts and not an abrupt, deep-seated, area wide change. Both lines appear to be in deep sediments at the edge of the Tillamook Highlands. Pfaff's (1981) gravity models across the Coast Range are similar to the models used here.

Local Models

Modelling of the local lines began with the addition of the measured gravity values to the regional values, and reduction of the area modelled to slightly larger than the measured line itself. The regional model was used at first and changes made to bring the model into agreement with the observed free-air gravity anomaly values. The local changes should not affect the regional model extending out from the ends of the gravity lines if the regional models are reasonably correct. Locations of the Apiary and Spitzenberg

gravity lines are shown in Figures 2 and 13.

The Apiary gravity line modelling began with a known block of Goble Volcanics on the east end, and observation of the location of surface outcrops of basalt and sediments along the line (Figure 16). The modelled blocks of basalt are quite irregular along their lower surfaces. Underlying sedimentary highs occur at 94.6 kilometers, 87 - 88 kilometers, and at 81 kilometers along the line. The thick, high density (2.9 - 3.0 g/cm^3) blocks required to model the west end of the line are an artifact caused by the nearby attraction of the Tillamook Highlands block to the southwest. Well data from about eight kilometers west of the end of the line indicate sediments at least 550 meters deep. Relatively accurate modelling can only be done east of 79 - 81 kilometers. A block of lower density material, about 100 meters (300 feet) deep, has been modelled from 88 - 89 kilometers, and may be weathered or less well consolidated sediments.

The Spitzenberg gravity line, when matched to the regional model, fit well in the west where sediments are seen in outcrop, but had a large anomaly at the center of the line (Figure 17). The anomaly at the east end modelled well with a basalt block thickening to the east. It thins somewhat in the center indicating a possible sedimentary high. The central anomaly was modelled with a block of low density (2.0 g/cm^3) material which extends thinly west along a stream valley. This block is about 700 meters (2100 feet)

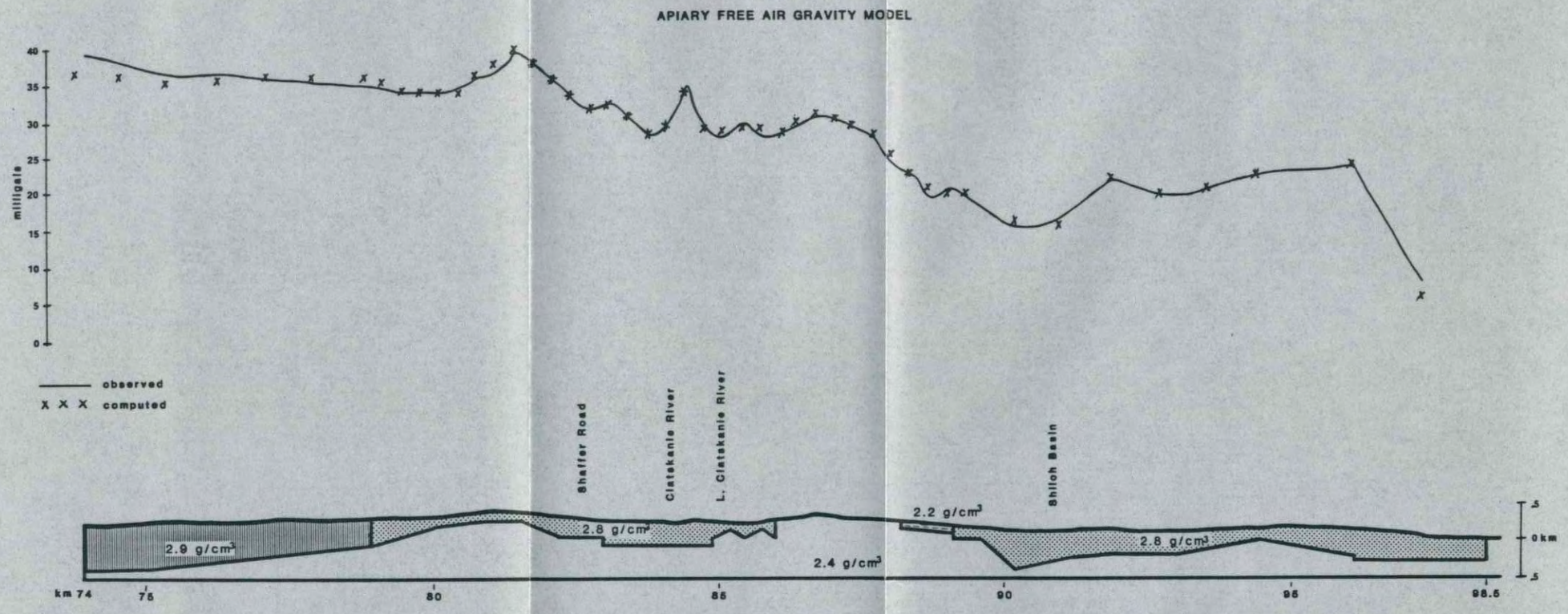

Figure 16. Apiary local gravity model.

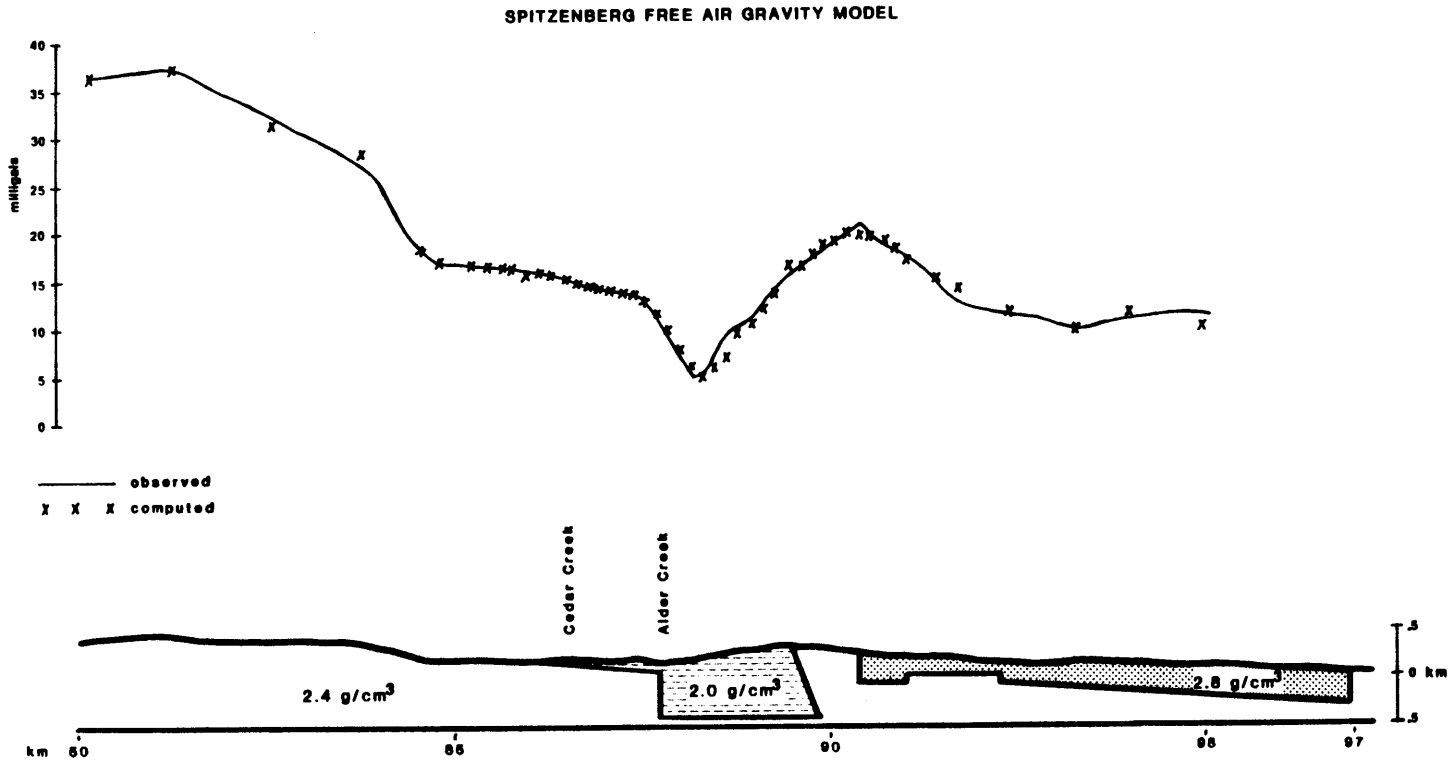

Figure 17. Spitzenberg local gravity model.

deep and two kilometers (6100 feet) wide. The low density material could be unconsolidated sand or clay, gravel, or some other poorly consolidated, or broken up, rock. It begins at the North Scappoose - Alder Creek lineament and extends east for two kilometers (6100 feet). This anomaly could also be modelled by a series of deeper and thinner blocks of the same material.

Comparison

Both the Apiary and Spitzenberg gravity models have blocks of 2.8 g/cm^3 density basalt in the eastern third of the model, thickening to the east. The thicknesses of the basalt blocks are similar with a more irregular lower surface on the Apiary model. Both lines generally fit the regional model of deep (6 kilometers) sediments in this area, but the central and western parts of each model differ. The Apiary model has sediments to the surface in the central part with a thin (200 - 300 meters) layer of 2.8 g/cm^3 basalt extending to the west. The Spitzenberg line has a section of low density material in the center and sediments to the west. Both models indicate a sedimentary high, with basalt to the east, with more basalt deposited to the west in the north but not in the south.

A contour map of complete Bouguer gravity values (Figure 18) using the Apiary, Pittsburg-Yankton and Spitzenberg gravity data (Table I) indicates an area of higher gravity anomaly (more dense material) in an arc,

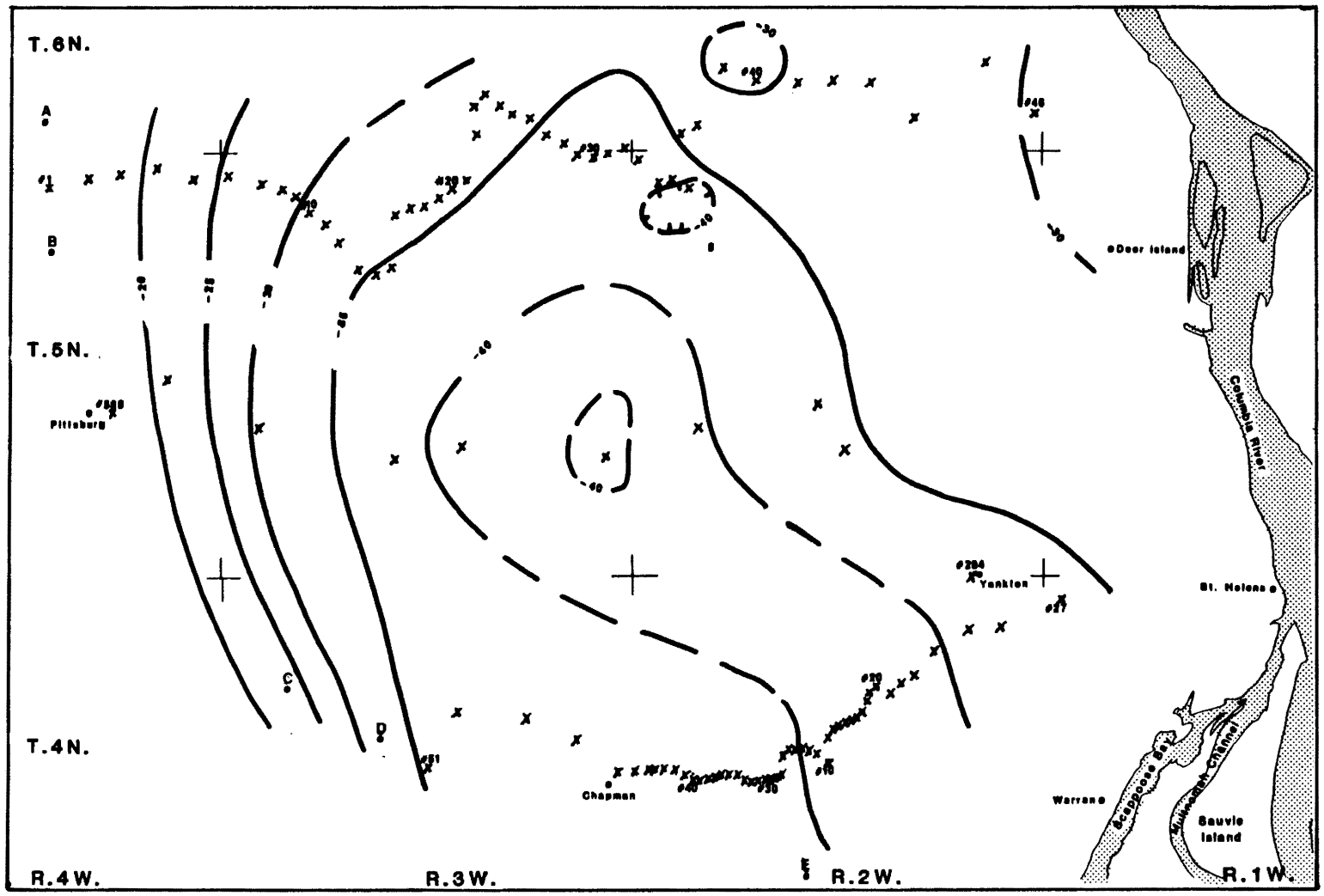

Figure 18. Bouguer gravity anomaly contour map.

TABLE I

COMPLETE BOUGUER GRAVITY ANOMALY VALUES FOR APIARY, PITTSBURG-YANKTON AND SPITZENBERG GRAVITY LINES

(East to West)

Apiary Line		Apiary Line		Pittsburg-Yankton Line		Spitzenberg Line		Spitzenberg Line		OSU Stations (north to south)	
Station	Anomaly	Station	Anomaly	Station	Anomaly	Station	Anomaly	Station	Anomaly	Station	Anomaly
46	-29.3	16	-34.9	BM284	-37.2	27	-36.0	34	-38.4	A	-12.2
45	-32.0	15	-35.6	BM277	-35.7	26	-37.9	35	-38.2	B	-13.5
44	-33.5	14	-35.8	BM439	-37.8	25	-38.5	36	-38.2	C	-23.8
43	-32.6	13	-34.6	BM848	-40.1	24	-40.5	37	-38.1	D	-31.0
42	-31.3	12	-33.2	BM1005	-38.9	23	-41.4	38	-37.9	E	-38.9
41	-32.5	11	-32.0	BM1683	-42.5	22	-41.1	39	-37.7		
40	-28.8	10	-30.8	BM1751	-39.3	21	-42.0	40	-37.5		
38	-30.2	9	-29.3	BM1403	-31.5	20	-43.2	41	-37.2		
37	-34.4	8	-28.4	BM855	-21.4	19	-43.7	42	-36.7		
36A	-34.4	7	-27.9	BM586	-16.4	18	-44.1	43	-36.8		
36	-40.3	6	-26.4			17	-44.0	44	-37.0		
35	-39.5	5	-23.7			16	-44.2	45	-36.4		
34	-39.5	4	-20.4			15	-43.9	46	-36.1		
33	-38.6	3	-19.4			14	-44.1	47	-36.3		
32	-38.4	2	-16.9			13	-44.2	48	-38.7		
31	-38.4	1	-13.8			12	-44.1	49	-38.2		
30	-38.7					11	-44.3	50	-37.2		
29	-38.0					10	-43.1	51	-36.2		
28	-37.3					9	-42.2				
27	-36.4					8	-41.1				
26	-34.7					7	-40.0				
25	-34.8					6	-38.8				
24	-33.7					5	-39.3				
23	-31.2					4	-38.8				
22A	-31.5					3	-39.5				
22	-33.3					2	-39.1				
21	-33.4					1	-39.4				
20	-32.2					31	-39.0				
19	-34.8					32	-39.1				
18	-34.8					33	-38.9				
17	-34.6					33A	-38.6				

open to the south, around an area of lower gravity (less dense material). This gives an indication that there is a continuity of features which show up on the models, among the three gravity lines. Four gravity values on the western margin and one on the south edge were added from Oregon State University gravity data to make contouring more accurate.

REFRACTION

General

Interpretation of seismic refraction data is based on Fermat's principle that energy will travel from source to receiver along the path taking the least time, and Snell's Law which states that the sine of the critical angle equals the ratio of the velocities of the materials on each side of an interface. Energy arriving at an interface at the critical angle will travel along the interface. This creates a disturbance in the upper medium generating waves which travel up through the upper medium at the critical angle. The time required for energy to travel from source to receiver gives information on the velocities and general structure of the materials beneath the surface (See formulas in Appendix B).

Several assumptions, or boundary conditions, are made in refraction interpretation. 1) The velocity of each successively deeper layer of material is greater than the layer above it. 2) The velocity is constant within each

layer (isotropic). 3) Each layer is sufficiently thick to be seen by refraction. 4) The interface between layers can be approximated by a plane.

Increasing velocity with depth is a necessary assumption since energy travelling from a faster to a slower layer will be refracted down through the slower layer. Thus a slower layer beneath a faster layer will not be seen in a time-distance plot, and the next high velocity layer will appear deeper than it really is. This assumption is reasonable since sediments compact with burial, and the deeper, less porous sediments will have a higher velocity than the shallower ones. Weathering also reduces velocity which results in an increase of velocity with depth. In the study area sediments lie above and below basalt. The sediments below the basalt generally will not show up on time-distance plots because they should have a slower velocity than the basalts.

Constant velocity within each layer is often not an accurate assumption. A linear increase of velocity with depth, as in sediments being compacted, will show on the time-distance plot as a curved line. Usually the average velocity over the interval being investigated is used and provides an adequate approximation of the actual conditions. Velocity may also vary laterally within a layer but is usually averaged out over the length of the total refraction line (Dobrin, 1976; Redpath, 1973).

The minimum detectable thickness of a layer depends on the velocity and thickness of the layers above and below it. Thin layers of sediments or basalt will not show up on the time-distance plots. Redpath (1973) describes a procedure for determining this value. Well logs and bore hole data are indispensable here.

Many interfaces between layers are non-planar and surface irregularities in the interface affect the transmission of energy. High frequency energy (short wavelength) is absorbed faster than low frequency energy as distance from the source increases, and is scattered more by irregularities. This is seen as less distinct arrivals at greater distances from the source (Redpath, 1973). Large irregularities may produce a shadow, a gap of no arrivals in the seismic record (Dix, 1952).

Errors in refraction are due to three general causes: 1) incorrect reading of the data, 2) incorrect assumptions, 3) incorrect geologic interpretation (Northwood, 1967). Incorrect picking of first breaks leads to errors in depth and dip calculations, and is especially likely when velocity contrasts are less than 3 to 4 (.75). Incorrect assumptions can be minimized by using all available data on the local geology and checking interpretations against bore hole data. In all cases in this study the simpler interpretation was given precedence to avoid over interpretation of the data.

The depth to interface values shown on the cross sections are not exact. The depth values cover a range, due

to different velocity readings in opposite directions for each layer and variations in velocity along the line. The final values chosen are within the calculated range and agree with a reasonable geologic interpretation along the refraction line. Similarly, location of faults or vertical offsets cannot be determined exactly and may vary laterally up to 33 meters (100 feet), the distance between three geophones. Refraction data is listed in Appendix B.

Bunker Hill Line

The Bunker Hill refraction line (Figure 10), 1340 meters long, was the "best behaved" of the three lines run. The first breaks were cleaner and the records were of better quality than Shaffer Road or Little Clatskanie River Road. On a purely subjective rating of A (excellent) to F (marginally usable), all but three of the records were C or better.

Three velocity layers were observed on the time-distance plots (Figure 19). The surface or "weathering" layer has a velocity of about 1000 m/s (3300 f/s) continuously along the line except for a section between BH-0 and 1100E where it is approximately 520 m/s (1700 f/s). (Station numbers refer to distance in feet east and west of the Wilark 247 Road - Bunker Hill Road intersection.) The second layer averages 1675 m/s (5500 f/s) from 2200W to BH-0 but slows down to about 1525 m/s (5000 f/s) on the eastern half of the line. The third layer is composed of two parts, the slower part has a velocity of 2130 - 2440 m/s (7000 -

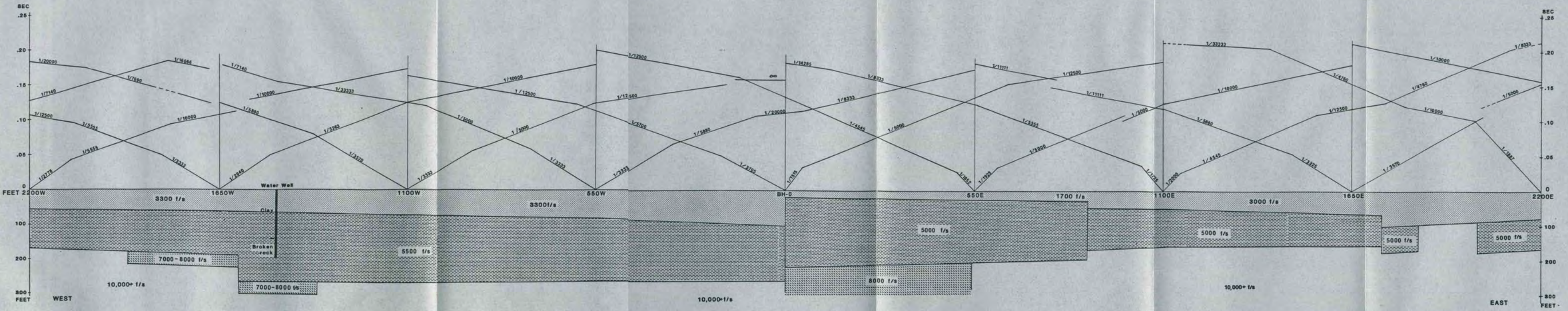

Figure 19. Bunker Hill refraction, time-distance plot.

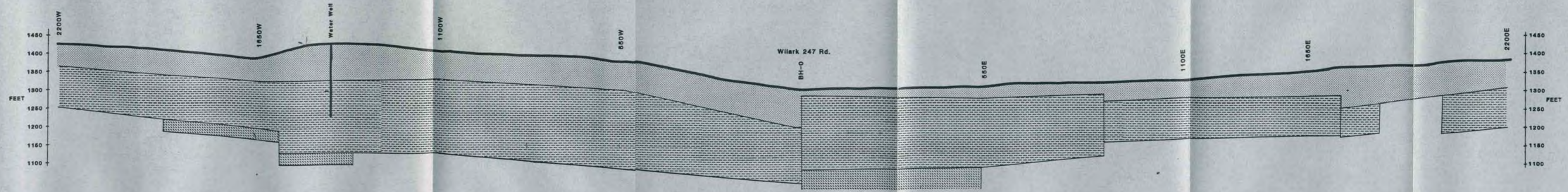

Projected from: Section	Angle to lineament
2200W-1650W	90°
1650W-650E	67°
650E-1250E	90°
1250E-1650E	30°
1650E-2200E	90°

Figure 20. Bunker Hill refraction, projected cross section.

8000 f/s) and the faster part has a velocity of 3050 m/s (10,000 f/s) and higher. The slower stratum is seen only in sections 2200W-1100W, BH-0-550E and 1650E-2200E. The high speed layer is continuous along the line.

The layer 1 - Layer 2 interface is basically flat-lying with dips less than two degrees from 2200W-1100E, except in section 550W-BH-0 (Figures 19 and 20). It dips about 6° to the east in section 1100E-1650E, and is faulted in section 1650E-2200E and at BH-0. The depth of this interface is about 18 meters (60 feet) at 2200W and slopes gently to a depth of 30 meters (100 feet) at BH-0. The slower (1525 m/s) layer 1 stratum is about 6 meters (20 feet) deep at BH-0 and slopes, with two vertical offsets, to about 24 meters (80 feet) at 2200E. The layer 2 - layer 3 interface has a discontinuity near 1650E and in section 550E-1100E, and dips gently east from BH-0 to 550W. It is broken in several places in section 1650E-2200E. The depth of this interface varies from 52 meters (170 feet) at 2200W to about 80 meters (260 feet) at BH-0, and 46 meters (150 feet) at 1100E.

All outcrops along this line are red clay, suggesting that the refraction survey is seeing basalt in various stages of weathering. The logs from two water wells, one 0.8 kilometer (0.5 mile) south of the line (T4N, R2W, Sec. 6, SW¼ NE¼), and one near the west end (T4N, R2W, Sec. 6, SW¼ NW¼) show 25 - 38 meters (80 - 125 feet) of clay above basalt

or "broken rock" (Figure 10 and Appendix B). The velocity of clay is 915 - 1830 m/s (3000 - 6000 f/s), claystone about 1800 m/s (5900 f/s), fractured basalt 2745 - 4270 m/s (9000 - 14,000 f/s), sandstone 1830 - 2440 m/s (6000 - 8000 f/s), and fresh basalt about 6100 m/s (20,000 f/s) (Redpath, 1973). Layer 1, with a velocity of 1000 m/s (3300 f/s) agrees well with clay while the section with a velocity of 520 m/s (1700 f/s) is more thoroughly weathered, contains some sandy clay, or is a layer of clayey topsoil. Soil that has been expanded by smectite has many air spaces and would give a very low velocity. Layer 2, with a velocity of 1525 - 1675 m/s (5000 - 5500 f/s), is probably a more consolidated claystone or layer of very broken and weathered basalt. This broken, weathered basalt is seen in outcrop throughout the study area. The high speed layer 3 is fairly fresh basalt, with variations in velocity probably due to fractures and slight weathering near the top. The lower velocity layer 3 may be due to a vesicular area near the top of a basalt flow, a highly fractured layer, weathering or a sediment (sandstone) layer. This layer occurs only next to discontinuities on the Bunker Hill refraction line, but this does not hold for the other lines.

The major discontinuities have been modelled as faults. They are shown with vertical movement only due to the limitations of this refraction survey, but this should not be interpreted to mean the fault planes do not dip or

that there is no horizontal component to the fault movement. It appears there are three faults along the Bunker Hill line, one near 1650W, one near BH-0 and a fault zone east of 1650E. Displacements cannot be modelled reliably, however the fault at BH-0 has about the same vertical displacement as the one at 1650W.

Shaffer Road Line

The Shaffer Road refraction line (Figure 12), 1340 meters (4400 feet) long, is rather complicated. The records are poorer than the other two lines, especially the 335 meter (1100 foot) sections. The seismic energy was absorbed very quickly (high attenuation), and in several sections first breaks were not seen beyond 245 meters (800 feet) from the source. On the A to F rating scale, 3/4 of the records were C to F.

Four layers were interpreted from the time-distance plots (Figure 21). A surface (weathered?) layer with a velocity of 1370 - 1657 m/s (4500 - 5500 f/s) is found in part of section 550-1100, near station 1100 and from 2200 - 3850. (Station numbers refer to the distance in feet from the west end of the refraction line.) From 2200 to 3850 the velocities vary from 730 - 1800 m/s (2400 - 5900 f/s) indicating significant anisotropy (lateral and vertical variation). Layer 2, with a velocity of 2350 - 2530 m/s (7700 - 8300 f/s) may be a separate layer, or it may be a lower velocity zone at the top of layer 3. It does seem to

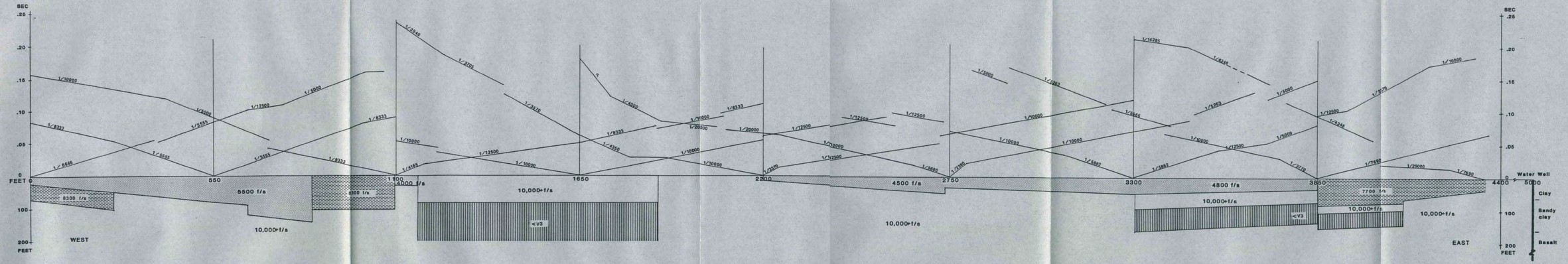

Figure 21. Shaffer Road refraction, time-distance plot.

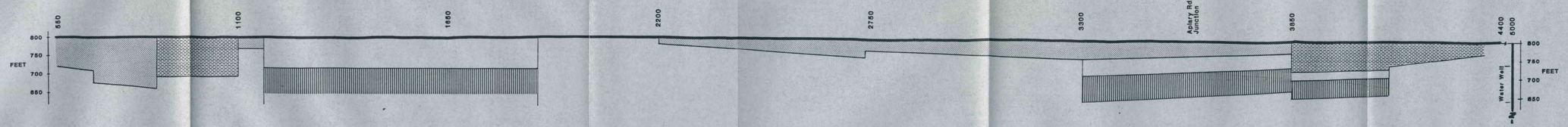

Figure 22. Shaffer Road refraction, projected cross-section.

be separate on this line however, and occurs as blocks in sections 0 - 1100 and 3850 - 4400 only. Layer 3 is the high speed stratum with velocities of 3050 m/s (10,000 f/s) and higher, and is continuous along the line. A low velocity layer occurs below layer 3 discontinuously from 1100 to the east end of the line. Only surface waves arrive at receivers beyond 92 meters (300 feet) from the source in some sections.

Dips were difficult to determine for this line due to the many discontinuities in the records. The interfaces between layers generally appear to be flat or dipping less than 3^{o}. More steeply dipping sections may occur in sections 550 - 1100 and 3850 - 4400 (Figures 21 and 22).

The Shaffer Road line is quite broken up. All nearby outcrops are basalt or clay suggesting that, like the Bunker Hill line, the different velocities indicate different stages of weathering of the basalt. A water well at the east end of the line (T5N, R3W, Sec. 3, SE¼ NE¼) (Figure 12 and Appendix B) was drilled through 18 meters (60 feet) of clay, 30 meters (100 feet) of sandy clay, 92 meters (300 feet) of basalt, and bottomed in sandstone. In several places the time-distance plots indicate fresh basalt at the surface, and, except in section 550 - 1100, the weathered surface layer is no deeper than 15 meters (50 feet). It was not possible to determine the depths of other layers or blocks. The low velocity layer beneath layer 3 may be an interflow weathered zone, a more weathered less competent flow, a

vesicular zone, or sediments. There is no way to tell from the data available. The discontinuities have been modelled as faults. This line may cross two fault zones, or branches of the Shaffer Road - Clatskanie River lineament, since it is between two 90° jogs in the Clatskanie River (Figure 23). This may help explain its broken and discontinuous nature. Here also the faults modelled with vertical movement may have other directional components but this refraction survey would not how them.

Little Clatskanie River Road Line

The Little Clatskanie River Road refraction line, located about 2.4 kilometers (1.5 miles) north of the Shaffer Road line, is an eastward continuation across the lineaments (Figure 12). It has a similar style and is 915 meters (3300 feet) in length. On the A to F rating scale 2/3 of the records are C to F.

The time-distance plots indicate three layers, with the fastest layer again having slow and fast strata (Figure 24). The surface (weathering?) layer velocity of 1370 m/s (4500 f/s) near the west end declines steadily to 915 m/s (3000 f/s) at the east end of the line. The second layer has a velocity of about 1740 m/s (5700 f/s) and appears at the surface in section 0-550. (Station numbers are distances in feet from the west end of the line.) It is seen as blocks in sections 1650 - 2200 and 2200 - 2750, then becomes continuous from 2750 east (Figures 24 and 25). The

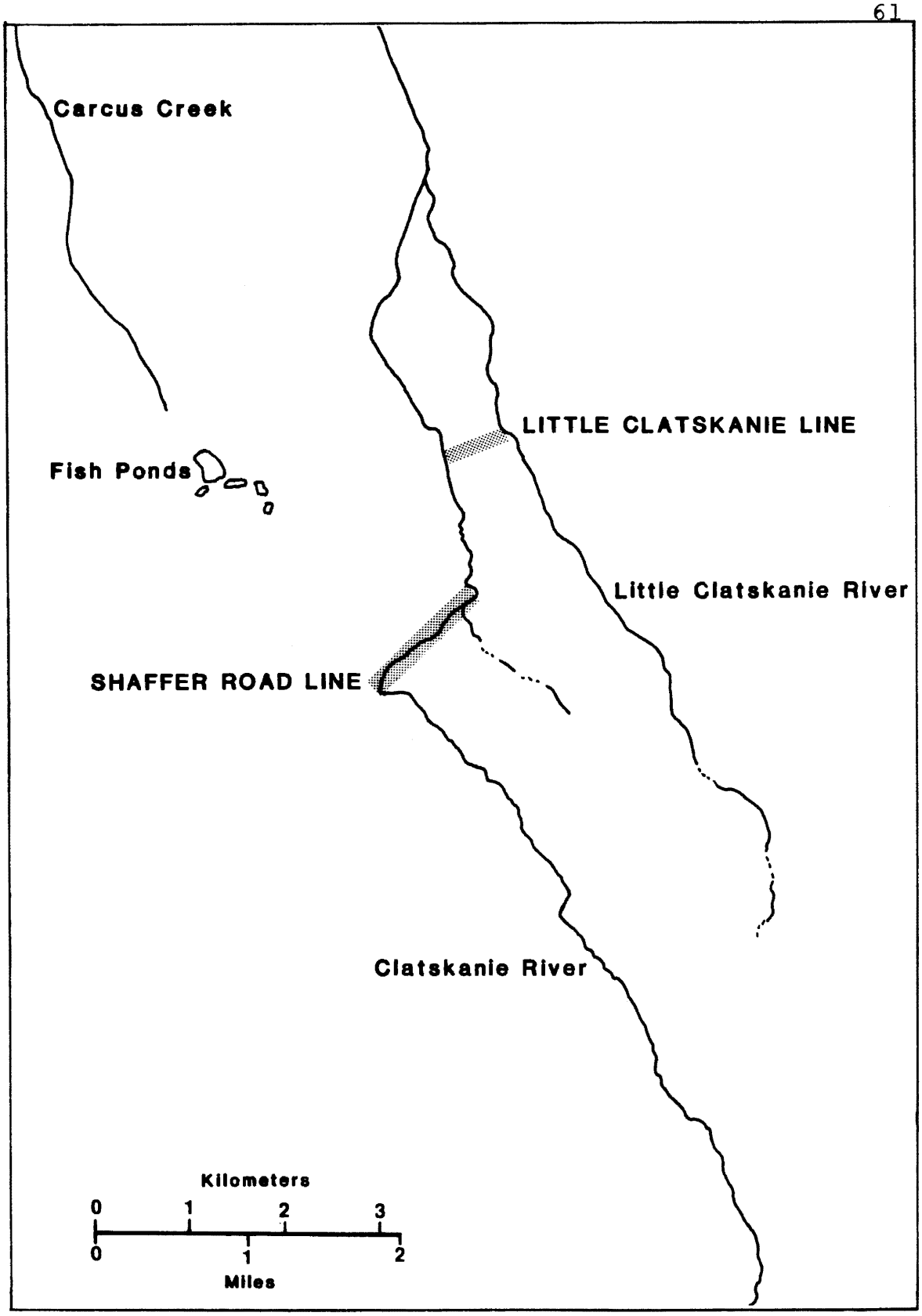

Figure 23. Lineament offset at north end of Shaffer Road.

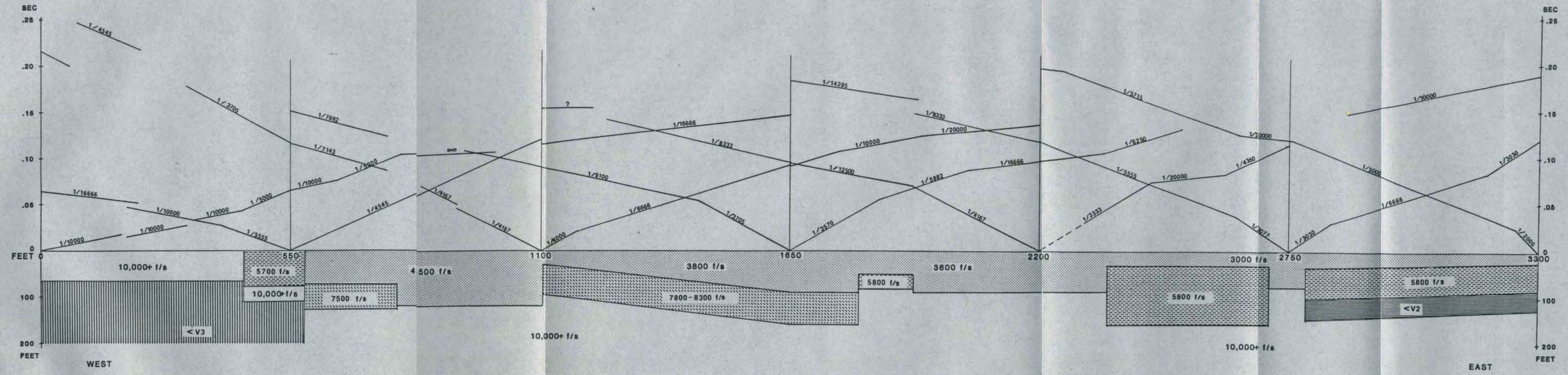

Time-distance graph
velocities in feet/second

- Layer 1
- Layer 2 (v2)
- Layer 3 (v3)
- Layer 3A

Figure 24. Little Clatskanie refraction, time-distance plot.

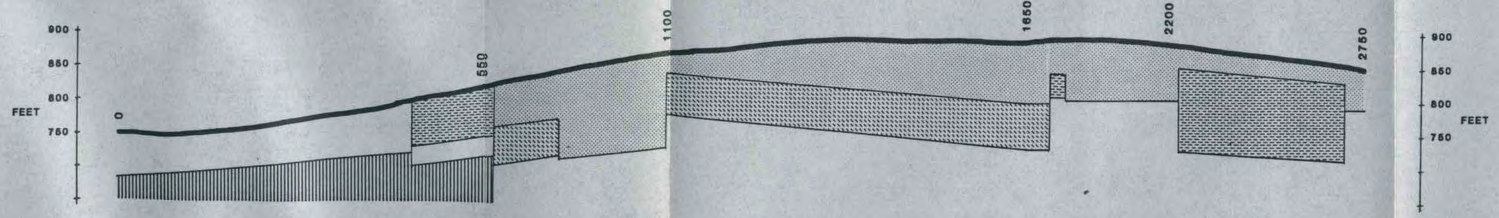

Figure 25. Little Clatskanie refraction, projected cross-section.

Projected from: Section	Angle to lineament
0-550	90°
550-1100	30°
1100-1650	90°
1650-2200	12°
2200-2750	48°
2750-3300	0°

layer 3 fast stratum has velocities greater than 3050 m/s (10,000 f/s), occurs at the surface in section 0 - 550, and is continuous under the rest of the line. The slower part of the layer has velocities of 2380 - 2530 m/s (7800 - 8300 f/s) and occurs discontinuously along the line. A low velocity zone occurs beneath layer 3 in sections 0 - 550 and 2200 - 2750, and is indicated by the arrival of surface waves only at distances beyond about 180 meters (600 feet) from the energy source.

The dip on the layer 1 - layer 2 interface can be determined in only three sections and veries from 5^{o} to the east to 2^{o} - 4^{o} to the west. All interfaces are assumed to be relatively flat-lying or with shallow dips similar to the other two lines. Layer 1 varies in depth from about 9 meters (30 feet) at 1100 to approximately 30 meters (100 feet) at 1650 and 2200, and is about 9 meters (30 feet) deep in section 2750 - 3300. The depth of the layer 2 - layer 3 interface can be estimated only near 550 where it is about 23 meters (75 feet). Both interfaces are discontinuous and broken.

Outcrops along the Little Clatskanie line are clay or broken basalt, with a basalt quarry across the Apiary Road at the west end. The velocity of layer 1 decreases to the east suggesting a topsoil or more weathered, less compacted clay at the east end. Layer 2, with velocities around 1740 m/s (5700 f/s), may be claystone or clayey sandstone, particularly at the east end (see magnetics model). Layer 3

is relatively unweathered basalt with velocities of 3050 - 6100 m/s (10,000 - 20,000 f/s). The slower stratum may be a vesicular area at the top of the basalt flow, or a broken or fractured layer of the basalt, or sediments. The many discontinuities have been modelled as faults, with vertical movement. The downdropped blocks near 2750 and in section 550 - 1100 may be channels cut in the basalt but some sediments, which do not show up, would be expected in them. There are no extensive non-broken areas, but most of the discontinuities are concentrated near 550 and from 1650 to 2750.

The faulted area near 550 is near the Clatskanie River, and the down to the east movement agrees with what can be seen at the Apiary Road, where there is a basalt outcrop and quarry on the west side and a canyon with the Clatskanie River on the east side of the road. The sense of movement on faults along the line varies.

Comparison

The Shaffer Road and Little Clatskanie lines have similar velocities and style of time-distance plots, and are different from the Bunker Hill line. The Shaffer Road and Little Clatskanie lines have four layers of 1370 - 1675 m/s (4500 - 5500 f/s), 2135 - 2440 m/s (7000 - 8000 f/s), 3050+ m/s (10,000+ f/s) and a slow layer occasionally below the fastest one. They have discontinuities along the line, and the seismic records for both are generally poor, even for the

shortest refraction line segments. The material along both lines absorbed energy quickly. The Bunker Hill line is the only line with a slow "weathering" layer of 520 - 1000 m/s (1700 - 3300 f/s). Other layers of 1675 m/s (5500 f/s), 2135 - 2440 m/s (7000 - 8000 f/s) and 3050+ m/s (10,000+ f/s) are also present, but there is no slow layer below layer 3. This line is less broken, with faulted areas occurring at three distinct places along the line and relatively undisturbed areas in between.

MAGNETICS

General

Interpretation of this magnetic survey can be only qualitative since the magnetic susceptibility (k), the magnetite content of the rock, local earth field vectors, and the remnant magnetization are not known. Magnetic anomalies are caused by local variations in magnetization of the rocks. These local changes are primarily determined by variations in the susceptibility, k, which in turn depends on the amount of magnetite present in the rock. Since the remnant magnetization is usually variable and too small to measure, it is assumed, in interpretation, that the entire anomaly is due to induced magnetization. The nuclear precession magnetometer used in this survey measures the total magnetic field along the earth's field vector. This is because where F (the earth's field) is much larger than T (the local disturbance) the resultant, from vector

addition, is not noticeably different from F. The earth's magnetic field near Portland is approximately 55,000 gammas (.55 gauss) and the inclination is 70^{o}. For interpretation, an inclination of 70^{o} for the total field vector is approximately the same as the vertical field (Van Blaricom, 1980).

The amplitude and shape of a magnetic anomaly is a function of depth and contrast in magnetic susceptibility between two rock types. Generally, the broader the anomaly, the deeper the source. Depths determined by any method are maximum depths and the source may be closer to the surface. Depths for the interpretation of the anomalies in the three lines were determined by the ½ width rules (Van Blaricom, 1980, p.234) for symmetrical anomalies, and Peters' slope method (Dobrin, 1976, p.544) for asymmetrical anomalies. The ½ width rules are usually accurate within 20%, and both methods are within 10% to 50% of the real depth. Anomalies of several hundred gammas are due to magnetization contrasts, not irregularities in uniformly magnetized rock. The magnetic susceptibility for basalt is 10^{-3} to 10^{-4} cgs units, and for sediments it is about 10^{-5} to 10^{-6}.

Interpretation of magnetic anomalies assumes 1) the source can be modelled by a simple shape such as a sphere, cylinder or sheet, 2) magnetization within the model shape is uniform, and 3) magnetization within the shape is different from magnetization outside it. Error can occur from 1) the survey method, 2) local electrical noise or magnetic

objects such as cars and fences, 3) magnetic storms, and 4) misinterpretation of anomalies. Magnetic data is listed in Appendix C.

Bunker Hill Line

The Bunker Hill magnetics line has a background level of 55,200 to 55,300 gammas (Figure 26). The area from 2200W to 550W contains a broad anomaly with several smaller ones superimposed upon it (Figures 26 and 27). A shallow sharp anomaly occurs at 225E. An increase in k, magnetic susceptibility, is seen near 1000E and continues to 1650E. Two anomalies occur between 1650E and 1750E. The anomalies do not follow the topography, therefore they represent subsurface contrasts in magnetization.

All of the anomalies can be modelled as vertical cylinders, or thick or thin slabs. There is no direct evidence of tilting or dipping. The area between 2200W and 550W is modelled by large blocks raised and lowered (faulted?) in relation to one another, with maximum depths of 21 - 76 meters (70 - 250 feet). The anomaly at 225E is interpreted to be a vertical slab less than 25 meters (80 feet) deep. The increase in magnetic susceptibility between 1000E and 1650E is probably due to a broad slab or faulted block. The anomaly in section 1800E - 2400E may be two faulted blocks at maximum depths of 43 - 49 meters (140 - 160 feet). A horizontal slab at about 18 meters (60 feet) depth is a possible interpretation for the asymmetric anomaly in

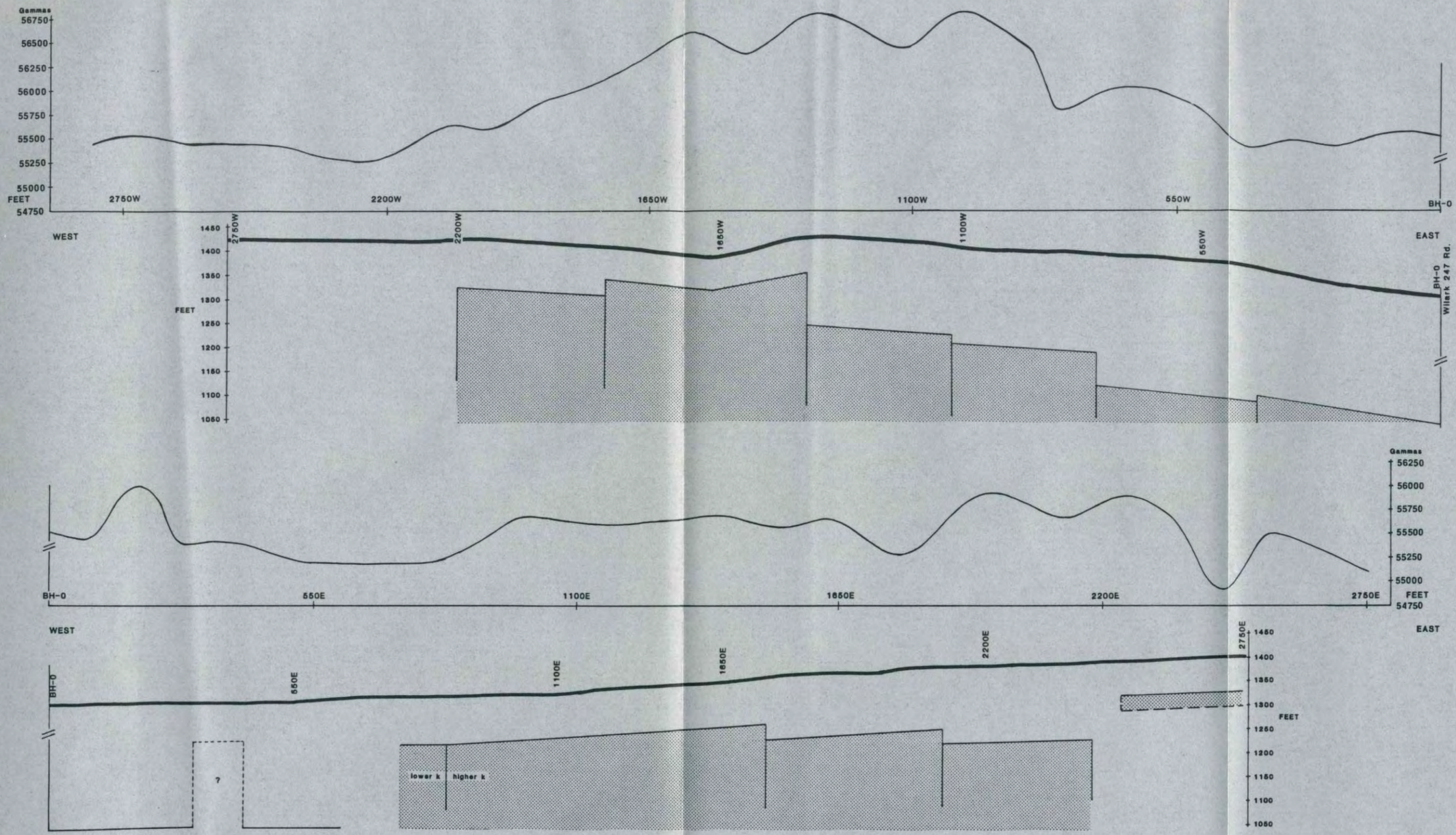

Material with higher magnetic susceptibility (k)

Depths to anomalous materials are ≤ to depths shown.

Projected from: Section	Angle to lineament
2750W-2200W	55°
2200W-1650W	90°
1650W-650E	67°
650E-1250E	90°
1250E-1650E	30°
1650E-2750E	90°

Figures 26 and 27. Bunker Hill magnetic data, graph and projected cross section.

section 2500E - 2750E. The magnetization contrasts could be due to blocks of basalt with different amounts of weathering being faulted up or down in relation to each other, although contrasts with large lateral extent may be parts of different flows, or lateral variations in a single flow.

Shaffer Road Line

The Shaffer Road magnetics line is more complex than the Bunker Hill line, following the same relationship as the refraction lines. Sharp anomalies are present near 1300 and 3400 with a broad area containing several anomalies from 2000 to 3000 (Figures 28 and 29). The general background level of magnetization agrees with the regional average of 55,000 gammas.

The anomaly at 1300 can be interpreted as a gently dipping slab (or broken, tilted, thin layer) a little more than 30 meters (100 feet) beneath the surface. Wide thick blocks, less than 18 meters (60 feet) deep, can be modelled for the similar anomalies in sections 1400 - 1800 and 2700 - 3000. The blocks dip slightly in opposite directions, away from the large broken area in section 2000 - 2600. This broad anomaly can be separated into smaller blocks and a horizontal slab (or thin plate) from 9 to 36 meters (30 to 120 feet) deep. An area of negative anomaly occurs from 3000 - 3850, about 200 gammas below the regional average, which is modelled by a shallow vertical slab at 3450. This decrease in magnetization may be due to a lateral change in

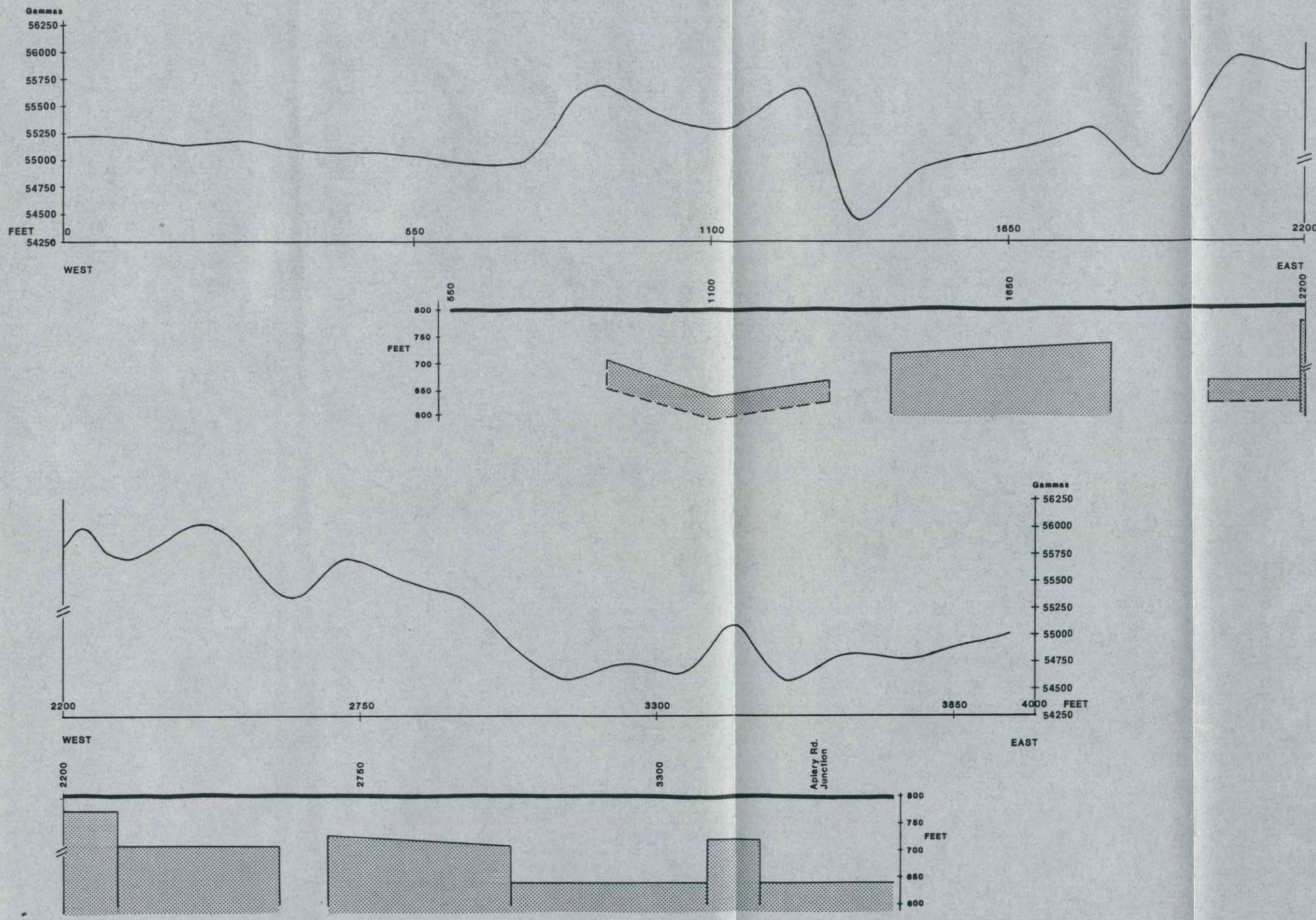

Material with higher magnetic susceptibility (k)

Depths to anomalous materials are ≤ to depths shown.

Projected from: Section	Angle to lineament
0-550	0°
550-1100	55°
1100-4000	90°

Figures 28 and 29. Shaffer Road magnetic data, graph and projected cross section.

the basalt or a sedimentary layer.

Little Clatskanie River Road Line

The Little Clatskanie River Road magnetics line shows a background level which agrees with the regional value (Figure 30). A relatively large anomaly occurs at the west end of the line, with a wide area of anomalies from 1000 - 2400. East of 2400 no large anomalies are evident (Figures 30 and 31).

This line can be modelled as a series of faulted blocks with a deep horizontal slab at the western end. A large mass of basalt occurs across the road from the west end and this may have an influence on the large anomaly near that end of the line. The section from 600 - 2000 appears to be a series of faulted blocks at depths of 18 - 76 meters (60 - 250 feet). Near 2400 a change in magnetization occurs with the remaining area to the east showing no significant anomalies, possible representing sediments near the surface, or a thick, deeply weathered layer in this area.

Comparison

The Bunker Hill line has a different magnetic character than the Shaffer Road and Little Clatskanie River lines, however even these two lines differ more from each other than they did in refraction. All three lines contain one large, broad anomaly with smaller anomalies superimposed on it. The Bunker Hill line has a background level higher than

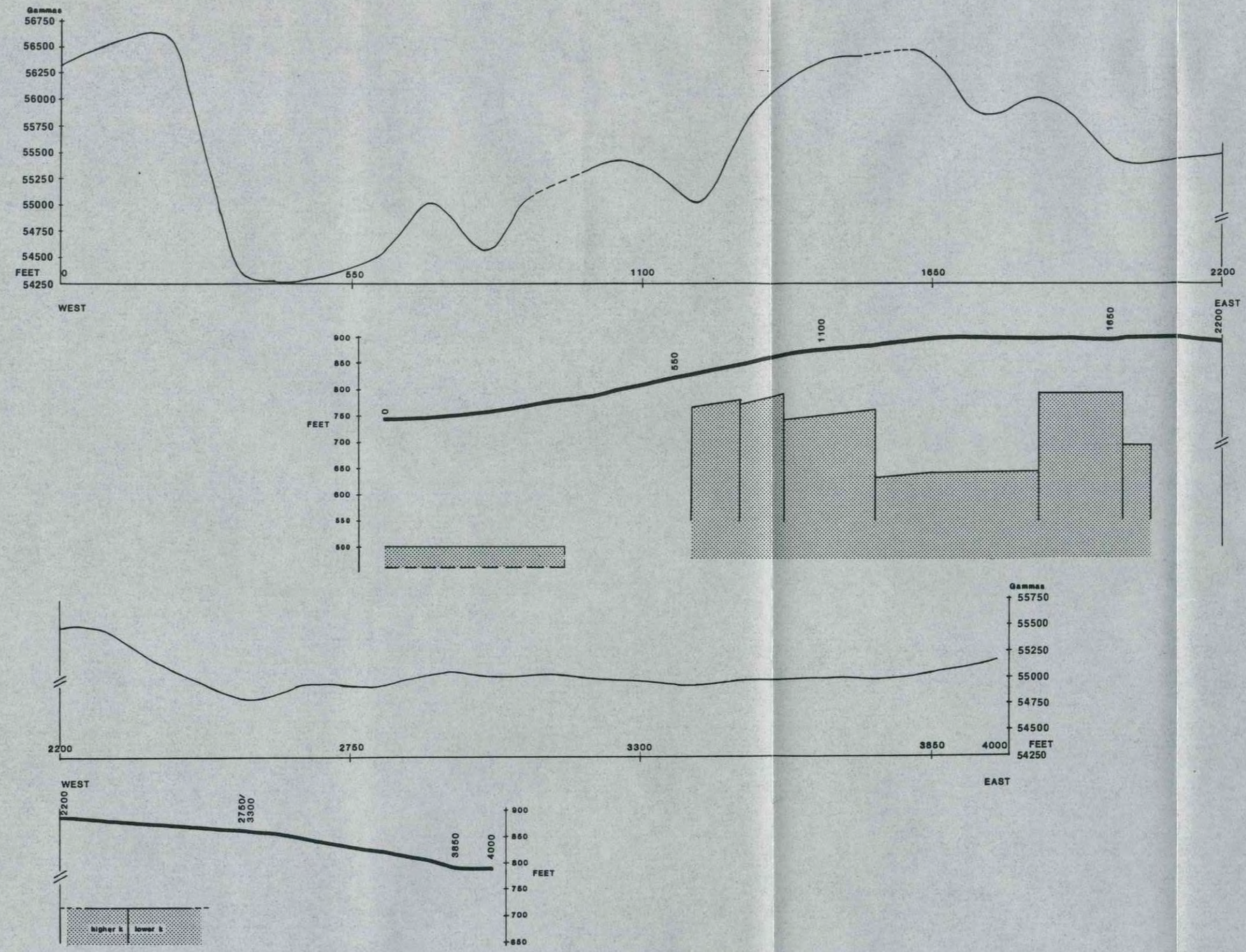

Figures 30 and 31. Little Clatskanie magnetic data, graph and projected cross section.

Material with higher magnetic susceptibility (k)

Depths to anomalous materials are ≤ to depths shown.

Projected from:

Section	Angle to lineament
0-550	90°
550-1100	30°
1100-1650	90°
1650-2200	12°
2200-2750	48°
2750-3300	0°
3300-3850	40°

the regional average while the two northern lines are close to the regional value of 55,000 gammas. On the Bunker Hill and Little Clatskanie lines a horizontal slab or thin plate is located near suspected faults, while the Shaffer Road line has these features near areas which are not seen as faults in the modelling. Depths to basalt (high k) are similar on all three lines.

DISCUSSION AND CONCLUSIONS

DISCUSSION

The Spitzenberg gravity line is the southernmost geophysical line in this study (Figure 2). The gravity readings for this line show a low at Alder Creek which continues east for about two kilometers. This low was modelled (Figure 17) with a zone of low density material, possibly unconsolidated sand, gravel or broken rock. A sedimentary high extends one kilometer east of this zone, then basalt is found over sediments to the east end of the line. The basalt block models with a relatively smooth lower surface indicating it was probably deposited on a sedimentary surface with few irregularities. A fault has been mapped along North Scappoose Creek and Alder Creek and lines up with the western edge of the low density zone (Wilkinson and others, 1946; Marty, 1983, in preparation). A fault has been mapped east of Alder Creek, occurring in the low density and sedimentary material (Marty, 1983, in preparation). The basalt seen at the surface does not show up in the gravity model, and therefore is probably less than 30 meters (100 feet) thick in the three kilometers east of Alder Creek. Any thicker layer of basalt would require modelling thicker, less dense, material below it to match the measured gravity.

The Bunker Hill refraction/magnetics line is about five kilometers northwest of the Spitzenberg line along a ridge which separates the Alder Creek and Clatskanie River drainages (Figures 2 and 10). A ponded marshy area, which could be sag ponds, follows the lineament northwest from Bunker Hill for about 1.5 kilometers. The Bunker Hill refraction data shows a fault with approximately 33 meters of offset, up on the east. This offset coincides with a saddle where the lineament crosses Bunker Hill. There is a possible fault with about the same offset approximately 500 meters west, and a zone of broken blocks approximately 500 meters east of the Alder Creek - Clatskanie River lineament. The magnetics data does not show a sharp boundary for the fault in the saddle but does indicate the general westward decrease in depth to the top of the basalt. The blockiness of the model could be smoothed. The anomalous area from 400W to 2200W could be modelled as a larger structure, and not only as individual blocks (Figures 26 and 27). The sharp anomaly at 225E is different from others on the line and is probably an artifact due to a cultural feature, such as a drain pipe crossing under the road.

The Shaffer Road refraction/magnetics line, Apiary gravity line and Little Clatskanie River refraction/magnetics line are 12 kilometers northwest of the Bunker Hill line (Figure 2). These geophysical lines cross three lineaments, the Clatskanie River, its offset, and the Little Clatskanie

River. The Apiary gravity line models with a layer of basalt across the lineaments, between two sedimentary highs (Figure 16). It is not obvious from the gravity model whether these were highs when the basalt was deposited, whether they were the result of folding after basalt deposition, or resulted from continuous uplift during deposition. The irregular nature of the lower surface of the basalt blocks suggests they were deposited on an irregular erosional surface. The non-uniform thickness of the basalt may be due to non-uniform deposition, uplift and erosion after deposition, non-uniform coverage by different basalt flows, or a combination of these. The basalt block is thickest between Shaffer Road and the Little Clatskanie River, thinning to the east and west. The Clatskanie River, which has been following the lineament northwest, is offset approximately 1.5 kilometers to the northeast along the Apiary line, then turns northwest and parallels the lineament trend (Figure 23). The Little Clatskanie River parallels the offset Clatskanie River about one kilometer east. The original Alder Creek - Clatskanie River lineament continues northwest across the Apiary line for several kilometers, including an area of ponds, possibly sag ponds. The refraction/magnetics line is offset across the three lineaments, with the Shaffer Road line along the Clatskanie River offset section, and the Little Clatskanie River line approximately 2.5 kilometers north, between the Clatskanie and

Little Clatskanie Rivers (Figure 12). Refraction (Figures 22 and 25) indicates that relatively unweathered basalt is at or very near the surface along most of the line, with a dropped down section near the east end. The magnetic data (Figures 29 and 31) generally follows the increasing depth to basalt to the east, after smoothing out the anomalous area from 2000 to 3000. The anomaly at 3300 may relate to the fault at the same location shown on the refraction model. The Little Clatskanie line is quite faulted and this is indicated by both refraction and magnetics. Here again the magnetics model, after smoothing, generally follows the basalt surface as shown by the refraction model.

The three geophysical methods used, gravity, magnetics, and seismic refraction produce complimentary but not necessarily identical results. The spacing between gravity stations equals an entire refraction section, or several magnetics stations. Thus the scale of modelling is different for each method. In this study refraction models from ground level down to the top of the basalt, typically less than 100 meters deep. Magnetics, with 30.5 meter (100 foot) spacing between stations, models to a similar depth, however the magnetic data can be smoothed (eliminating one or two point anomalies) to give a deeper model. Gravity, on the scale modelled here, requires a layer of anomalous material to be approximately 30 meters thick to be seen on the model. Density contrasts within a few kilometers of the surface are

modelled here. Therefore, progressively deeper features are seen from refraction to magnetics to gravity. The specific features on each type of model may not correlate well due to the scale differences, and they may be from different sources.

Gravity and magnetics are potential fields and the interpretation of an anomaly does not have a unique solution. A shallow wide body may produce a disturbance in the potential field similar to a deeper narrower body. This emphasizes again the need for integration and comparison of data from all geophysical methods with available geologic data, which allows a reasonable range of possible solutions to be proposed.

CONCLUSIONS

Available evidence tends to confirm the hypothesis that the North Scappoose Creek - Alder Creek - Clatskanie River lineament indicates a northwest-trending fault zone. The lineament is quite distinctive on SLAR, air photos and topographic maps and appears to represent the western margin of the proposed fault zone. The zone extends east from the lineament approximately two kilometers. The zone is better defined to the south, on the Spitzenberg gravity and Bunker Hill refraction lines, and is less well defined on the northern lines. The lineament becomes less obvious north of the Apiary Road but two lineaments, offset 1.5 and 2 kilometers to the east, continue the northwest trend. Sag ponds,

a feature sometimes associated with recent fault activity, occur along the lineament in at least two locations.

The three geophysical methods used differentiate basalt and sediments by indicating contrasts in various physical properties. Both gravity models show anomalies associated with the proposed fault zone, a block of very low density material on the Spitzenberg model, and a thicker section of basalt on the Apiary model between Shaffer Road (kilometer 83) and the Little Clatskanie River (kilometer 85). The low density material in the Spitzenberg model may be broken and fractured rock, or clay. On both models the proposed fault zone is bounded on the east by a sedimentary high. The refraction and magnetic models show that the surface, or near surface, basalt is broken and faulted. This may be due to fault zone activity, or it may be the reaction of a thin, brittle skin to regional compression. This may be one reason why there is no major offset indicated in the near surface data. The deeper evidence for faulting is not clear cut in the gravity models, however 2.4 g/cm^3 sediments faulted against 2.5 g/cm^3 sediments may not show up, particularly since the 2.5 g/cm^3 for the Cowlitz Formation is an average for sediments ($\sim$2.4 g/cm^3) and interbedded volcanics.

Probable recent activity along the proposed fault zone is indicated by the sag ponds, the linear nature and youthful appearance of the lineaments, and the occurrence at the

surface of unweathered basalt against well weathered basalt and clay. The thick (600 - 700 meter) low density material in the Spitzenberg gravity model may indicate continuing activity during the mid to late Tertiary, or earlier. This block, which is modelled as being above the upper Eocene sediments, could also be modelled as two or three narrower, thicker, blocks which might indicate continuous activity over a longer period of time (Wang and others, 1978). There is not enough evidence to determine the sense of movement along the porposed fault zone. Right lateral strike slip motion would fit with the regional north - south compressive stress.

The complete Bouguer gravity values, when plotted on the state gravity anomaly map, fit the -20 and -30 milligal contours. The -25 and -35 milligal contours also follow the local trend on the state map, however the -40 milligal contour does not agree with the state Bouguer anomaly map (Figure 32). The -40 milligal contour continues northwest farther into Columbia County then loops back and rejoins the state map's -40 milligal contour. This loop enphasizes the northwesterly trend of the Portland Hills fault and the North Scappoose Creek - Alder Creek - Clatskanie River lineament. This change in the state map fits with the more northwesterly trend in the -20 and -30 milligal contours found in the Portland area by Perttu (1980).

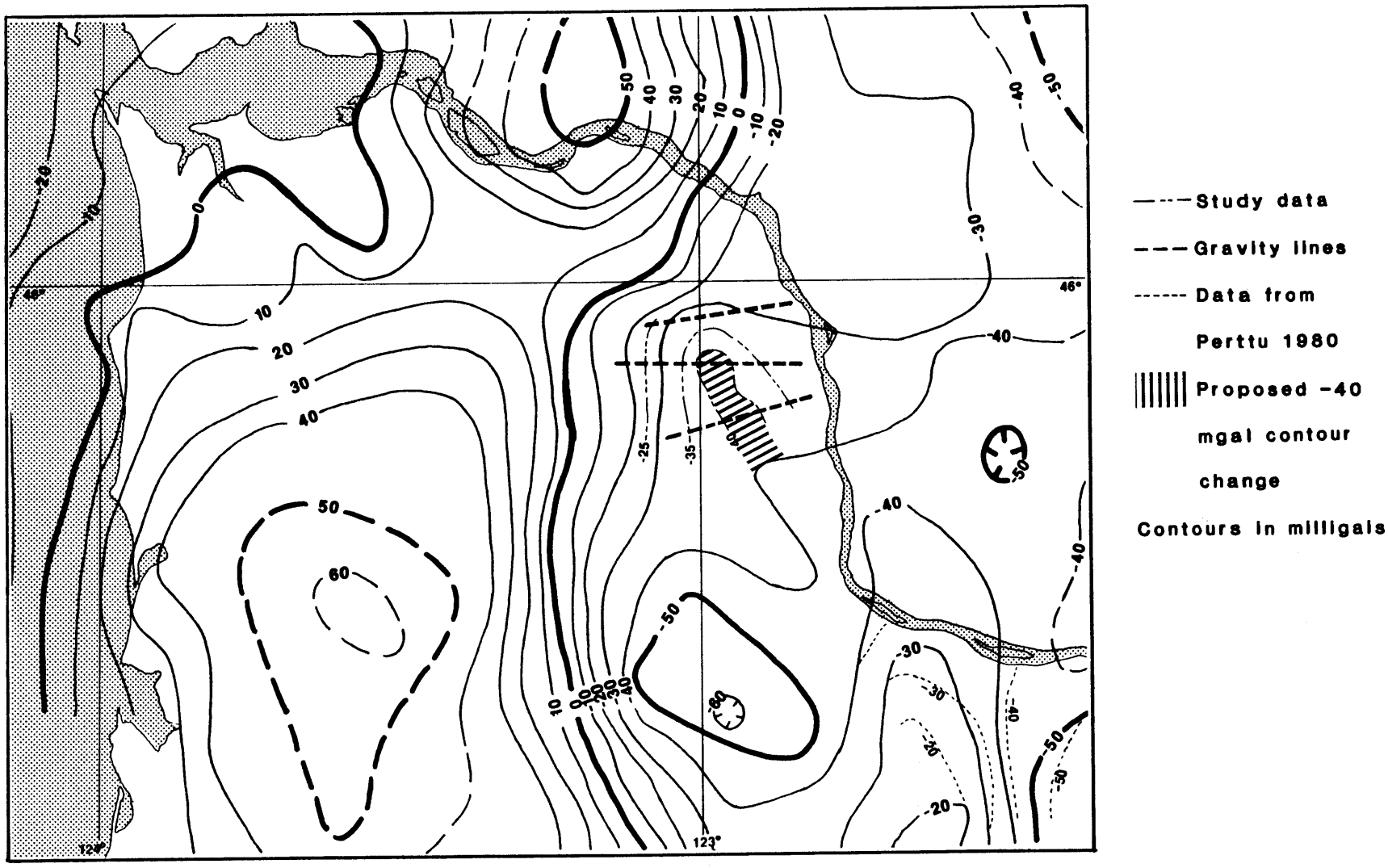

Figure 32. Complete Bouguer gravity map of northwestern Oregon with study data (from Berg and Thiruvathukal 1967, and Bonini and others 1974).

REFERENCES

Anderson, J.L., 1978, The stratigraphy and structure of the Columbia River Basalt in the Clackamas River drainage: unpublished thesis, M.S., Portland State University, Portland, Oregon.

Atwater, T.M., 1970, Implication of plate tectonics for the Cenozoic tectonic evolution of western North America: Geological Society of America Bulletin, V. 81, p. 3513 - 3536.

Balsillie, J.H., and Benson, G.T., 1971, Evidence for the Portland Hills fault: The Ore Bin, v. 33, no. 6, p. 109 - 118.

Barthelmes, A.J., 1946, Application of continuous profiling to refraction shooting: Geophysics, V. 11, no. 1, p. 24 - 42.

Beaulieu, J.D., and Peterson, N.V., 1981, Seismic and volcanic hazard evaluation of the Mount St. Helens area, Washington, relative to the Trojan nuclear site, Oregon: Oregon Department of Geology and Mineral Industries, Open File Report 0-81-9.

Beck, M.E., Jr., 1980, Paleomagnetic record of plate margin tectonic processes along the western edge of North America: Journal of Geophysical Research, v. 85, no. B12, p. 7115 - 7131.

Beck, M.E., Jr., and Burr, C.D., 1979, Paleomagnetism and tectonic significance of the Goble Volcanic Series, southwest Washington: Geology, v. 7, p. 175 - 179.

Beck, M.E., Jr., and Plumley, P., 1980, Paleomagnetism of intrusive rocks in the Coast Range of Oregon: Microplate rotations in middle Tertiary time: Geology, v. 8, p. 573 - 577.

Beeson, M.H., Johnson, A.G., Moran, M.R., 1976, Portland environmental geology - fault identification; Final technical report to United States Geological Survey: Earth Sciences Dept., Portland State University, Portland, Oregon.

Beeson, M.H., Johnson, A.G., Moran, M.R., 1977, Fault identification and structural evolution of the Portland area: Proc. Oregon Academy of Science, p. 58 (abstract).

Benson, G.T., and Donovan, J.C., 1974, Preliminary tectonic map of the greater Portland area: in Hammond, P.E., and others, 1974, A preliminary geological investigation of the ground effects of earthquakes in the Portland metropolitan area, Oregon: unpublished report to the United States Geological Survey (PEG I report), Portland State University, Portland, Oregon.

Berg, J.W., Jr., and Baker, C.D., 1962, Oregon earthquakes, 1841 through 1958: The Ore Bin, v. 24, no. 9, p. 143 - 149.

_____, 1963, Oregon earthquakes, 1841 through 1958: Seismological Society of America Bulletin, v. 53, p. 95 - 108.

Berg, J.W., Jr., and others, 1966, Crustal refraction profile, Oregon Coast Range: Seismological Society of America Bulletin, v. 56, p. 1357 - 1362.

Berg, J.W., and Thiruvathukal, J.V., 1967a, Free air gravity anomaly map of Oregon: Oregon Department of Geology and Mineral Industries, GMS 4a, scale 1:500,000.

_____, 1967b, Complete Bouguer gravity anomaly map of Oregon: Oregon Department of Geology and Mineral Industries, GMS 4b, scale 1:500,000.

Bonini, W.E., Hughes, D.W., and Danes, Z.F., 1974, Complete Bouguer gravity anomaly map of Washington: Division of Geology and Earth Resources, State of Washington, Department of Natural Resources, geologic map GM-11, scale 1:500,000.

Bromery, R.W., and Snavely, P.D., Jr., 1964, Geologic interpretation of reconnaissance gravity and aeromagnetic surveys in northwestern Oregon: United States Geological Survey Bulletin 1181-N.

Bruer, W.G., 1980, Mist gas field, Columbia County, Oregon: American Association of Petroleum Geologists Bulletin, v. 64, no. 3, p. 439 (abstract).

Cash, D.J., 1973, A gravity survey in northeast Portland: unpublished paper, Portland State University, Portland, Oregon.

Couch, R., Johnson, S., and Gallagher, J., 1968, The Portland earthquake of May 13, 1968, and earthquake energy release in the Portland area: The Ore Bin, v. 30, no. 10, p. 185 - 190.

Couch, R., and Lowell, R.P., 1971, Earthquakes and seismic energy release in Oregon: The Ore Bin, v. 33, no. 4, p. 61 - 84.

Couch, R.W., and Mac Farlane, W.T., 1971, A fault plane solution of the October 1969, Mt. Rainier earthquake and tectonic movements in the Pacific Northwest: Derived from fault plane and first motion studies: EOS, v. 52, p. 428 (abstract).

Crosson, R.S., 1972, Small earthquakes, structure and tectonics of the Puget Sound region: Seismological Society of America Bulletin, v. 62, no. 5, p. 1133 - 1171.

Dehlinger, P., 1969, Tectonic processes in the Juan de Fuca and Gorda ridges, and their implications for global tectonics: EOS, v. 50, p. 186 (abstract).

Dehlinger, P., and Berg, J.W., Jr., 1962, The Portland earthquake of November 5, 1962: The Ore Bin, v. 24, no. 11, p. 185 - 188.

Dehlinger, P., Bowen, R.G., Chilburis, E.F., and Westphal, W.H., 1963, Investigations of the earthquake of November 5, 1962, north of Portland: The Ore Bin, v. 25, no. 4, p. 53 - 68.

Dehlinger, P., and Couch, R.W., 1969, Synthesis of geophysical results in the Juan de Fuca and Gorda Ridge areas (Northeast Pacific Ocean): EOS, v. 50, p. 186 (abstract).

Dehlinger, P., Rinehart, R.W., Couch, R.W., and Gemperle, M., 1967, Free air gravity anomaly map west of Oregon: Oregon Department of Geology and Mineral Industries, GMS 4c, scale 1:500,000.

Dickinson, W.R., 1976, Sedimentary basins developed during evolution of the Mesozoic - Cenozoic arc-trench system in western North America: Canadian Journal of Earth Sciences, v. 13, p. 1268 - 1287.

Dickinson, W.R., 1979, Cenozoic plate tectonic setting of the cordilleran region in the U.S.: in Cenozoic paleogeography of the western U.S., J.M. Armentrout, ed., Pacific Coast Paleogeography Symposium No. 3, SEPM, Los Angeles, California.

Diller, J.S., 1896, A geological reconnaissance in the northwest Oregon: United States Geological Survey, 17th Annual Report, part 3, p. 441 - 520.

Dobrin, M.B., 1960, Introduction to geophysical prospecting: New York, McGraw Hill Book Company; 1976, 3rd edition.

Dix, C.H., 1939, Refraction and reflection of seismic waves, I. Fundamentals: Geophysics, v. 4, no. 2, p. 81 - 101.

_____, 1939, Refraction and reflection of seismic waves, II. Discussion of the physics of refraction prospecting: Geophysics, v. 4, no. 4, p. 238 - 241.

_____, 1941, Notes on refraction prospecting: Geophysics, v. 6, no. 4, p. 378 - 396.

_____, 1952, Seismic prospecting for oil: New York, Harper and Row.

DOGAMI, 1978, Geologic hazards review, Trojan nuclear power plant site, Columbia County, Oregon: Open file report 78-1.

Donath, F.A., and Kuo, J.T., 1962, Seismic refraction study of block faulting, south-central Oregon: Geological Society of America Bulletin, v. 73, no. 4, p. 429 - 434.

Ewing, M., Wollard, G.P., and Vine, A., 1939, Geophysical investigations in the emerged and submerged Atlantic coastal plain, Part III: Geological Society of America Bulletin, v. 50, p. 257 - 296.

Hamilton, W., 1978, Mesozoic tectonics of the Western U.S.: in Mesozoic paleogeography of the western U.S., D.G. Howell, ed., Pacific Coast Paleogeography Symposium, No. 2, SEPM, Los Angeles, California.

Hammer, S., 1939, Terrain corrections for gravimeter stations: Geophysics, v. 4, no. 3, p. 184 - 194.

Hammond, P.E., 1979, A tectonic model for evolution of the Cascade Range: in Cenozoic paleogeography of the western U.S., J.M. Armentrout, ed., Pacific Coast Paleogeography Symposium No. 3, SEPM, Los Angeles, CA.

_____, 1980, Reconnaissance geologic map and cross sections of southern Washington Cascade Range: Department of Earth Sciences, Portland State University, scale 1:125,000, 2 sheets, booklet.

Hammond, P.E., Benson, G.T., Cash, D.J., Palmer, L.A., Donovan, J., and Gannon, B., 1974, A preliminary geologic investigation of the ground effects of earthquakes in the Portland Metropolitan area, Oregon: unpublished report to the United States Geological Survey.

Hales, F.W., 1958, An accurate graphical method for interpreting seismic refraction lines: Geophysical Prospecting, v. 6, p. 285 - 304.

Hawkins, L.V., 1961, The reciprocal method of routine shallow seismic refraction investigations: Geophysics, v. 26, no. 6, p. 806 - 819.

Heiland, C.A., 1968, Geophysical exploration: New York, Hafner Publishing Company.

Heinrichs, D.F., and Pietrafesa, L.J., 1968, The Portland earthquake of January 27, 1968: The Ore Bin, v. 30, no. 2, p. 37 - 40.

Jakosky, J.J., 1940, Exploration geophysics: Los Angeles, Los Angeles Times Mirror Press.

Johnson, A.G., 1976, Gravity profiles across the northeast side of the Tualatin Mountains, Portland, Oregon: Transactions, American Geophysical Union, v. 57, no. 2, p. 89 (abstract).

Johnson, A.G., and Jones, T., 1976, Gravimetric investigations of the tectonics of the Portland Hills: Transactions, American Geophysical Union, v. 57, no. 20, p. 897 (abstract).

Johnson, A.G., Jones, T., and Perttu, J.D., 1977, Interpretation of gravity in the Portland area: Proc. of Oregon Academy of Science, p. 60 (abstract).

Jones, D.L., Cox, A., Coney, P., and Beck, M., 1982, The growth of western North America: Scientific American, v. 247, no. 5, p. 70 - 84.

Jones, T.D., 1977, Analysis of a gravity traverse south of Portland, Oregon: unpublished thesis, B.S., Portland State University, Portland, Oregon.

Kadri, Moinoddin, 1982, Structure and influence of the Tillamook uplift on the stratigraphy of the Mist area, Oregon: unpublished thesis, M.S., Portland State University, Portland, Oregon.

Kelty, K.B., 1981, Stratigraphy, lithofacies and environment of deposition of the Scappoose Formation in central Columbia County, Oregon: unpublished thesis, M.S., Portland State University, Portland, Oregon.

Lawrence, R.D., 1976, Strike-slip faulting terminates the Basin and Range Province in Oregon: Geological Society of America Bulletin, v. 87, no. 6, p. 846 - 850.

Levorsen, A.I., 1960, Paleogeologic maps: San Francisco, W.H. Freeman and Company.

Magill, J., and Cox, A., 1980, Tectonic rotation of the Oregon western Cascades: Oregon Department of Geology and Mineral Industries, special paper 10.

_____, 1981, Post-Oligocene tectonic rotation of the Oregon western Cascade Range and the Klamath Mountains: Geology, v. 9, no. 3, p. 127 - 131.

Magill, J., Cox, A., and Duncan, R., 1981, Tillamook Volcanic Series: Further evidence for tectonic rotation of the Oregon Coast Range: Journal of Geophysical Research, v. 86, no. B4, p. 2953 - 2970.

Magill, J.R., Wells, R.E., Simpson, R.W., and Cox, A.V., 1982, Post 12 m.y. rotation of southwest Washington: Journal of Geophysical Research, v. 87, no. B5, p. 3761 - 3776.

Marty, R., 1983, Formation and zonation of ferruginous bauxite deposits, Columbia County, Oregon: thesis in preparation, M.S., Portland State University, Portland, Oregon.

Mota, Lindonor, 1954, Determination of dips and depths of geological layers by the seismic refraction method: Geophysics, v. 19, no. 2, p. 242 - 254.

Musgrave, A.W., 1967, Seismic refraction prospecting: Tulsa, Society of Exploration Geophysicists.

Nettleton, L.L., 1940, Geophysical prospecting for oil: New York, Mc Graw-Hill Book Company.

_____, 1971, Elementary gravity and magnetism for geologists and seismologists: Tulsa, SEG Monograph, Series 1.

Newton, V.C., Jr., 1969, Subsurface geology of the Lower Columbia and Willamette Basins, Oregon: Oregon Department of Geology and Mineral Industries, Oil and Gas Investigation, No. 2.

_____, 1979, Subsurface correlations in the Mist area, Columbia County, Oregon: Oregon Geology, v. 41, no. 12, p. 193 - 196.

Newton, V.C., and Van Atta, R.O., 1976, Prospects for natural gas production and underground storage of pipeline gas in the upper Nehalem River basin, Columbia and Clatsop Counties, Oregon: Oregon Department of Geology and Mineral Industries, Oil and Gas Investigation, No. 5.

Northwood, E.J., 1967, Notes on errors in refraction interpretation: in Musgrave, A.W., ed., 1967, Seismic refraction prospecting: Tulsa, SEG.

Perttu, J.D., 1980, An analysis of gravity surveys in the Portland Basin, Oregon: unpublished thesis, M.S., Portland State University, Portland, Oregon.

Pfaff, V.J., 1981, Geophysical and geochemical analyses of selected Miocene coastal basalt features, Clatsop County, Oregon: unpublished thesis, M.S., Portland State University, Portland, Oregon.

Redpath, B.B., 1973, Seismic refraction exploration for engineering site investigations: U.S. Army Engineer Waterways Experiment Station, Livermore, California, Technical report E-73-4.

Riddihough, R.P., 1978, The Juan de Fuca Plate: EOS, v. 59, no. 9, p. 836 - 842.

Rockwell, D.W., 1967, General wavefront method: in Musgrave, A.W., ed., 1967, Seismic refraction prospecting: Tulsa, SEG.

Sabins, F.F., Jr., 1978, Remote sensing: principles and interpretation: San Francisco, W.H. Freeman and Company.

Schlicker, H.G., Deacon, R.J., and Twelker, N.H., 1964, Earthquake geology of the Portland area, Oregon: The Ore Bin, v. 26, no. 12, p. 209 - 230.

Schmela, R.J., 1971, Geophysical and geological analysis of a fault-like lineation in the Lower Clackamas River area, Clackamas County, Oregon: unpublished thesis, M.S., Portland State University, Portland, Oregon.

Simpson, R.W., and Cox, A.V., 1977, Paleomagnetic evidence for tectonic rotation of the Oregon Coast Range: Geology, v. 5, p. 585 - 589.

Skeels, D.C., 1963, An approximate solution of the problem of maximum depth in gravity interpretation: Geophysics, v. 28, p. 724 - 735.

Slotnick, M.M., 1950, A graphical method for the interpretation of refraction profile data: Geophysics, v. 15, no. 2, p. 163 - 180.

Smith, R.B., and Eaton, G.P., eds., 1980, Cenozoic tectonics and regional geophysics of the western Cordillera: Geological Society of America Memoir 152.

Snavely, P.D., Jr., and Wagner, H.C., 1963, Tertiary geologic history of western Oregon and Washington: Washington Division of Mines and Geology, R.I. 22.

_____, 1964, Geologic sketch of northwest Oregon: United States Geological Survey Bulletin, no. 1181-M.

_____, 1982, Geologic cross-section across the continental margin of southwestern Washington: United States Geological Survey, open-file report 82-459.

Snavely, P.D., Jr., Wagner, H.C., and Lander, D.L., 1980, Interpretation of the Cenozoic geologic history, central Oregon continental margin: cross-section summary: Geological Society of America Bulletin, Part I, v. 91, p. 143 - 146.

Talwani, M., Worzel, J.C., and Landisman, M., 1959, Rapid gravity computations for two-dimensional bodies with application to the Mendocino submarine fracture zone: Journal of Geophysical Research, v. 64, no. 1, p. 49 - 59.

Tatel, H.E., and Ture, M.A., 1955, Seismic exploration of a continental crust: Geological Society of America Special Paper 62, p. 35 - 50.

Tchalenko, J.S., 1970, Similarities between shear zones of different magnitudes: Geological Society of America Bulletin, v. 81, p. 1625 - 1640.

Telford, W.M., Geldart, L.P., Sheriff, R.S., and Keys, D.A., 1976, Applied geophysics: Cambridge, Cambridge University Press.

Thiruvathukal, J.V., Berg, J.W., Jr., and Heinrichs, D.F., 1970, Regional gravity of Oregon: Geological Society of America Bulletin, v. 81, no. 3, p. 725 - 738.

Timmons, D.M., 1981, Stratigraphy, lithofacies and depositional environment of the Cowlitz Formation T4 and 5N, R5W, northwest Oregon: unpublished thesis, M.S., Portland State University, Portland, Oregon.

Trimble, D.E., 1963, Geology of Portland, Oregon and adjacent areas: United States Geological Survey Bulletin, 1119, map scale 1:62,500.

Van Blaricom, R., Ed., 1980, Practical geophysics for the exploration geologist: Spokane, Northwest Mining Association.

Veen, C.A., 1979, A geophysical definition of a Klamath Falls Graben fault: unpublished thesis, M.S., Portland State University, Portland, Oregon.

Venkatakrishnan, R., Bond, J.G., and Kauffman, J.D., 1980, Geological linears of the northern part of the Cascade Range, Oregon: Oregon Department of Geology and Mineral Industries, special paper 12.

Wang, C., Lin, W, and Wu, F.T., 1978, Constitution of the San Andreas Fault zone at depth: Geophysical Research Letters, v. 5, no. 9, p. 741 - 744.

Warren, W.C., and Norbisrath, H., 1946, Stratigraphy of the Upper Nehalem Basin, northwest Oregon: American Association of Petroleum Geologists Bulletin, v. 30, no. 2, p. 213 - 237.

Warren, W.C., Norbisrath, H., and Grivetti, R.M., 1945, Geology of northwest Oregon: United States Geological Survey, Oil and Gas Investigations Preliminary Map 42, scale 1:250,000.

Warrick, R.E., Hoover, D.B., Jackson, W.H., Pakiser, L.C., and Roller, J.C., 1961, The specification and testing of a seismic-refraction system for crustal studies: Geophysics, v. 26, p. 820 - 824.

White, W.R.H., and Savage, J.C., 1965, A seismic refraction and gravity study of the earth's crust in British Columbia: Seismological Society of America Bulletin, v. 55, p. 463 - 486.

Wilkenson, W.D., Lowry, W.D., and Baldwin, E.M., 1946, Geology of the St. Helens Quadrangle, Oregon: Oregon Department of Geology and Mineral Industries Bulletin no. 31.

Zietz, I., Hearn, B.C., Jr., Higgins, M.W., Robinson, G.D., and Swanson, D.A., 1971, Interpretation of an aeromagnetic strip across the northwestern United States: Geological Society of America Bulletin, v. 82, no. 12, p. 3347 - 3371.

APPENDIX A

SPITZENBERG GRAVITY DATA

Station	Latitude	Longitude	Elevation (meters)	Observed Gravity (mgals)	Terrain Correction (mgals)	Free Air Anomaly (mgals)	Complete Bouguer Anomaly (mgals)
27	45°51.68'	122°51.62'	89.55	980653.53	0.08	-25.97	-36.04
26	45°51.33'	122°52.75'	109.27	980647.20	0.21	-25.69	-37.87
25	45°51.32'	122°53.33'	95.51	980648.98	0.43	-28.15	-38.54
24	45°51.05'	122°53.89'	129.94	980639.17	1.12	-26.93	-40.54
23	45°50.77'	122°54.32'	155.11	980633.63	0.45	-24.28	-41.42
22	45°50.65'	122°54.50'	166.09	980631.43	0.64	-22.91	-41.10
21	45°50.54'	122°54.74'	180.98	980627.54	0.52	-22.05	-42.03
20	45°50.64'	122°54.94'	198.62	980622.88	0.69	-21.42	-43.23
19	45°50.60'	122°55.04'	226.67	980616.55	1.01	-19.02	-43.69
18	45°50.52'	122°55.11'	240.29	980613.35	0.97	-17.90	-44.14
17	45°50.37'	122°55.20'	253.56	980610.27	1.40	-16.66	-43.99
16	45°50.27'	122°55.29'	261.73	980608.59	1.11	-15.67	-44.21
15	45°50.23'	122°55.40'	262.02	980608.91	0.95	-15.20	-43.94
14	45°50.18'	122°55.52'	270.91	980606.91	1.02	-14.39	-44.05
13	45°50.15'	122°55.64'	280.13	980604.80	1.12	-13.61	-44.22
12	45°50.11'	122°55.76'	289.43	980602.95	1.20	-12.53	-44.11
11	45°50.04'	122°55.85'	302.82	980599.95	1.30	-11.29	-44.30
10	45°49.71'	122°55.85'	276.05	980605.89	1.27	-13.12	-43.12
9	45°49.79'	122°56.00'	257.99	980610.67	1.01	-14.03	-42.24
8	45°49.84'	122°56.13'	240.08	980615.38	1.03	-14.92	-41.10
7	45°49.86'	122°56.30'	223.87	980619.72	1.01	-15.61	-39.97
6	45°49.86'	122°56.45'	198.87	980625.50	1.25	-17.54	-38.84
5	45°49.85'	122°56.57'	181.76	980628.03	1.60	-20.28	-39.28
4	45°49.78'	122°56.66'	168.50	980630.85	1.78	-21.44	-38.76
3	45°49.52'	122°56.72'	162.06	980631.31	1.46	-22.57	-39.46
2	45°49.52'	122°56.82'	167.64	980630.60	1.45	-21.56	-39.11
1	45°49.51'	122°56.94'	172.03	980629.60	1.28	-21.20	-39.40
31*	45°49.50'	122°57.07'	180.00	980628.54	1.18	-19.78	-39.00
32	45°49.48'	122°57.21'	187.59	980627.04	1.04	-18.91	-39.14
33	45°49.48'	122°57.31'	185.15	980627.76	1.00	-18.94	-38.94
33A	45°49.56'	122°57.43'	182.02	980628.87	0.95	-18.92	-38.59
34	45°49.58'	122°57.54'	181.83	980629.18	0.91	-18.69	-38.40
35	45°49.57'	122°57.64'	182.93	980629.11	0.94	-18.41	-38.20
36	45°49.55'	122°57.78'	182.07	980629.20	0.98	-18.56	-38.19
37	45°49.53'	122°57.92'	182.90	980629.14	0.97	-18.33	-38.08
38	45°49.51'	122°58.04'	184.29	980629.04	0.95	-17.98	-37.91
39	45°49.50'	122°58.17'	185.58	980629.02	0.94	-17.58	-37.68
40	45°49.52'	122°58.31'	187.20	980628.93	0.93	-17.20	-37.48
41	45°49.59'	122°58.48'	186.85	980629.42	0.88	-16.93	-37.22
42	45°49.63'	122°58.65'	187.15	980629.55	1.27	-16.76	-36.71
43	45°49.65'	122°58.80'	190.54	980628.82	1.31	-16.48	-36.75
44	45°49.63'	122°58.95'	195.68	980627.57	1.31	-16.11	-36.98
45	45°49.64'	122°59.07'	193.42	980628.43	1.51	-15.96	-36.36
46	45°49.63'	122°59.33'	196.84	980627.89	1.60	-15.44	-36.14
47	45°49.62'	122°59.60'	212.02	980624.63	1.74	-13.99	-36.28
48	45°50.07'	123°00.44'	312.38	980603.28	1.76	- 5.06	-38.70
49	45°50.30'	123°01.23'	347.72	980597.86	1.15	+ 0.07	-38.16
50	45°50.34'	123°02.49'	386.88	980591.01	1.37	+ 5.25	-37.19
51	45°49.68'	123°03.04'	370.63	980594.26	1.27	+ 4.48	-36.23

* no station 28, 29, 30

PITTSBURG-YANKTON GRAVITY DATA

Station	Latitude	Longitude	Elevation (meters)	Observed Gravity (mgals)	Terrain Correction (mgals)	Free Air Anomaly (mgals)	Complete Bouguer Anomaly (mgals)
BM284	45°51.99'	122°53.17'	86.38	980653.30	0.21	-27.65	-37.23
BM277	45°53.61'	122°55.57'	83.60	980656.61	1.38	-27.64	-35.72
BM439	45°54.15'	122°55.90'	133.54	980646.21	0.82	-23.44	-37.75
BM848	45°53.83'	122°58.14'	258.10	980618.90	0.93	-11.84	-40.14
BM1005	45°53.48'	122°59.87'	305.99	980610.04	1.13	- 5.40	-38.92
BM1683	45°53.63'	123°02.43'	512.80	980565.91	1.45	+14.05	-42.54
BM1751	45°53.50'	123°03.62'	533.63	980563.70	2.76	+18.45	-39.18
BM1403	45°53.88'	123°06.10'	427.33	980593.19	2.33	+14.58	-31.47
BM855	45°54.45'	123°07.68'	260.24	980638.10	1.01	+ 7.09	-21.37
BM586	45°54.09'	123°08.64'	178.25	980658.64	0.88	+ 2.87	-16.44

APIARY GRAVITY DATA

Station	Latitude	Longitude	Elevation (meters)	Observed Gravity (mgals)	Terrain Correction (mgals)	Free Air Anomaly (mgals)	Complete Bouguer Anomaly (mgals)
46	45°57.66'	122°52.03'	16.99	980682.72	0.82	-28.17	-29.27
45	45°58.26'	122°53.02'	182.23	980648.74	0.69	-12.07	-32.03
44	45°57.60'	122°54.25'	185.93	980645.69	0.54	-12.98	-33.52
43	45°58.03'	122°54.99'	161.86	980652.27	0.21	-14.47	-32.61
42	45°58.07'	122°55.67'	144.31	980656.98	0.25	-15.25	-31.34
41	45°58.03'	122°56.32'	170.18	980650.59	0.38	-13.59	-32.49
40	45°58.08'	122°57.00'	97.41	980668.43	0.52	-18.28	-28.80
38*	45°58.21'	122°57.68'	98.99	980666.73	0.72	-19.68	-30.17
37	45°57.50'	122°58.20'	172.25	980647.47	0.44	-15.28	-34.35
36A	45°57.45'	122°58.44'	186.46	980644.20	0.83	-14.09	-34.39
36	45°56.77'	122°58.33'	219.21	980631.27	0.45	-15.89	-40.28
35	45°56.86'	122°58.63'	243.08	980627.49	0.49	-12.43	-39.49
34	45°56.84'	122°58.89'	253.41	980625.32	0.57	-11.39	-39.53
33	45°57.08'	122°59.18'	280.72	980621.31	0.58	- 7.34	-38.55
32	45°57.26'	122°59.48'	291.67	980619.48	0.66	- 6.06	-38.44
31	45°57.20'	122°59.74'	303.91	980616.85	0.82	- 4.83	-38.43
30	45°57.17'	123°00.00'	308.09	980615.95	0.62	- 4.39	-38.66
29	45°57.22'	123°00.28'	292.66	980619.88	0.45	- 5.29	-38.00
28	45°57.35'	123°00.56'	274.16	980624.41	0.39	- 6.67	-37.34
27	45°57.47'	123°00.85'	262.20	980627.74	0.56	- 7.21	-36.35
26	45°57.68'	123°01.15'	264.42	980629.45	0.44	- 5.13	-34.65
25	45°57.73'	123°01.39'	246.42	980632.84	0.45	- 7.37	-34.83
24	45°57.78'	123°01.68'	246.40	980634.00	0.56	- 6.29	-33.65
23	45°57.92'	123°01.97'	280.37	980630.10	0.45	+ 0.06	-31.21
22A	45°57.80'	123°02.19'	235.89	980627.98	0.78	- 5.58	-31.52
22	45°57.43'	123°02.12'	237.87	980635.30	0.78	- 7.09	-33.27
21	45°56.85'	123°02.30'	258.62	980630.17	0.83	- 4.95	-33.40
20	45°56.78'	123°02.53'	273.12	980628.25	1.02	- 2.29	-32.18
19	45°56.67'	123°02.78'	282.42	980623.76	0.95	- 3.75	-34.77
18	45°56.58'	123°03.05'	299.42	980619.99	1.24	- 2.14	-34.79
17	45°56.54'	123°03.30'	317.03	980617.07	0.85	+ 0.43	-34.61
16	45°56.49'	123°03.55'	340.84	980612.19	0.69	+ 2.98	-34.93
15	45°55.82'	123°03.68'	364.12	980605.54	1.11	+ 4.52	-35.59
14	45°55.74'	123°03.95'	345.92	980608.11	1.78	+ 1.59	-35.80
13	45°55.80'	123°04.22'	330.05	980612.65	1.61	+ 1.15	-34.61
12	45°56.13'	123°04.55'	307.86	980618.46	2.08	- 0.39	-33.18
11	45°56.36'	123°04.82'	295.87	980621.93	2.45	- 0.96	-32.02
10	45°56.52'	123°05.15'	290.02	980623.44	3.55	- 1.50	-30.79
9	45°56.70'	123°05.42'	279.59	980627.25	3.54	- 1.17	-29.30
8	45°56.79'	123°05.68'	274.70	980629.56	3.34	- 0.51	-28.43
7	45°56.85'	123°05.95'	268.19	980631.84	2.85	- 0.33	-27.86
6	45°56.95'	123°06.60'	247.15	980638.52	1.87	- 0.29	-26.43
5	45°56.92'	123°07.20'	231.64	980644.48	1.57	+ 0.93	-23.74
4	45°57.02'	123°07.94'	211.14	980651.78	1.81	+ 1.76	-20.35
3	45°56.98'	123°08.59'	192.47	980656.88	1.25	+ 1.16	-19.40
2	45°56.84'	123°09.23'	182.29	980661.76	0.62	+ 3.11	-16.93
1	45°56.77'	123°09.81'	171.12	980666.82	0.75	+ 4.82	-13.81

* no station 39

GRAVITY DATA CORRECTIONS

Latitude - $\sim$1.307 sin 2ϕ mgal/mile

ϕ = latitude

Free-Air - 0.3085 mgal/m

Bouguer - 0.112 mgal/m

Free Air anomaly = OG - GØ + FAC

Bouguer anomaly = OG - GØ + FAC - BC + TC

OG - observed gravity

GØ - theoretical gravity

FAC - Free Air correction

BC - Bouguer correction

TC - terrain correction

PSU base station:

Location: Lobby of Geology Department Office
Cramer Hall, Room 17

Gravity: 980641.35 milligals, established using the 1930 International Formula.

DEEP WELL DATA USED IN GRAVITY MODELLING

T5N, R5W, Sec. 14, NW¼ *

Total depth 558 meters (1832 feet)

American Quasar Petroleum Co.
Crown Zellerbach #14-21

All sediments.

T4N, R3W, Sec. 8, NW¼ *

Total depth 1768 meters (5805 feet)

Reichhold Energy Corp.
"NNG-CZ" #2

All sediments except volcanics from 870 to 930 meters.

T5N, R4W, Sec. 36, NW¼

Total depth 1848 meters (6063 feet)

Reichhold Energy Corp.
Crown Zellerbach #4

All sediments except volcanics from 745 to 760 meters.

Well locations noted on Figure 2.

* Projected onto cross sections, Figures 14 and 17.

```
10C          FREE AIR GRAVITY FIT PROGRAM
20C    THIS PROGRAM COMPUTES THE GRAVITATIONAL ATTRACTION ACROSS THE SURFACE
30C    OF A RECTANGLE COMPOSED OF A NUMBER OF ARTITRARILY SHAPED BLOCKS.
40C    THE TERRAIN MAY BE INCLUDED ALONG THE TOP OF THE RECTANGLE. THE
50C    ORIGIN OF THE COORDINATE SYSTEM IS IN THE UPPER LEFT HAND CORNER
60C    OF THE RECTANGLE. Z IS POSITIVE DOWNWARDS. ALL DISTANCES ARE IN
70C    KM. THE RECTANGLE IS ORDINARILY EXTENDED ABOUT 100 KM ON EITHER
80C    SIDE OF THE AREA OF INTEREST IN ORDER TO ELIMINATE EDGE EFFECTS.
90C    THE MODEL CHECK HAS NO SIGNIFICANCE WHEN THE TOPOGRAPHY IS INCLUDED.
100C    DRCX       COMMENT CARD                                          20A4
110C    GRAD1      FIRST REGIONAL GRADIENT                               F10.0
120C    GRAD2      SECOND REGIONAL GRADIENT                              F10.0
130C    GRADS      CHANGE IN REGIONAL GRADIENT                           F10.0
140C    SAM        CROSS SECTION NUMBER                                  F10.0
150C    M          TOTAL NUMBER OF COMPUTED POINTS                       I5
160C    N          TOTAL NUMBER OF BLOCKS IN MODEL                       I5
170C    PX         X COORDINATE OF CALCULATED POINT                      F10.0
180C    PZ         Z COORDINATE OF CALCULATED POINT                      F10.0
190C    RHO        BLOCK DENSITY                                         F5.2
200C    J          NUMBER OF CORNERS IN BLOCK                            I3
210C    ISALT      BLOCK NUMBER                                          I5
220C    X          X COORDINATE OF BLOCK CORNER                          F10.0
230C    Z          Z COORDINATE OF BLOCK CORNER                          F10.0
240C
250C
260C
270       DIMENSION PX(200),PZ(200),X(400),Z(400),TOT(200),TIT(200),DRCX(20)
280       READ (22,901)(DRCX(J),J=1,20)
290$901    FORMAT (20A4)
300       WRITE (23,902)(DRCX(J),J=1,20)
310$902    FORMAT ('1',20A4////)
320$100    READ (22,469) GRAD1,GRAD2,GRADS, GRADA, GRAD
330$469    FORMAT (5F10.0)
340        IF (GRADS) 255,9999,255
350$255       WRITE (23,468) GRAD1,GRAD2,GRADS, GRADA, GRAD
360$468    FORMAT (' ',F10.3,' =GRAD1',F10.3,' =GRAD2',F10.3,' =GRADS'
361&      , F10.3, ' = GRADA', F10.3, ' = GRAD')
370       PI=3.1415927
380       PIT2=2.*PI
390       READ (22,1) SAM,M,N
400$1      FORMAT (F10.0,2I5)
410       DO 721 J=1,M
420$721    CONTINUE
430$903    WRITE (23,201) SAM,M,N
440$201    FORMAT (' ',F10.2,' CROSS SECTION ID NUMBER'/,I9,'   POINTS AT WHI
450&      CH GRAVITY IS TO BE COMPUTED'/,I9,2X,' BLOCKS IN MODEL'//////)
460       DO 52 I=1,M
470       READ (22,301) PX(I) ,PZ(I)
480$301    FORMAT (2F10.0)
490       WRITE (23,303) PX(I),PZ(I)
500$303    FORMAT (' ',2F10.4)
510       TIT(I)=0.
520       TOT(I)=0.
530$52     CONTINUE
540       DO 106 IN=1,N
550       READ (22,2) RHO,J,ISALT
560$2      FORMAT (F5.2,I3,I5)
570       WRITE (23,304)RHO,J,ISALT
580$304    FORMAT ('0'F6.2,' DENSITY'/ I7,' CORNERS IN BLOCK'/I7,' BLOCK NUMB
590&      ER'///)
600       WRITE (23,305)
610$305    FORMAT (' ',7X,'X',9X,'Z',6X,' COORDINATES OF BLOCK CORNERS')
620       DO 300 I=1,J
```

```
630       READ (22,301) X(I),Z(I)
640       WRITE (23,306) X(I),Z(I)
650$306    FORMAT (' ',2F10.3)
660$300    CONTINUE
670       K=J+1
680       X(K)=X(1)
690       Z(K)=Z(1)
700       SUM=0.
710       DO 101 I=1,M
720       DO 5 J=1,K
730       Z(J)=Z(J)-PZ(I)
740       X(J)=X(J)-PX(I)
750$5      CONTINUE
760       DO 122 J=1,K
770        IF (X(J))  253,256,253
771$256     IF (Z(J)) 853,851,853
780$853    IF (X(J)) 253,499,253
790$253       GO TO 852
800$851    TH=0.
810       GO TO 498
820$852    IF (Z(J)) 252,861,252
830$252       GO TO 854
840$861    IF (X(J)) 251,251,863
850$251       TH=-1*PI
860       GO TO 498
870$863    TH=0.
880       GO TO 498
890$854    TH=ATAN2(Z(J),X(J))
900       GO TO 498
910$499    TH=PI*.5
920        IF (Z(J)) 250,498,498
921$250    TH = -1 * TH
930$498    IF (Z(J)) 501,502,502
940$501    TH=TH+PIT2
950$502    IF (J-1) 10,503,10
960$503    TH1=TH
970       GO TO 122
980$10     TH2=TH
990       L=J-1
1000       A=Z(J)-Z(L)
1010       B=X(J)-X(L)
1020       JJ=5
1030       IF (X(L)) 505,504,505
1040$504    JJ=1
1050$505    IF (X(J)) 507,506,507
1060$506    JJ=2
1070$507    IF (A) 509,508,509
1080$508    JJ=3
1090$509    IF (B) 511,510,511
1100$510    JJ=4
1110$511    IF (TH1-TH2) 19,512,19
1120$512    S=0.
1130       GO TO 102
1140$19     IF (X(L)) 22,513,22
1150$513    IF (Z(L)) 22,514,22
1160$514    S=0.
1170       GO TO 102
1180$22     IF (X(J)) 25,515,25
1190$515    IF (Z(J)) 25,516,25
1200$516    S=0.
1210       GO TO 102
1220$25     GO TO (26,27,28,29,30),JJ
1230$26     V6=TH2-.5*PI
1240       IF (ABS(V6)-PI) 518,518,517
1250$517    V6=V6-SIGN (PIT2,V6)
1260$518    S=(X(J)*X(J)*Z(L)/(A*A+X(J)*X(J)))*(V6+(A/X(J))*(ALOG(ABS(Z(L)))
```

```
1270&      -.5*ALOG(X(J)*X(J)+Z(J)*Z(J))))
1280       S1=S
1290       GO TO 102
1300$27     V7=TH1-.5*PI
1310       IF(ABS(V7)-PI)519,519,520
1320$520    V7=V7-SIGN (PIT2,V7)
1330$519    S=(X(L)*X(L)*Z(J)/(A*A+X(L)*X(L)))*(V7-(A/X(L))*(ALOG(ABS(Z(J)))
1340&      -.5*ALOG(X(L)*X(L)+Z(L)*Z(L))))
1350       S2=S
1360       S=-S
1370       GO TO 102
1380$28     V8=TH2-TH1
1390       IF(ABS(V8)-PI) 522,522,521
1400$521    V8=V8-SIGN (PIT2,V8)
1410$522    S=Z(L)*V8
1420       GO TO 102
1430$29     V=SQRT((Z(J)*Z(J)+X(J)*X(J))/(Z(L)*Z(L)+X(L)*X(L)))
1440       V1=V
1450       S=X(L)*ALOG((X(L)/X(J))*V)
1460       S3=S
1470       GO TO 102
1480$30     T=X(J)-(Z(J)*B/A)
1490       V=TH1-TH2
1500       U=B*A/(B*B+A*A)
1510       IF(ABS(V)-PI) 524,524,523
1520$523    V=V-SIGN (PIT2,V)
1530$524    W=(A/B)*.5*ALOG((Z(J)*Z(J)+X(J)*X(J))/(Z(L)*Z(L)+X(L)*X(L)))
1540       S=T*U*(V+W)
1550$102    SUM=SUM+S
1560       TH1=TH2
1570$122    CONTINUE
1580       DO 103 J=1,K
1590       Z(J)=Z(J)+PZ(I)
1600       X(J)=X(J)+PX(I)
1610$103    CONTINUE
1620       DUM=SUM*13.346
1630       TIT(I)=TIT(I)+DUM
1640       SUM=SUM*RHO*13.346
1650       TOT(I)=TOT(I)+SUM
1660       SUM=0.
1670$101    CONTINUE
1680$106    CONTINUE
1690       DO 1000 KT=2,M
1700       TIT(KT)=TIT(KT)-TIT(1)
1710$1000   CONTINUE
1720       DO 633 I=1,M
1730       IF (PX(I) - GRADS) 254,254,621
1740$254        TOT(I)=TOT(I)+SUM-PX(I)*GRAD1
1750       GO TO 622
1751$621   IF(PX(I) - GRAD) 701, 701, 702
1752$701    TOT(I) = TOT(I) + SUM-GRADS*GRAD1 - GRAD2*(PX(I)-GRADS)
1753       GO TO 622
1754$702   TOT(I)=TOT(I) + SUM - GRADS*GRAD1 - (GRAD-GRADS)*GRAD2 - GRADA*
1755&      (PX(I) - GRAD)
1770$622    SUM=0.
1780$633    CONTINUE
1790       TIT(1)=0.
1800       WRITE (23,315)
1810$315    FORMAT('1',3X,'PX',8X,'PZ',9X,'TOT',10X,'TIT')
1820       WRITE (23,200)  (PX(I),PZ(I),TOT(I),TIT(I),I=1,M)
1830$200    FORMAT (' ',F8.2,F12.4,F12.2,F12.4)
1840       GO TO 100
1850$9999   STOP
1860       END
```

PROGRAM FOR REDUCING SURVEY DATA TO STATION ELEVATIONS IN FEET, TO RUN ON TEKTRONIX 4051 COMPUTER.

```
100 INIT
110 PAGE
120 SET DEGREES
130 REM ENTER DATA
140 PRINT "ENTER BM ELEVATION"
150 INPUT E
160 PRINT "ENTER HI, SLOPE DIST, VERT ANGLE(D/M/S), MID X-HAIR"
170 INPUT I,S,D,M1,S1,M
180 PRINT "ENTER 1-FORESIGHT OR 2-BACKSIGHT"
190 INPUT D1
200 PRINT "IS ANGLE 1-POS OR 2-NEG"
210 INPUT D2
220 A=D+M1/60+S1/3600
230 H=S*COS(A)*COS(A)
240 V=S*COS(A)*SIN(A)
250 IF D1=1 THEN 270
260 IF D1=2 THEN 320
270 IF D2=1 THEN 300
280 E1=E+V-M+I
290 GO TO 360
300 E1=E+I+V-M
310 GO TO 360
320 IF D2=1 THEN 350
330 E1=E+M-V-I
340 GO TO 360
350 E1=E+M-V-I
360 IMAGE "H= ",5D,2X, "V= ",-3D.2D,2X, "ELEV= ",5D.2D
370 PRINT USING 360:H,V,E1
380 E=E1
390 INPUT A$
400 GO TO 160
410 END
```

BM - benchmark

HI - instrument height

$\frac{+ \mid +}{- \mid -}$ - sign of vertical angle

A - vertical angle

H - horizontal distance between survey stations

V - vertical distance between survey stations

E - known elevation

E1 - elevation to be determined

A$ - pause in program, hit RETURN to continue

APPENDIX B

BUNKER HILL REFRACTION DATA

(East to West)

		Arrival time at geophone (seconds)												
Line	Shotpoint	1	2	3	4	5	6	7	8	9	10	11	12	Record Quality
2200E-1650E	1650E	0	.018	.031	.047	.058	.067	.086	.098	.132	.137	.145	.150	B
	2200E	.159	.147	.135	.122	.119	.110	.108	.107	.085	.057	.029	0	B+
	2750E	.213	.202	.200	.199	.199	.191	.182	.174	.173	.166	.162	.155	D
	1100E	.155	.159	.165	.173	.186	.201	.210	.222	.232	.239	.245	.260	C
1650E-1100E	1100E	.118	.115	.110	.101	.089	.079	.067	.057	.045	.036	.025	0	A
	1650E	0	.017	.031	.046	.064	.066	.075	.084	.091	.099	.109	.118	B
	2200E	.126	.134	.148	.161	.169	.164	.177	.178	.182	.182	.187	.199	C-
	550E	.185	.175	.170	.168	.162	.156	.148	.142	.137	.135	.132	.126	B
1100E-550E	550E	0	.027	.040	.050	.060	.074	.081	.093	.099	.105	.114	.124	B
	1100E	0	.029	.041	.053	.064	.076	.080	.087	.097	.107	.116	.125	A
	1650E	.189	.174	.172	.181	.168	.154	.149	.144	.139	.133	.130	.126	B
	BH-0	.126	.137	.141	.148	.153	.155	.160	.165	.166	.168	.174	.177	B
550E-BH-0	BH-0	0	.033	.042	.053	.067	.076	.084	.093	.106	.115	.124	.134	A
	550E	.134	.125	.113	.105	.095	.089	.072	.062	.050	.037	.027	0	A
	1100E	.185	.177	.176	.174	.167	.159	.157	.147	.140	.135	.132	.126	B
	550W	.126	.129	.135	.140	.149	.152	.159	.164	.169	.174	.185	.191	B
BH-0-550W	BH-0	0	.015	.027	.039	.051	.062	.067	.077	.086	.094	.100	.105	C+
	550W	.112	.107	.105	.097	.086	.079	.071	.063	.050	.027	.012	0	B
	1100W	.160	.159	.159	.161	.149	.148	.144	.138	.138	.134	.127	.126	C
	550E	.128	.126	.137	.146	.148	.157	.159	.163	.168	.170	.178	.180	B+
550W-1100W	550W	0	.012	.026	.047	.062	.072	.080	.093	.103	.108	.120	.125	B
	1100W	.118	.114	.104	.097	.086	.078	.068	.055	.044	.030	.013	0	A
	1650W	.181	.169	.167	.166	.159	.155	.150	.145	.139	.135	.129	.126	C
	BH-0	.126	.138	.139	.145	.148	.152	.155	.160	.165	.167	.170	.179	C+
1100W-1650W	1100W	0	.013	.032	.044	.057	.068	.072	.080	.088	.097	.106	.113	C+
	1650W	.121	.119	.105	.095	.085	.080	.068	.066	.050	.037	.020	0	B
	2200W	.188	.188	.186	.176	.170	.168	.160	-	.150	.148	.131	.126	D
	550W	.126	.130	.135	.138	.141	.146	.148	.176	.158	.167	.173	.180	C
1650W-2200W	1650W	.103	.100	.102	.094	.081	.075	.065	.058	.047	.031	.019	0	B
	2200W	0	.019	.036	.048	.058	.067	.072	.082	.093	.095	.102	.108	C+
	2750W	.126	.136	.140	.148	.159	.160	.164	.177	.187	.178	.176	.094	D
	1100W	.184	.181	.177	.177	.169	.165	.157	.150	.131	.134	.127	.126	C

SHAFFER ROAD REFRACTION DATA

(West to East)

Line	Shotpoint	1	2	3	4	5	6	7	8	9	10	11	12	Record Quality
0-550	0	0	.011	.013	.022	.031	.036	.043	.052	.055	.064	.074	.082	B+
	550	.084	.078	.068	.062	.058	.053	.046	.036	.026	.018	.008	0	A
	1100	.090	.101	.111	.119	.121	.131	.135	.140	.140	.150	.153	.162	D
550-1100	550	.092	.080	.080	.072	.059	.050	.044	.034	.028	.020	.010	0	B+
	1100	0	.004	.010	.014	.022	.027	.028	.041	.059	.066	.077	.098	C
	0	-	.160	.159	.148	.133	.128	.119	.109	.103	.101	.092	.082	D
1100-1650	1100	0	.013	.018	.020	.021	.028	.030	.033	.041	-	.045	.052	C+
	1650	.055	.047	.045	.035	.031	.026	.020	.018	.011	.008	.004	0	D
	2200	.060	.080	.090	.098	.118	.147	.158	.172	.184	.202	.218	.248	F
1650-2200	1650	.057	.053	.045	.040	.032	.028	.021	.019	.012	.011	.004	0	B
	2200	0	.004	.013	.015	.019	.024	.027	.028	.028	.038	.054	.062	B
	2750	.050	.057	.061	.068	.074	.075	.078	.084	.088	.099	.106	.111	C+
	1100	.180	.142	.119	.104	.097	.082	.080	.080	.077	.071	.071	.065	F
2200-2750	2200	0	.013	.017	.022	.023	.028	.032	.032	.038	.047	.048	.059	B+
	2750	.066	.063	.056	.047	.042	.035	.028	.026	.024	.017	.005	0	B
	3300	.182	-	.121	-	.129	.091	.088	.082	.097	.092	.088	.070	F
	1650	.060	.075	.071	.068	.075	.076	-	.095	-	-	-	-	F
2750-3300	2750	0	.021	.025	.032	.036	.042	.044	.051	.054	.059	.066	.072	B+
	3300	.070	.065	.059	.055	.048	.045	.037	.033	.023	.015	.010	0	B
	3850	.165	-	.158	.148	.161	.157	.147	.131	.124	.116	.104	.095	D-
	2200	.065	.069	.077	.080	.084	.090	.097	.100	.107	.112	.113	.115	C-
3300-3850	3300	0	.009	.013	.025	.029	.038	.045	.049	.054	.058	.068	.084	B-
	3850	.095	.091	.080	.065	.053	.050	.044	.043	.034	.025	.015	0	C-
	4400	.202	.209	.203	.201	.194	.181	.128	.160	.146	.097	.084	.075	D-
	2750	.070	.079	.080	.084	.105	.112	.119	.129	.129	.131	.140	.150	D-
3850-4400	3850	0	.011	.017	.021	.024	.036	.040	.042	.046	.057	.066	.096	C
	4400	.079	.063	.049	.043	.021	.016	.016	.013	.013	.007	0	.004	C
	3300	.095	.123	.125	.151	.166	.173	.180	.188	.188	.194	.218	-	D

LITTLE CLATSKANIE REFRACTION DATA

(West to East)

Line	Shotpoint	Arrival time at geophone (seconds) 1	2	3	4	5	6	7	8	9	10	11	12	Record Quality
0-550	0	0	.005	.009	.015	.016	.021	.024	.034	.038	.045	.057	.067	B
	550	.065	.059	.057	.055	.046	.038	.036	.029	.027	.019	.012	0	B+
	1100	.217	.204	.243	.232	.222	.222	.222	.172	.155	.134	.134	.115	F-
550-1100	550	0	.014	.023	.033	.046	.065	.066	.076	.082	.088	.098	.115	B-
	1100	.112	.108	.102	.091	.087	.089	.066	.054	.037	.025	.013	0	C
	1650	.151	.150	.140	.131	.123	-	.120	.102	.102	.101	.093	.092	D-
	0	.065	.069	.074	.084	.094	.103	.103	.103	.103	.172	.182	-	F-
1100-1650	1100	.086	.081	.076	.068	.059	-	.042	.036	.030	.026	.013	0	B+
	1650	0	.015	.027	.042	.052	.058	.062	.065	.076	.081	.084	.092	B
	2200	.095	.108	.105	.108	.115	.121	.128	.131	.137	.153	.153	.153	C-
	550	.145	.141	.139	.137	.132	.128	.127	.119	.119	.120	.117	.115	D-
1650-2200	1650	0	.018	.028	.043	.056	.062	.072	.082	.087	.087	.095	.097	B+
	2200	.090	.090	.083	.076	.076	.072	.062	.048	.038	.027	.011	0	A-
	2750	.184	.179	.173	.168	.166	.166	.147	.136	.128	.126	.119	.116	C
	1100	.092	.102	.106	.107	.114	.118	.124	.126	.126	.132	.132	.136	C+
2200-2750	2200	0	-	.034	.047	.060	.073	.073	.080	.081	.095	.100	.114	B
	2750	.104	-	.094	.090	.076	.072	.059	.057	.039	.033	.016	0	B-
	3300	.197	.194	.188	.172	.172	.155	.143	.141	.132	.124	.124	.120	C-
	1650	.095	-	.101	.107	.113	.123	.130	-	-	-	-	-	F
2750-3300	2750	0	.018	.031	.039	.045	.055	.061	.072	.077	.088	.104	.121	B
	3300	.117	.111	.090	.088	.072	.061	.051	.046	.033	.020	.009	0	C
	3850	.126	.119	.113	.097	.077	.069	.060	.036	.019	.009	.007	0	D-
	2200	.116	.116	.118	.151	.155	.163	.163	.172	.137	.182	.183	.192	F

REFRACTION DATA REDUCTION FORMULAS

A. Critical angle, dip, depth and thickness of layers

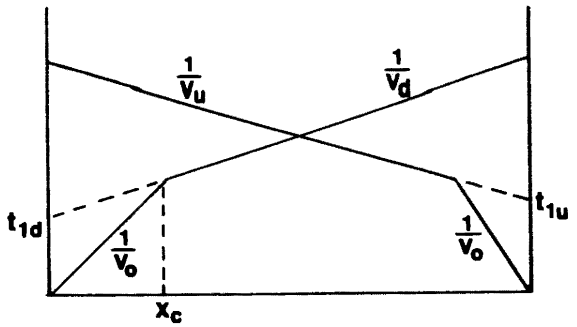

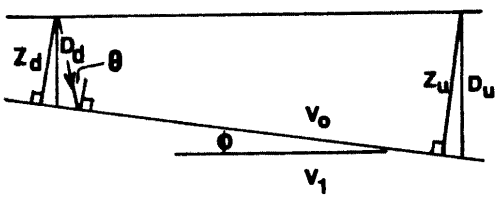

$$\theta \text{ (critical angle)} = \frac{1}{2}\left[\sin^{-1}\frac{V_o}{V_d} + \sin^{-1}\frac{V_o}{V_u}\right] \qquad \sin\theta = \frac{V_o}{V_1}$$

$$\phi \text{ (dip)} = \frac{1}{2}\left[\sin^{-1}\frac{V_o}{V_d} - \sin^{-1}\frac{V_o}{V_u}\right] \qquad V_u > V_d$$

$$Z_d = \frac{t_{1d} V_o}{2\cos\theta} \qquad Z_u = \frac{t_{1u} V_o}{2\cos\theta}$$

$$D_d = \frac{Z_d}{\cos\phi} \qquad D_u = \frac{Z_u}{\cos\phi}$$

Multiple dipping layer formulas in Ewing, Woollard and Vine, 1938, and Mota, 1954.

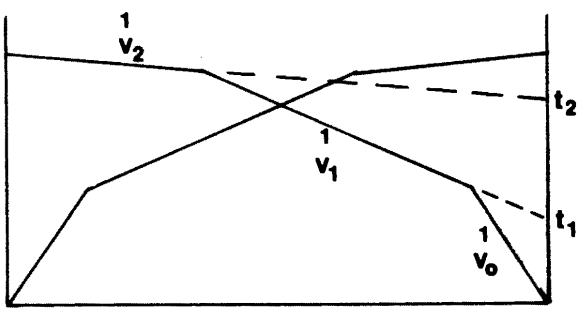

$$V_o < V_1 < V_2$$

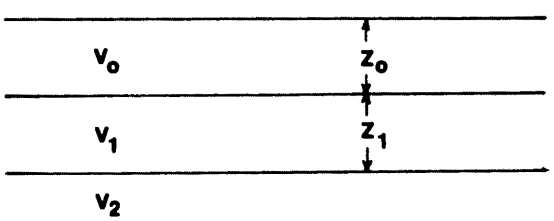

$$Z_o = \frac{t_1}{2}\frac{V_1 V_o}{\sqrt{V_1^2 - V_o^2}}$$

or

$$Z_o = \frac{1}{2}\sqrt{\frac{V_1 - V_o}{V_1 + V_o}}\, X_c$$

$$Z_1 = \frac{1}{2}\left(t_2 - 2Z_o\frac{\sqrt{V_2^2 - V_o^2}}{V_2 V_o}\right)\left(\frac{V_2 V_1}{\sqrt{V_2^2 - V_1^2}}\right)$$

As a quick approximation $\frac{X_c}{2} \leq Z$.

B. Fault throw:

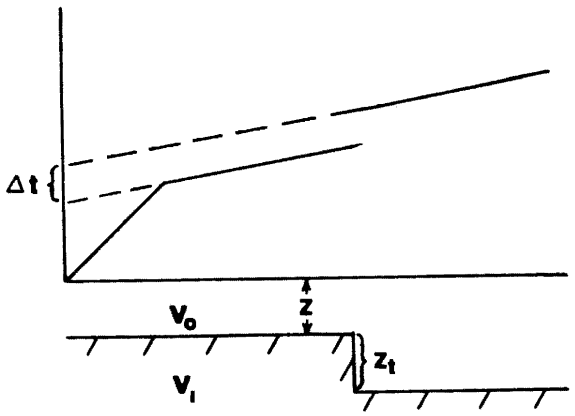

$$Z_t = \frac{\Delta t V_o}{\cos\theta} = \Delta t\left(\frac{V_o V_1}{\sqrt{V_1^2 - V_o^2}}\right)$$

C. Elevation correction:

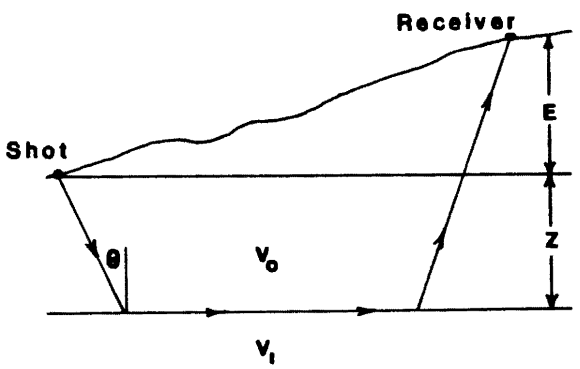

Depth to V_o/V_1 interface = $Z + \frac{E}{2}$.

APPENDIX C

BUNKER HILL MAGNETIC DATA

(East to West)

Station*	Gammas	Station	Gammas	Station	Gammas
BH-0	55523	420	55370	1235	56715
E2750	55107	315	55366	1345	56725
2650	55331	265	55400	1450	56380
2550	55504	240	55786	1560	56609
2450	54930	210	55935	1665	56329
2350	55626	160	55934	1765	56062
2250	55894	135	55786	1865	55913
2145	55697	110	55569	1965	55606
2040	55826	BH-0	55515	2065	55630
1935	55884	105	55559	2165	55381
1830	55436	210	55419	2275	55263
1725	55353	310	55481	2380	55381
1630	55651	365	55563	2485	55390
1530	55575	395	55724	2590	55383
1435	55663	415	55415	2700	55524
1335	55664	520	55812	2800	55455
1240	55638	615	56004	BH-0	55524
1140	55603	720	55992		
1040	55664	820	55818		
935	55539	870	56440		
830	55248	920	56613		
725	55186	975	56763		
620	55190	1025	56775		
525	55211	1125	56447		

*Distance in feet east or west of BH-O (Figure 10).

SHAFFER ROAD MAGNETIC DATA

(East to West)

Station*	Gammas	Station	Gammas
S2200	55850	1685	55175
3950	55012	1580	55033
3850	54884	1470	54889
3745	54777	1365	55453
3640	54809	1255	55654
3540	54586	1145	55341
3435	55078	1055	55333
3330	54626	950	55056
3230	54715	845	55086
3125	54591	740	54963
3025	54910	635	54961
3925	55377	540	55046
2820	55527	435	55073
2720	55701	330	55081
2620	55352	230	55186
2520	55866	125	55130
2420	55982	20	55203
2320	55712	-80	55221
2220	55986	S2200	55829
S2200	55834		
2120	55909		
2010	55556		
1905	54884		
1795	55040		

*Distance in feet from west end of line (Figure 12).

LITTLE CLATSKANIE MAGNETIC DATA

(West to East)

Station*	Gammas	Station	Gammas
LC1650	56353	2175	55467
LC-0	56333	2270	55481
100	56539	2370	55186
200	56601	2465	54968
300	54981	2560	54800
400	54268	2655	54953
500	54372	2750	54942
600	54505	2840	54961
700	55019	2935	55066
800	54578	3025	55018
900	55101	3120	55027
1000	55324	3210	54987
1100	55369	3300	54964
1205	55026	3395	54923
1310	55870	3490	54971
1410	56282	3590	54975
1515	56405	3685	54992
1620	56466	3780	54992
LC1650	56356	3880	55048
1715	55948	3975	55165
1810	55932	LC1650	56341
1900	55901		
1995	55440		
2085	55413		

*Distance in feet from west end of line (Figure 12).

APPENDIX D

WATER WELL DATA USED IN REFRACTION MODELLING

T4N, R2W, Sec. 6, SW¼ NE¼ (Bunker Hill line)

Total depth 150 feet

0 -	82 feet	clay
82 -	150 feet	basalt

T4N, R2W, Sec. 6, SW¼ NW¼ (Bunker Hill line) *

Total depth 200 feet

0 -	125 feet	clay
125 -	200 feet	broken rock

T5N, R3W, Sec. 3, SE¼ NE¼ (Shaffer Road line) *

Total depth 483 feet

0 -	60 feet	clay
60 -	158 feet	sandy clay
158 -	455 feet	basalt
455 -	483 feet	sandstone

Well locations noted on Figures 2, 10 and 12.

* Projected on cross sections, Figures 19, 20, 21, 22.